Final Report

ASSESSMENT OF AVAILABLE HABITAT AND OCCURRENCE OF THE BLACK-SPOTTED NEWT (*NOTOPHTHALMUS MERIDIONALIS*) IN TEXAS

Prepared for the Texas Comptroller of Public Accounts
#18-6656CS
(Principal Investigators: Richard J. Kline, A. Faiz Rahman)

by

DREW R. DAVIS, PADRAIC S. ROBINSON, SEAN M. COLLINS, CAITLIN R. HELMAN, ABDULLAH F. RAHMAN, AND RICHARD J. KLINE

School of Earth, Environmental, and Marine Sciences,
The University of Texas Rio Grande Valley,
Brownsville, Texas 78520

11 April 2023

TABLE OF CONTENTS

ACKNOWLEDGEMENTS

We thank the Texas Parks and Wildlife Department (TPWD), National Park Service (NPS), U.S. Fish and Wildlife Service (USFWS), and The Nature Conservancy (TNC) for issuing permits to allow for sampling on their property. All research was conducted under a TPWD Scientific Research Permit (SPR-1018-294), TPWD State Park Scientific Study Permits (2018_R2_RGV_07, 2019_R2_RGV_02, 2020_R2_RGV_04), NPS Scientific Research and Collecting Permit (PAAL-2021-SCI-0001), USFWS Research and Monitoring Special Use Permits (STRC-12-17-18-CJP, 21530-20-7, 2021-LA-028), TNC (Texas Chapter) Scientific Investigation and Collection Permit, and The University of Texas Rio Grande Valley IACUC protocols (AUP-18-28, AUP-22-12). We also wish to thank the following private landowners and public organizations who granted us permission to sample and access sites on their property: East Foundation, Coastal Bend Bays and Estuaries Program, Coastal Bend College, Audubon Outdoor Club of Corpus Christi, E. Salinas, L. Lopez, B. Glick, and G. Glick. We also thank C. Guadiana, M. Schalk, M. Pons, Jr., D. Coyle, K. Ruppert, A. Bogolin, S. Bauer, and B. Genter for their assistance in the field, C. Guadiana and Gladys Porter Zoo for allowing eDNA sampling from captive animals, T. LaDuc (TNHC) for accessioning and cataloging voucher specimens and for the loan of tissue samples used when validating the eDNA analysis, the numerous curators and collection managers who have shared information on occurrence records, G. de la Fuente and Ducks Unlimited Mexico (DUMAC) for providing a Mexico wetlands inventory shapefile, and B. Chastain for helpful comments regarding Maxent.

EXECUTIVE SUMMARY

The goal of this project was to increase our understanding and knowledge about the current distribution of the Black-spotted Newt (*Notophthalmus meridionalis*) in Texas, USA, and the habitats that the species occupies. There was a paucity of information surrounding the Black-spotted Newt, and there have been few previous studies of this species across the entire species range. Here, we conducted six main tasks aimed at answering these research questions: 1) created a species occurrence database to guide surveys and to use in predictive models; 2) developed and validated a targeted environmental DNA (eDNA) assay for Black-spotted Newts; 3) surveyed for Black-spotted Newts across south Texas using eDNA and traditional methods; 4) examined environmental correlates of Black-spotted Newt detections; 5) developed an eDNA metabarcoding assay and compared its effectiveness to the targeted eDNA assay; and 6) developed current and future habitat suitability models for the Black-spotted Newt.

Occurrence records for the Black-spotted Newt were requested from 69 different sources, 34 of which had available records. In total, 1006 Black-spotted Newt occurrence records were aggregated from throughout the species' range. Our database revealed that recent (since 2000) verifiable records of Black-spotted Newts in Texas were confined to the three southernmost counties: Willacy, Hidalgo, and Cameron.

A sensitive, PCR based eDNA assay was developed for the Black-spotted Newt. This assay was successful at detecting newt eDNA at very low levels from field samples. In total, eDNA samples from 80 sites were analyzed, producing eight positive detections (10%). Using traditional methodologies and eDNA detection together, Black-spotted Newts were detected at 12 of 80 sites (15%) spanning five counties across south Texas. Five new Black-spotted Newt localities were reported as part of this study (eDNA: n = 4; traditional methods: n = 1), including one in Live Oak County, which is the first newt detection the county since 1938, and one in Calhoun County where there have been no previous confirmed Black-spotted Newt records. With so few confirmed Black-spotted Newt localities in the past 20 years, accurately locating breeding ponds is essential to better understand the current distribution of this species in south Texas.

The water, soil, and habitat data were used to characterize potentially suitable breeding ponds for Black-spotted Newts. We identified shared characteristics between the sites in which newts had been detected during this study combined with recent occurrences of this species. The analysis revealed that ephemerality, the absence of paved roads, higher soil copper concentration, lower soil sand percentage, and lower water conductivity can help predict Black-spotted Newt presence. In addition, higher levels of clay are likely important for this species, which aids soil moisture retention as individuals move into underground habitats during times of drought. Clay, silty clay loam, or clay loam were soil classifications that characterized newt habitat. The absence of nearby paved roads was a shared characteristic among all sites in which Black-spotted Newts have been detected in recent years. The maximum conductivity where Black-spotted Newts were found was 2073 µS/cm; conductivity in water bodies significantly greater than this value may not be suitable for this species.

Previous studies identified seven "metapopulation centers" for the Black-spotted Newt in south Texas. Among these, we obtained positive eDNA detections from two metapopulation centers. Our results indicate that breeding populations of Black-spotted Newts have persisted within these two areas for 30+ years. Possibly contributing to the persistence of this species is the conservation focus of the organizations that operate these sites. The remaining metapopulation centers were in Kleberg (n = 4) and Kenedy (n = 1) counties, where we obtained no positive Black-spotted Newt

detections after repeated sampling. During our study, many previously documented ponds and ditches were no longer present due to human development. Further, dirt roads running parallel to the US Hwy 77 were highly disturbed due to activities by U.S. Customs and Border Protection (CBP).

The eDNA metabarcoding assay was validated on 32 co-occurring native amphibian species. A number of different amphibians, as well as many other taxa, were detected in field samples using metabarcoding. For a portion of the study, eDNA metabarcoding, along with targeted eDNA assay and traditional survey methods, were used to provide information on amphibian community assemblages throughout south Texas. The eDNA metabarcoding offered more species-level detections and detected significantly more amphibian taxonomic units compared to paired traditional visual encounter surveys. eDNA metabarcoding was less efficient at detecting Black-spotted Newts compared to traditional survey methods. However, we found the most effective tool for detecting Black-spotted Newts across sites was the targeted eDNA assay.

Current habitat suitability was modelled for the Texas Black-spotted Newt using Maxent to find high-suitability habitat where previously unrecognized populations may be found. The model was projected under two different climate scenarios (SSP2-4.5 and SSP3-7.0) at two future time periods (2061–2080 and 2081–2100) using three general circulation models (ACCESS, CanESM5, MIROC6) to evaluate the range of possible effects of climate change on newt habitat suitability. The current model and future projections all placed the most high-suitability habitat for the Texas Black-spotted Newt in Hidalgo, Cameron, and Willacy counties and, under SSP3, even predicted improved suitability in these counties. However, Cameron and Hidalgo counties also contain the most pronounced areas of low-suitability habitat that correspond to high human population density and, along with Starr and Willacy counties, are predicted to experience continued population growth through the first half of the 21st Century. The rapidly growing population is accompanied by the conversion of native habitat and agricultural land to urban land cover and correlates with an increase in paved roads, drainage of ponds and low-lying areas, and fragmentation of habitat.

While agriculture has historically been the primary driver of habitat loss and fragmentation in south Texas, urbanization is predicted to become the dominant cause of habitat destruction, degradation, and fragmentation in the Lower Rio Grande Valley. Predicted expansions of suitable habitat occurring along the inland margins of the distribution may aid in the expansion of Black-spotted Newt range only if individuals are geographically and physiologically capable of dispersal to these areas. Our recent detections of Texas Black-spotted Newts and the estimation of high suitability habitat in these areas suggests that tracts of relatively undisturbed native habitat are critical for the presence and persistence of this populations, particularly in Cameron and Hidalgo counties, where land conversion for urban use is most prominent.

While there were a few surprising new detections of Black-spotted Newts during this project, the overall pattern was one of decline. Of the previously described seven metapopulation centers in Texas, only two appear to remain after repeated sampling using multiple detection methods. It is clear that Black-spotted Newts and human urban development are incompatible, and habitat should be set aside in these remaining areas to limit their further decline. Considering the challenges in detecting this species, a dual approach utilizing the targeted eDNA assay developed in this project and traditional survey methods with repeated sampling is recommended for future work. Accurate detection of this species, given its cryptic nature, depends on the timing of sampling, which, should occur following rainfall throughout the year.

CHAPTER 1

Background Information

BLACK-SPOTTED NEWT

The Black-spotted Newt (*Notophthalmus meridionalis*) is a small- to medium-sized salamander with granular skin and is characterized by an olive-green or grey-brown dorsum with yellow-gold broken dorsolateral bars and a bright orange-yellow venter. The entire body is covered with black spots, which are more apparent against the orange-yellow underside (Mecham 1968a). The historic range of this species extended from Victoria County, Texas, USA, south to the state of Veracruz, Mexico, along the Gulf of Mexico. Black-spotted Newt populations have been reported 30–50 km from the Gulf of Mexico (Rappole and Klicka 1991), although some specimens have been collected further inland (ca. 150–175 km; Taggart 1997; Carbajal-Marquez et al. 2014). Currently, two subspecies are recognized: the Texas Black-spotted Newt (*N. meridionalis meridionalis*), and the Mexican Black-spotted Newt (*N. meridionalis kallerti*). The Texas Black-spotted Newt occupies the northern extent of the species range that includes south Texas, USA and northern Tamaulipas, Mexico, while the Mexican Black-spotted Newt occupies the southern portion of the species range, consisting of northern Veracruz, eastern Puebla, eastern San Luis Potosi, and southeastern Hidalgo, Mexico. Additionally, the Mexican Black-spotted Newt is found at higher elevations (ca. 800 m elev.) in the Sierra Madre Oriental Mountains as well as low-elevation wetlands. Mecham (1968b) identified a zone of intergradation between the two subspecies in southern Tamaulipas, Mexico (ca. 22.75–23.4°N).

Throughout their range in the Tamaulipan Biotic Province, the Black-spotted Newt has been found in ephemeral ponds, resacas, roadside ditches, pools of small streams, and other quiet waters (Bishop 1947; Mecham 1968a). This ecosystem is unique in its climate and wildlife and is typically characterized by dense and thorny vegetation, such as Texas Ebony (*Ebenopsis ebano*), Retama (*Parkinsonia aculeata*), Spiny Hackberry (*Celtis ehrenbergiana*), Huisache (*Acacia farnesiana*), Prickly Pear (*Opuntia lindheimeri*), and Honey Mesquite (*Prosopis glandulosa*). Rainfall is irregular, both seasonally and annually (Gutzler 2004), and temperatures regularly exceed 37°C (Jahrsdoerfer and Leslie 1988), thus wildlife within this semi-arid environment must be adapted to drought and heat. Rappole and Klicka (1991) anecdotally reported that the Black-spotted Newt is well-suited to the harsh climate that it occupies, persisting for long periods of drought in an inactive or semi-active state. The Black-spotted Newt spends a considerable amount of time below ground, utilizing burrows and cracks in the soil (Rappole and Klicka 1991; Bare and Kline 2017). Rainfall is a likely cue for Black-spotted Newts to emerge to forage or reproduce as individuals have been seen moving across roads on rainy nights (Thornton 1977; Taggart 1997). The Black-spotted Newt is an opportunistic breeder, as eggs can be laid at any time of the year, although the activity of captive newts slowed considerably below 10°C indicating that individuals are less likely to reproduce during cooler winter months (Rappole and Klicka 1991). Female newts lay eggs (up to 300 at a time) that are attached singly or in small clusters to submerged vegetation (Altig and McDiarmid 2015); eggs hatch ca. 12–14 d after laying, thus considerable rainfall is required to fill ephemeral ponds that this species is thought to utilize for reproduction.

The Black-spotted Newt is considered a species of conservation concern by many agencies and organizations, including the IUCN which lists it as Endangered with the "current population trend" described as decreasing (Flores-Villela 2008), NatureServe which lists is as a G3 species, meaning

"Vulnerable" (NatureServe 2019), Texas Parks and Wildlife Department (TPWD) which lists it as Threatened (TPWD 2020) and Mexico's Secretary of Environment and Natural Resources which lists it as a species "in danger of extinction" (Flores and Herrera 2010). However, the Black-spotted Newt holds no status with the U.S. Fish and Wildlife Service (USFWS) under the Endangered Species Act, although Judd (1985), in a report to the USFWS Office of Endangered Species, suggested that it should be listed as threatened. The Black-spotted Newt is up for a listing decision by the USFWS in fiscal year 2024 (USFWS 2021).

One of the likely drivers for the decline of Black-spotted Newt populations is habitat loss and fragmentation, which has been implicated as the primary driver of biodiversity loss (Brooks 2002; Wilson et al. 2016). Amphibians are particularly affected by habitat loss due to their relatively low ability to move about their environment, high susceptibility to death when moving across roads or inhospitable landscapes, narrow habitat tolerances, and vulnerability to pathogens (Cushman 2006). South Texas, USA, has experienced significant habitat loss due to human activity (Jahrsdoerfer and Leslie 1988; Fulbright and Bryant 2002). In particular, >95% of native brushland in the Lower Rio Grande Valley (LRGV) has been cleared since the 1920s (Jahrsdoerfer and Leslie 1988). The clearing of land for agriculture, rangeland, roads, and urban development has served to fragment suitable Black-spotted Newt habitat; the remaining tracts of native brushland exist patchily throughout the LRGV, with most being maintained by federal and state agencies, nongovernmental organizations, and private entities. The LRGV is one of the most heavily farmed areas in the United States and agriculture serves as a direct threat to remaining Black-spotted Newt populations and their habitats (Jahrsdoerfer and Leslie 1988; Rappole and Klicka 1991). Dixon (2013) suggested that pesticide and herbicide usage adversely affect Black-spotted Newts, and although this has not been explicitly tested, Brühl et al. (2013) suggested that pesticide exposure is an underestimated driver of amphibian declines. Aside from the risk posed by agriculture, alteration of habitat on large cattle ranches has been suggested to negatively impact newt breeding habitat through the loss or conversion of ephemeral ponds or depressions into permanent cattle tanks (Rappole and Klicka 1991). This threat is most prevalent on large contiguous ranches that make up significant portions of several counties in south Texas including Brooks, Kenedy, Kleberg, and Jim Wells (Fulbright and Bryant 2002). Further, urbanization and the subsequent construction of roads causes direct and indirect threats to amphibians (Jochimsen et al. 2004) including the drainage and destruction of newt breeding habitat (Judd 1985). Hydrologic changes such as the damming of the Rio Grande for flood control and agriculture, have disrupted the natural flood-pulse cycle which, in the past, had created ephemeral wetlands and filled dried resacas that the Black-spotted Newt would utilize (Small et al. 2009).

HABITAT AND ENVIRONMENTAL CHARACTERISTICS

Understanding characteristics of the wetlands and surrounding uplands that amphibians utilize as breeding and non-breeding habitat are important to inform conservation efforts. Rappole and Klicka (1991) previously provided the most comprehensive account of Black-spotted Newt natural history, however, much of their report was anecdotal. Rappole and Klicka (1991) associated Black-spotted Newts with shallow, "clean", temporary, freshwater environments with a firm clay bottom. The same study indicated that the absence of Black-spotted Newts was associated with large, permanent water bodies greater than 2 m deep. Although Black-spotted Newts are most commonly associated with ephemeral water bodies (Mecham 1968a; Rappole and Klicka 1991), there are historic records in Texas from streams (e.g., Coleto Creek, Victoria County) and large permanent water bodies (e.g., Lake La Joya and Walker Lake, Hidalgo County). However, it is possible that

some of these specimens were collected from ephemeral sites nearby or adjacent to more the permanent, named water bodies, which is reflected in the catalogued specimen record. Rappole and Klicka (1991) suggested that the Black-spotted Newt is not associated with water bodies near agricultural fields or impacted by cattle. However, Black-spotted Newts have been recently collected along the periphery of agricultural fields (e.g., TNHC 116642) and rangeland ponds (e.g., TNHC 116644). Scott (1996) suggested that the Black-spotted Newt may be common on large cattle ranches that are difficult to access to conduct biological surveys (e.g., King Ranch, Yturria Ranch). Considering the variation in where Black-spotted Newts have been found, it is important to define the water body characteristics that this species utilizes in order to inform management and conservation efforts.

Water quality parameters can be important predictors of amphibian species richness and presence/absence. Hecnar and M'Closkey (1996) identified conductivity, total hardness, and turbidity as negative correlates of amphibian species richness. Lane et al. (2007) found that pH and salinity were important predictor variables for five Australian amphibian species. Rappole and Klicka (1991) reported salty or brackish water bodies with salinity greater than 1.0 PSU were not suitable for Black-spotted Newts. In ponds where Rappole and Klicka (1991) found Black-spotted Newts, the salinity ranged from 0.5–1.0 PSU. Further, Rappole and Klicka (1991) reported that Black-spotted Newts "avoid" water bodies with large amounts of agricultural runoff, which could be indicated by hypoxic conditions (Boyer and Grue 1995), nitrogen contamination (Rouse et al. 1999), and elevated conductivity (Egea-Serrano et al. 2012).

Floral and faunal associations can also be important predictors of amphibian presence/absence. Hecnar and M'Closkey (1997) showed that amphibian species richness decreased in ponds with predatory fish. However, Black-spotted Newts have been associated with the Western Tiger Salamander (*Ambystoma mavortium*) and Lesser Siren (*Siren intermedia*; Rappole and Klicka 1991). In the two localities where Judd (1985) found Black-spotted Newts, Lesser Sirens were present, and fish were absent. Rappole and Klicka (1991) reported water bodies with large fish were not suitable for Black-spotted Newts. Dodd (1993) reported that breeding ponds of a closely related species, Striped Newt (*Notophthalmus perstriatus*), generally do not contain predatory fish, however this is more likely a result of the unpredictable hydroperiod than an ecological interaction. Lane et al. (2007) found that ponds with a greater proportion of emergent vegetation had a greater diversity of amphibians. Black-spotted Newt presence has been associated with abundant aquatic vegetation, particularly rooted macrophytes (Rappole and Klicka 1991) and green algae of the genus *Chara* (Mecham 1968a).

Soil type and composition has been shown to be important for other amphibians (Loredo et al. 1996; Groff et al. 2014; Renan et al. 2017). Wyman (1988) found soil moisture impacted Eastern Newt (*Notophthalmus viridescens*) distribution in New York, USA. For Black-spotted Newts, soil parameters including pH and organic carbon content at the surface were found to be significant contributors to a constrictive Maxent distribution model (Bare 2018). Black-spotted Newts can spend a considerable amount of time beneath the surface of the soil during times of drought (Rappole and Klicka 1991; Bare 2018), and individuals have been found within cracks in the soil as deep as 20 cm (Rappole and Klicka 1991) and in artificial burrows up to 50 cm (Bare 2018). Rappole and Klicka (1991) also found Black-spotted Newts within crevices in clay soils adjacent to a drift fence, hypothesizing that such soils hold moisture and attract invertebrate prey. These cracks are likely important refugia for these newts as they are unable to burrow in clay soils. Rappole and Klicka (1991) associated Black-spotted Newts with Tiocano and Edroy clay soils with a firm bottom. Tiocano, Edroy, and similar soils make up 1% of Cameron County, 1.1% of

Hidalgo County, 1% of Willacy County, and 6.7% of Kenedy and Kleberg counties (USDA 2019). These soil types are characterized as deep and slowly draining with a slope of one percent or less (USDA 2013).

ENVIRONMENTAL DNA (eDNA)

Given the limited distribution of the Black-spotted Newt in south Texas, accurate detection of populations is essential to inform policy and conservation. Traditional survey methods have proved ineffective: Rappole and Klicka (1991) seined one pond on 20 separate occasions, detecting Black-spotted Newts only twice. Rappole and Klicka (1991) and Judd (1985) reported finding Black-spotted Newts by searching under debris that held moisture or by digging when such debris was absent. Bare (2018) and Bare and Kline (2020) detected Black-spotted Newts in crevices within dry soils using a borescope, which was moderately effective in times of drought. Despite some success with traditional survey techniques, more efficient sampling methodologies are required.

One promising methodology to survey for cryptic species is environmental DNA (eDNA), which describes DNA collected from the environment that originated from an organism's shed skin, feces, urine, or saliva (Ficetola et al. 2008). For aquatic or semi-aquatic organisms, water can be filtered and analyzed for the presence of species-specific DNA (Laramie et al. 2015). Collected DNA must be extracted before analysis, and extraction methods vary between studies from commercial kits to liquid phase separation using organic solvents (Tsuji et al. 2019). Extracted DNA is then amplified with species-specific primer sets using polymerase chain reaction (PCR) assays. Short-sequence mitochondrial DNA barcodes are generally used for species detection as longer fragments are more likely to degrade rapidly and mitochondrial DNA (mtDNA) is present at a greater copy number than nuclear DNA (Rees et al. 2014). Commonly targeted mtDNA genes include cytochrome b, cytochrome c oxidase subunit 1 (CO1), and 12s and 16s ribosomal RNA (Tsuji et al. 2019). Closely related species often have enough sequence divergence in the CO1 region to differentiate species (Herbert et al. 2003). To avoid amplifying DNA of non-target species, the designed primers should be tested both in-silico (using programs to compare sequences) and in-vitro through testing primers against tissue from target species as well as co-occurring closely related species (Bohmann et al. 2014). eDNA analysis can occur through either probe-based quantitative PCR (qPCR) methods (Goldberg et al. 2016) or through endpoint PCR in which amplified DNA is visualized for the presence of a fluorescent band of the appropriate size on an agarose gel and confirmed through sequencing the amplified product (Ficetola et al. 2008). Further specificity can be achieved through nested PCR, in which a second round of PCR is performed with primers "nested" within the amplified region from the first round (Nix et al. 2010; Jackson et al. 2017).

The bi-phasic lifestyle of most amphibians makes eDNA a powerful tool for their detection by taking advantage of aquatic reproduction and aquatic larval stages. eDNA allows for the non-invasive detection of rare or cryptic amphibians (Goldberg et al. 2016). Olson et al. (2012) used eDNA to detect the Eastern Hellbender (*Cryptobranchus alleganiensis alleganiensis*), a species of conservation concern that is typically surveyed with disruptive, high-effort snorkel surveys. Sasso et al. (2017) showed that eDNA assays can be more time-effective than traditional methods; four days of eDNA sampling allowed for the detection of 90% of aquatic or semiaquatic amphibian species that had been found during a long-term (five year) survey in the Brazilian Atlantic Forest. DeJean et al. (2012) found that eDNA (38 detections) can be more sensitive than traditional methodologies (seven detections with visual encounter and auditory surveys) for the American Bullfrog (*Rana catesbeiana*). While eDNA assays can have relatively high upfront costs including

primer development, sequencing non-target species, and laboratory equipment purchase (Smart et al. 2016), ultimately, they can be more cost-effective. Biggs et al. (2015) employed a Great Crested Newt (*Triturus cristatus*) eDNA assay at a large scale, utilizing citizen scientists to collect water samples, and found the initiative to be more than 10 times cheaper than traditional methods.

One major limitation to solely using eDNA is that researchers cannot directly observe animals to assess individual health, size, or reproductive status. Roussel et al. (2015) highlighted some of the deficiencies of eDNA surveys, namely that non-detection of target small fragments does not definitively mean that a species is absent from a given site as DNA could be present in small amounts or degraded below the detection threshold. While eDNA techniques can inform presence/absence, it is less effective at determining species abundance (Pilliod et al. 2013; Goldberg et al. 2015). Yates et al. (2019), in a meta-analysis, showed that eDNA concentrations are correlated to species abundance in laboratory experiments, however, in natural environments this linkage is much weaker. Future developments will likely allow for eDNA abundance estimates in the field, however, at this time, it is not reliable. False positives are another potential drawback that can occur due to contamination. To avoid laboratory contamination, DNA extractions and PCR set-ups should occur in separate locations from PCR machines. Field blanks are often used as a negative control for equipment contamination where deionized water is treated and filtered in the same manner as field-collected water (Goldberg et al. 2013). While eDNA has several benefits over traditional survey techniques, it cannot replace them completely. Thomsen et al. (2012) recommended eDNA as a complementary survey technique to traditional methodologies that can increase the likelihood of detection as well as the detection window for transient species.

METABARCODING

Presently, there are two popular eDNA survey strategies: targeted assays (e.g., Ruppert et al. 2022; Robinson et al. 2022) and metabarcoding assays (e.g., Lacoursière-Roussel et al. 2016; Valentini et al. 2016). Targeted assays are designed to specifically detect a single species and only that species. Targeted assays can be useful for early detection and monitoring of invasive species as well as monitoring the presence of rare or cryptic species (Ficetola et al. 2008; Dejean et al. 2012; Vörös et al. 2017). Targeted assays generally rely on qPCR or PCR and Sanger sequencing (Harper et al. 2018; Ruppert et al. 2022; Robinson et al. 2022). Metabarcoding assays are designed to detect groups of related taxa, such as all amphibians or even all vertebrates, and thereby are useful for examining community assemblages and generally rely on PCR and next-generation sequencing (NGS; Valentini et al. 2016; Sasso et al. 2017; Evans et al. 2017; Ruppert et al. 2019; Harper et al. 2020). NGS is required for metabarcoding assays because qPCR and PCR assays and Sanger sequencing are designed around detecting one-specific sequence and metabarcoding assays produce a variety of unique sequences that can all be read individually using a NGS platform (Valentini et al. 2016; Sasso et al. 2017; Evans et al. 2017; Ruppert et al. 2019). When considering results from metabarcoding assays, it is important to be mindful that certain primers can have a bias for particular species (or groups of species) based on primer affinity and that polymerases found in PCR master mixes can have an amplification bias towards certain sequence GC percentages. Both of these can skew DNA concentrations among different species and thus result in inaccurate abundance estimates (Fonseca 2018; Nichols et al. 2018; Beng and Corlett 2020).

HABITAT SUITABILITY MODELS

The use of habitat suitability models (HSMs), also commonly referred to as ecological niche models (ENMs), has increased dramatically in the past 20 years (Araújo et al. 2019; Peterson and

Soberón 2012), driven by their utility in estimating the distribution of suitable habitat for species based on the occurrence of abiotically suitable conditions in geographic space (Soberón and Peterson 2005; Hirzel et al. 2006; Peterson and Soberón 2012). HSMs are often used to provide estimates of species' potential distributions by modeling the fundamental niche, which describes species-environment relationships in the absence of biotic interactions or historical impediments to dispersal that limit their distribution (Hirzel et al. 2006; Hirzel and Le Lay 2008).

Improvements in model building, evaluation, and the quality of occurrence data has expanded the application of HSMs to a range of fields in recent years (Araújo et al. 2019). Increasingly, HSMs are used for diverse conservation purposes including selecting locations for new protected areas (Peterson 2006), identifying areas of high species richness (Rondinini et al. 2011), anticipating the spread of invasive species (Peterson 2003), and predicting distribution shifts in response to environmental change (Abrahms et al. 2017; Khwarahm et al. 2021). Despite not directly modeling species presence, presence-only HSMs exhibit similar predictive performance to methods explicitly designed for this purpose (Hirzel et al. 2006), and are used to guide surveys aimed at detecting previously unrecognized populations (Rhoden et al. 2017; Tronstad et al. 2018; Eyre et al. 2022).

We selected Maxent as the most suitable method to develop and project a predictive habitat suitability model for the Texas Black-spotted Newt. Maxent approximates the habitat distribution by finding the distribution of maximum entropy (closest to uniform) that satisfies the constraint that the expected mean of each environmental variable in the distribution matches its empirically observed average (Phillips et al. 2006). Maxent requires only presence data (Phillips et al. 2006), is robust to collinearity of predictor variables and sampling bias when corrective methods are employed (Phillips et al. 2009; Kramer-Schadt et al. 2013; Boria et al. 2014), and shows strong predictive performance when evaluated against independent presence/absence data (Elith et al. 2006), even with a small number of occurrence records (Pearson et al. 2007). Surveys guided by Maxent models have successfully detected previously unrecognized populations of cryptic amphibians (Groff et al. 2014), including those of conservation concern (Peterman et al. 2013), and geographically limited reptiles with few known occurrences (Pearson et al. 2007). Maxent's strong predictive performance using a limited number of presence-only records, its robustness to sampling bias and predictor correlation, and its utility for identifying new populations of similarly rare and cryptic amphibians make it an ideal method for modeling current and future distributions of suitable habitat for the Texas Black-spotted Newt to guide surveys for new populations and understand the potential effects of climate change on newt habitat.

PROJECT SCOPE

The Black-spotted Newt is a chronically understudied species. Further, challenges associated with international fieldwork have limited access to Mexico for research activities as was possible with past studies (e.g., Judd 1985; Rappole and Klicka 1991). There is a critical need to understand more about Black-spotted Newt distribution and habitat preferences throughout south Texas using both traditional survey methods, targeted eDNA assays, and eDNA metabarcoding techniques. The numerous threats to Black-spotted Newts, combined with their cryptic nature, pose an interesting research challenge. Is this species extirpated from much of its historic range and can novel survey methods and habitat suitability modeling help increase our understanding of this species? The goals of this research under this project were to:

1. Collect data to refine the Black-spotted Newt range map developed by Agency in 2017 for TPWD by identifying habitat characteristics, natural conditions and land management practices that are correlated with presence of the Black-spotted Newt via a robust, range-wide survey effort.
2. Refine and document repeatable, Black-spotted Newt environmental DNA ("eDNA") sampling methodology.
3. Address challenges to eDNA analysis caused by PCR inhibitors and provide protocols that will be useful to subsequent eDNA studies.
4. Address range-wide data gaps for the species.
5. Develop a range-wide predictive model for Black-spotted Newts by adding all data gathered in this study in conjunction with available spatial data from available sources.
6. Provide all Sharable Data to FWS to assist with the species status assessment of the Black-spotted Newt.

Data associated with this project are available at: https://doi.org/10.18738/T8/ARZS5G

CHAPTER 2

TASK 1. Creating a Black-spotted Newt occurrence database to inform field sampling and predictive modeling

OVERVIEW

Chapter 2 discusses how a Black-spotted Newt occurrence database was created and describes steps used in QA/QC and georeferencing. Previously, an occurrence database was created by Bare (2018) for purposes that included the creation of an initial habitat suitability model. However, this previous occurrence database overlooked several important sources of occurrence data and did not include full metadata concerning occurrence records, limiting its usefulness. Only verifiable specimen occurrence records are included given the verifiable nature of these sources. Important literature occurrence records are discussed, but are not formally included in this occurrence database. This chapter addresses Goals 1 (in part), 4 (in part), and 6 (in part) of the project.

METHODS

Queries for occurrence records of Black-spotted Newts were made through both museum aggregating platforms (e.g., VertNet, Arctos Database) and through direct queries with collection managers and curators of smaller collections. Both natural history collections and community science reporting platforms were queried. When needed, locality information was georeferenced using GEOLocate (www.geo-locate.org) or Google Earth Pro v7.3.4.8642 following MANIS/HerpNet/ORNIS Georeferencing Guidelines (available at: www.georeferencing.org/georefcalculator/docs/GeorefGuide.html). On occasion, descriptive localities were lacking, and occurrence records were unable to be georeferenced. Additionally, occurrence records with obscured GPS coordinates were included in the occurrence database, but never mapped due to their positional uncertainty.

RESULTS

Black-spotted Newt occurrence records were compiled from 34 different sources, which included 32 different natural history museums across the USA (n = 28), Canada (n = 2), and Europe (n = 2) and two citizen science reporting platforms (iNaturalist, HerpMapper; Table 2.1). The largest collection of Black-spotted Newt occurrence records is at the Biodiversity Collections, The University of Texas at Austin (TNHC), primarily due to holding the collections made by John Mecham in the 1960s as part of his studies on the species. iNaturalist had significantly more Black-spotted Newt occurrence records (n = 79) than did HerpMapper (n = 2), however, a large percentage (30.4%; n = 24 records) were unable to be mapped due to obscured or private GPS points. An additional 35 natural history collections of citizen science reporting platforms were also queried directly, but contained no Black-spotted Newt occurrence records (Table 2.2).

In total, 1006 Black-spotted Newt occurrence records were aggregated from throughout the species' range. Unfortunately, 54 occurrence records were unable to be mapped due to: 1) missing locality data, 2) locality information that was unable to be georeferenced, or 3) obscured GPS locations (iNaturalist occurrence records only). This resulted in 952 georeferenced specimen occurrence records (Figure 2.1). These occurrence records are from Texas, USA (n = 543; Figure 2.2), and Tamaulipas (n = 272), San Luis Potosí (n = 65), Puebla (n = 47), Veracruz (n = 24), and Hidalgo (n = 1), Mexico (Figure 2.1). Occurrence records spanned from 1896–2022.

DISCUSSION

The creation of a Black-spotted Newt occurrence database early as the start of our research efforts has helped to inform subsequent fieldwork (see Chapter 4) and habitat suitability modeling (see Chapter 7) conducted as part of this project. Previously, an occurrence database was created by Bare (2018) for purposes that include the creation of a habitat suitability model. However, this previous occurrence database overlooked several important sources of occurrence data and did not include full metadata concerning occurrence records, limiting its utility.

Though our database is larger and more complete than that of Bare (2018), areas for improvement remain. Notably, Black-spotted Newt occurrence records from Mexican institutions are lacking from our database as these collections are not publicly available through either VertNet or Arctos and correspondence has been challenging. Efforts to query museum collections across Mexico, particularly those within and near the range of the Black-spotted Newt, should continue.

Within Texas, Black-spotted Newt occurrence records were located across 13 counties (Figure 2.2). This distribution has two notable differences with the most recently published distribution map for Texas (Dixon 2013). The first difference is the addition of Live Oak County to our Texas distribution map (Figure 2.2). We discovered a series of six Black-spotted Newts part of the Oklahoma State University Collection of Vertebrates (OSU 848–853) that were collected in George West, Live Oak County in 1938. These six specimens represented a new county record for this species (Robinson et al. 2020) that was not reported by Dixon (2013), likely in part because specimen collection data for OSU is not provided on a museum aggregating platform (e.g., VertNet, Arctos Database).

The second difference is the exclusion of Starr County from our Texas distribution map, which has previously been included in maps since 2000 (Dixon 2000, 2013). Though specific reference to material is not provided for the inclusion of Starr County, it is likely based on Boundy (1994). In their publication, Boundy (1994) reported a series of four specimens from "Walker Lake" in Starr County (Louisiana Museum of Natural History, Louisiana State University [LSUMZ] 6827–6830), however this locality falls in Hidalgo County, though it is close to the Starr County line. Additionally, though not formally published, data on a museum specimen from La Joya Lake, Hidalgo County (American Museum of Natural History [AMNH] 182322) was incorrectly attributed to occurring in Starr County, but La Joya Lake occurs in Hidalgo County. This, there have been no verifiable records of Black-spotted Newts in Starr County. Irwin (1993) provides anecdotal evidence of a record from southeastern Starr County and there is anecdotal evidence of an observation along Old Military Highway, south of Buena Vista in southeastern Starr County (C. Roelke, pers. comm.). Until verifiable records of Black-spotted Newts from Starr County are provided, we recommend that distribution maps exclude it as part of the species' recognized range.

One trend which resulted from the creation of this occurrence database is that since 2000, Black-spotted Newts have only been observed in the three southernmost counties of Texas: Willacy, Hidalgo, and Cameron (Figure 2.2). Despite abundant records from the late-1970s and 1980s from Kleberg and Kenedy counties, no additional records of this species from recent decades are known. Though the exact reason for the absence of recent records, particularly in places where Black-spotted Newts previously seemed abundant, is troubling.

Table 2.1. List of natural history collections and citizen science reporting platforms that were queried that contained Black-spotted Newt occurrence records. Collection acronym, name, and number of records are provided.

Collection Acronym	Collection Name	# of Records
AMNH	American Museum of Natural History	116
ANSP	Academy of Natural Sciences of Drexel University	5
ASNHC	Angelo State Natural History Collections, Angelo State University	7
CHAS	Peggy Notebaert Nature Museum, Chicago Academy of Sciences	1
CM	Carnegie Museum of Natural History	5
CUMV	Cornell University Museum of Vertebrates	2
DRD	Drew R. Davis Field Series	24
EAB	Evan A. Bare Field Series	79
FMNH	Field Museum of Natural History	23
HM	HerpMapper	2
iNat	iNaturalist	79
KU	Biodiversity Institute, University of Kansas	34
KUDA	Kansas University Digital Archives	1
LACM	Natural History Museum of Los Angeles County	7
LSUMZ	Louisiana Museum of Natural History, Louisiana State University	51
MCZ	Museum of Comparative Zoology, Harvard University	8
MNHN	Muséum national d'Histoire naturelle	4
MVZ	Museum of Vertebrate Zoology, University of California at Berkeley	4
OSU	Oklahoma State University Collection of Vertebrates	7
RBINS	Royal Belgian Institute of Natural Sciences	1
ROM	Royal Ontario Museum	1
SMBU	Mayborn Museum Complex, Strecker Museum, Baylor University	23
TCWC	Biodiversity Research and Teaching Collections, Texas A&M University	18
TNHC	Biodiversity Collections, The University of Texas at Austin	333
UAMZ	University of Alberta	1
UF	Florida Museum of Natural History, University of Florida	21
UIMNH	University of Illinois Museum of Natural History	53
UMC	Univeristy of Missouri, Columbia	9
UMMZ	Museum of Zoology, University of Michigan	15
USNM	Smithsonian Institution, National Museum of Natural History	53
UTA	Amphibian and Reptile Diversity Research Center, University of Texas at Arlington	15
UTEP	University of Texas at El Paso Biodiversity Collections	1
WWF	Welder Wildlife Foundation	1
YPM	Peabody Museum of Natural History, Yale University	1

Table 2.2. List of natural history collections and citizen science reporting platforms that were queried that did not contain any Black-spotted Newt occurrence records. Collection acronym and name are provided.

Collection Acronym	Collection Name
ASNHC	Angelo State Natural History Collections, Angelo State University
ASU	Arkansas State University
AUM	Auburn University Museum of Natural History
BYU	Monte L. Bean Life Science Museum, Brigham Young University
CAS	California Academy of Sciences
CRCM	Charles R. Conner Museum, Washington State University
CUSC	Campbell Museum of Natural History, Clemson University
DURC	Drake University Vertebrate Collections
ENMU	Eastern New Mexico University
ESU	Emporia State University
FHSM	Sternberg Museum of Natural History, Fort Hayes State University
HERP	Herpetological Education and Research Project (H.E.R.P.)
INHS	Illinois Natural History Survey
ISU	Iowa State University
JFBM	James Ford Bell Museum, University of Minnesota
MPM	Milwaukee Public Museum
MSB	Museum of Southwestern Biology, University of New Mexico
MSUM	Michigan State University Museum, Michigan State University
NCSM	North Carolina Museum of Natural Sciences
OMNH	Sam Noble Oklahoma Museum of Natural History, University of Oklahoma
PSM	James R. Slater Museum of Natural History, University of Puget Sound
SDNHM	San Diego Natural History Museum
SDSM	Museum of Geology, South Dakota School of Mines
SDSU	South Dakota State University
SRSU	Sul Ross State University
UCM	Museum of Natural History, University of Colorado
UCM	University of Central Missouri
UCO	University of Central Oklahoma
UMM	University of Minnesota, Morris
UMNH	Utah Museum of Natural History
UNC	University of Northern Colorado
UNSM	University of Nebraska State Museum, University of Nebraska-Lincoln
UWSP	Museum of Natural History, University of Wisconsin-Stevens Point
UWZM	University of Wisconsin Zoological Museum
VMUNK	University of Nebraska at Kearney Vertebrate Museum

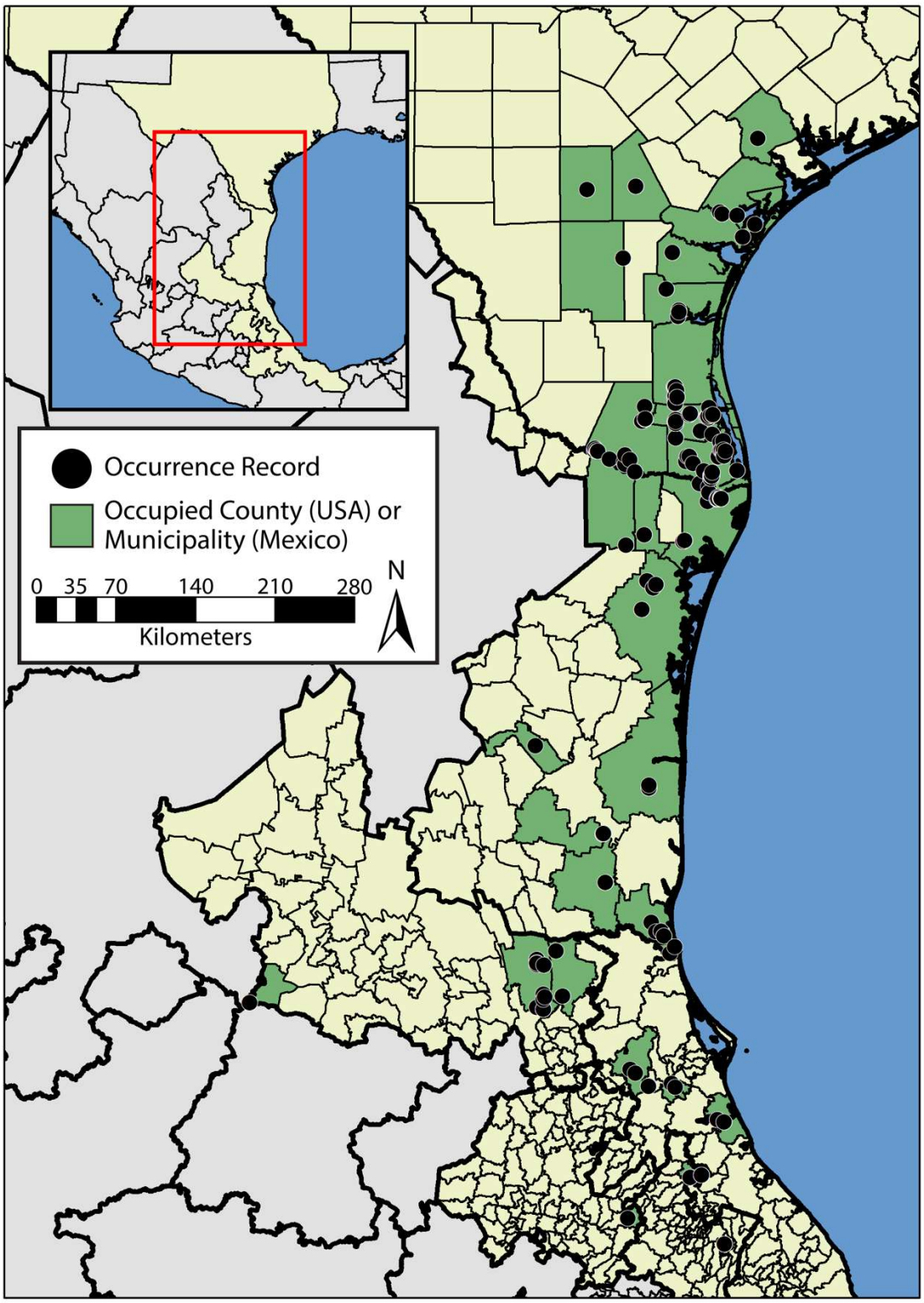

Figure 2.1. Occurrence records (black circles) of the Black-spotted Newt in Texas, USA, and northeastern Mexico. Green shading indicates counties (USA) or municipalities (Mexico) where records of newts are located. Bold lines indicate state boundaries.

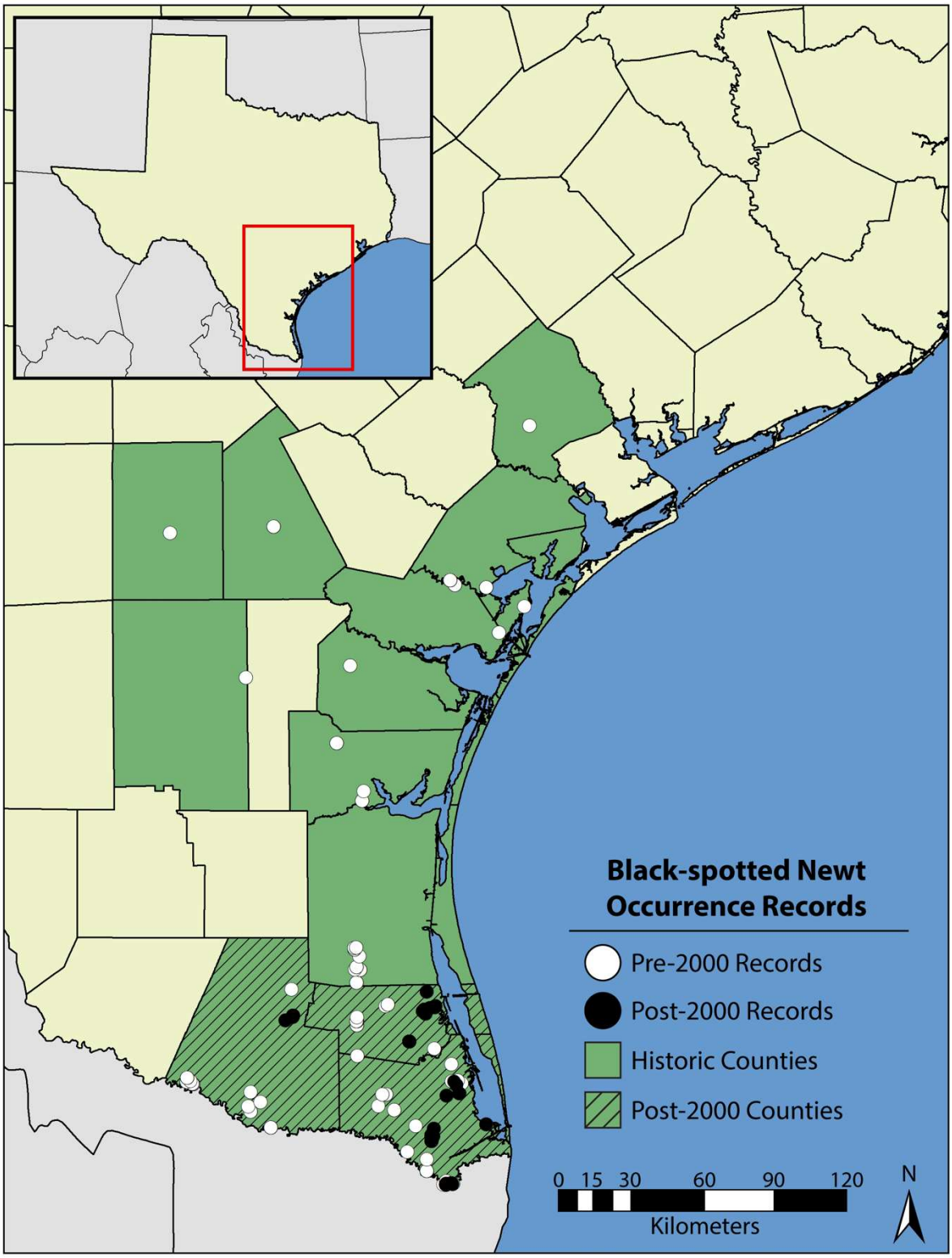

Figure 2.2. Occurrence records (circles) of the Black-spotted Newt in Texas, USA, showing pre- (white) and post-2000 records (black). Green counties indicate where records of newts are located and hashed counties are those where post-2000 occurrence records exist.

CHAPTER 3

TASK 2. Development and validation of an environmental DNA (eDNA) assay to detect Black-spotted Newts

OVERVIEW

Chapter 3 focuses on the development and validation of an environmental DNA (eDNA) assay for use in fieldwork to screen water samples for the presence of Black-spotted Newts. The development of the eDNA assay includes primer development, filter extraction and PCR optimization, and a comparison of gels stains used when visualizing the results. Assay validation included testing the developed primers with tissue from the Black-spotted Newt and other sympatric amphibians to ensure primer sensitivity and specificity, eDNA from captive settings, and eDNA from field-collected samples. This chapter addresses Goals 2, 3, and 6 (in part) of the project. Portions of this chapter were published in Robinson (2021) and Robinson et al. (2022).

METHODS

Extraction Protocol.—Previous work in our laboratory utilized a chloroform-based DNA extraction protocol (Bare 2018; Bogolin 2020), however, Ruppert (2020) suggested that PCR inhibitors were not fully removed from eDNA samples that were taken to detect the Lesser Siren (*Siren intermedia*), which occupy similar water bodies as Black-spotted Newts across south Texas. To determine the most efficient DNA extraction protocol, we tested the previously used chloroform extraction protocol, a phenol-chloroform extraction combined with a chemical cocktail to remove inhibitors (PC-CTAB), a modified PC-CTAB double extraction, and later, a modified extraction using the Epoch GenCatch Blood and Tissue Genomic Mini-Prep Kit (herein referred to as Epoch; Epoch Life Science, Missouri City, TX, USA). Extraction protocols are detailed in Appendix A. Extraction protocols were tested in conjunction with a commercial inhibitor removal kit (IRK), either the Zymo OneStep PCR Inhibitor Removal Kit (Zymo Research, Irvine, CA, USA) or the NucleoSpin Inhibitor Removal Kit (Macherey-Nagel, Düren, DEU). Extraction protocols were tested with water collected from an aquarium with ca. 30 L of water housing seven captive Black-spotted Newts at the Gladys Porter Zoo (GPZ) and diluted either with de-ionized (DI) or field-collected (F) water which should contain PCR inhibiting compounds based on previous sampling efforts.

For each extraction protocol, following sample filtration (1 L of water passed through a 25–30 μm pore size cellulose filter; described in more detail in Chapter 4), the filter papers were folded and placed in a 2-mL microcentrifuge tube containing 700 μL of DNAzol, where they remained at room temperature for at least 3 d. To reduce cross-contamination, filter extraction occurred in a fume hood, physically separate from PCR machines. As a negative control, the blank filter (the filter where only DI water was passed through it) was extracted in the same manner as the test samples. Each tube was heated at 55°C for 30 min in a heat bath, vortexed, and centrifuged at 5000 rpm for 2 min. Using forceps cleaned with bleach and rinsed with DI water, the filters slightly raised out of the tube and squeezed to remove DNAzol that had been absorbed by the filter and the filter was discarded. For field sites where three replicates were collected (where each replication was 1 L of field-collected water passed through each filter separately), the remaining DNAzol from each tube was then pooled in a 5-mL centrifuge tube (pooling did not occur for the field blanks). Gloves were discarded after all filters from a site had been pooled, and new gloves and forceps were used for each set of filters. Then, 600 μL from the pooled DNAzol was added to a

sterile 1.7-mL sterile microcentrifuge tube and extraction then occurred following one of the extraction protocols described in Appendix A. For a subset of extracted samples, eluted DNA was run through an IRK (following the manufacturer protocol) into a new 1.7-mL microcentrifuge tube. All extracted DNA was stored at -20°C until subsequent analyses.

Primer Design, Sensitivity, and Specificity.—Primers were designed based on the published mitochondrial genome for the Black-spotted Newt available on GenBank (accession numbers: MH367840.1, MH367841.1, MH367842.1, MH367843.1, MH367844.1). The cytochrome c oxidase subunit 1 (CO1) region within the mitochondrial genome is often used in eDNA assays (Tsuji et al. 2019). Accordingly, we designed primers to amplify a small segment (<200 base pairs [bp]) corresponding to the Black-spotted Newt CO1 gene. Primers were designed using Primer3 software and adjusted manually to create primers of similar length (19–21 bp) with similar melting temperatures (T_m) and guanine-cytosine (GC) content. In order to increase the sensitivity of the assay, nested primers were designed. The Eurofins Oligo Analysis Tool was used to check primers for hairpin loops and primer dimers, and these were avoided where possible. Primers were then analyzed in vitro, by optimizing annealing temperatures with dilute Black-spotted Newt tissue, and then by testing against dilute DNA extracts from the 32 potentially sympatric amphibians from south Texas (Table 3.1).

PCR Conditions.—PCR was performed using a T100 ThermoCycler (Bio-Rad Laboratories, Hercules, CA, USA). For each reaction, 12.5 µL GoTaq G2 HotStart MasterMix (Promega Corporation, Madison, WI, USA), 0.5 µL of 1 µM forward and reverse primers (Table 3.2), 5 µL of extracted sample, and 6.5 µL of nuclease-free water was added to a 0.2-mL PCR tube. To detect potential laboratory contamination or non-specific PCR products, a no-template control (NTC) was run in conjunction with other samples, where we used 5 µL molecular-grade water instead of extracted sample. These tubes were then run through the first round of PCR. For nested PCR, the product from the first round was purified with Exo-CIP Rapid PCR Cleanup Kit (herein referred to as Exo-CIP; New England Biolabs, Ipswich, MA, USA) and then used for the second round of PCR, which was set up as described above, but with a nested primer set (Table 3.2). Following the completion of the PCR, 20 µL of the PCR product was run on a 2% agarose gel for 40 min at 100 volts alongside a 50 bp GeneRuler ladder (Thermo Fisher Scientific, Waltham, MA, USA). The gel was visualized using a UVP transilluminator. The remaining 5 µL of PCR product was purified using Exo-CIP, combined with 5µL of 1 µM reverse primer (BSN_CO1_RV_7; Table 3.2), and sent to Eurofins Genomics (Louisville, KY, USA) for Sanger sequencing to confirm the presence of Black-spotted Newt DNA.

Gel Stain.—Ethidium bromide (EtBr) is a widely used intercalating agent that is used in DNA visualization for gel electrophoresis. However, EtBr is thought to be toxic and potentially mutagenic (Helfgott and Kallenbach 1979). EtBr and a commercial alternative GelRed Nucleic Acid Stain (herein referred to as GelRed stain; Biotium Inc., Hayward, CA, USA) were tested using a dilution series of PCR-amplified Black-spotted Newt DNA from tissue samples to compare the ability of each stain to visualize the results of PCR.

Validation.—Validation of the sensitivity and specificity of the primers as well as the extraction protocol occurred using field-collected water samples collected from a site in Willacy County where Black-spotted Newts were directly observed in the water. Water from this pond was

collected and filtered on-site. Three aliquots (up to 1 L) were filtered through a sterile 47-mm diameter, Grade 4 (25–30 μm pore size) Whatman cellulose filter and preserved in DNAzol (Molecular Research Center Inc., Cincinnati, OH, USA). After 3 d in DNAzol, the filters were squeezed, pooled, and extracted with the Epoch extraction protocol with and without each IRK, and then through the initial and nested rounds of PCR. From the nested PCR product, 20 μL was visualized on an agarose gel and 5 μL was purified and sent for Sanger sequencing as described previously.

RESULTS

Extraction Protocol.—Initial testing showed that the chloroform extraction performed better than the PC-CTAB extraction and a PC-CTAB double extraction (Figure 3.1). Combining the chloroform protocol with an IRK allowed for detection of Black-spotted Newt DNA in samples diluted with field water with the presence of potential inhibitors (Figure 3.1), showing that the chloroform extraction alone did not sufficiently remove inhibitors. In the GPZ:F 1:300 samples, the Epoch + IRK extraction protocol produced a brighter band for than the chloroform + IRK protocol (Figure 3.2). There were no bands visible for either protocol when an IRK was not used (Figure 3.2). In subsequent testing, more dilute samples (GPZ:F 1:500; GPZ:F 1:1000) extracted with the Epoch + IRK protocol produced a band of the correct size when run through the nested primer set. These samples were sent for Sanger sequencing and were a 100% match for Black-spotted Newt when queried on GenBank. The Epoch + IRK extraction protocol was the most efficient at capturing small amounts of DNA and removing potential PCR inhibitors.

Primer Design, Sensitivity, and Specificity.—A nested primer set (initial: BSN_CO1_6; nested: BSN_CO1_7) was designed (Table 3.2) and Sanger sequencing for dilute Black-spotted Newt DNA amplified and matched the correct sequences when queried on GenBank. The initial and nested primer sets were optimized with dilute Black-spotted Newt DNA (ca. 0.1, 1.0 pg/μL) using a temperature gradient in which the annealing temperature of the PCR was varied (Figure 3.3). The BSN_CO1_6 primers for the initial round of PCR produced the brightest band at an annealing temperature of 55.5°C (Figure 3.3A). For the nested round, using the BSN_CO1_7 primer set, another temperature gradient was run with a lower concentration of tissue that had been amplified and purified following the initial round of PCR, and there was only amplification at an annealing temperature of 53°C (Figure 3.3C). These annealing temperatures were used for all subsequent rounds of PCR.

In the sympatric species tests, following the initial round of PCR, there was no amplification for all 32 species tested. Following the nested round of PCR, no samples produced a band of the correct size (Figure 3.4) except for the congeneric Eastern Newt (*N. viridescens*; Figure 3.4A). The purified PCR product from the Eastern Newt sample was sent for Sanger sequencing, and when the resulting sequence was queried on GenBank, it was a 97.26% match for Eastern Newt and there was no significant similarity to Black-spotted Newt.

Gel Stain.—The EtBr allowed for visualization for only the highest concentration (ca. 100 pg/μL; Figure 1A) while the GelRed stain allowed for visualization of bands of Black-spotted Newt DNA at all concentrations tested (ca. 100, 10, and 1 pg/μL; Figure 1B). It should be noted that the GelRed stain also visualizes excess primer, which is the lower broad band (<50 bp; Figure 1B).

Validation.—At one sampling location in Willacy County, eight Black-spotted Newts were captured in the water. The eDNA samples that were collected and filtered from this pond were used to validate this assay under real field conditions. The filters extracted without the use of an IRK produced no visible bands (Figure 3.6A), while extraction combined with use of a Zymo IRK (Figure 3.6B) and NucleoSpin IRK (Figure 3.6C) produced bright bands. These samples were then sent for Sanger sequencing and were a 100% match for Black-spotted Newts when queried on GenBank.

DISCUSSION

The designed nested primers successfully amplified Black-spotted Newt DNA at low concentrations. The Epoch extraction combined with an IRK (either Zymo or NucleoSpin) successfully captured Black-spotted Newt DNA and removed PCR inhibitors from both positive control samples and samples collected under natural conditions from a field site. Finally, the more sensitive GelRed gel stain decreased the chances of false negatives from field samples. Taken together, the results of this study lend confidence to the utility of this assay to detect Black-spotted Newt eDNA from field samples.

Both the initial (BSN_CO1_6) and nested (BSN_CO1_7) primers were capable of amplifying dilute Black-spotted Newt DNA from tissue extracts at a concentration of ca. 1 pg/µL, and the BSN_CO1_7 primers amplified tissue at a concentration of ca. 0.1 pg/µL. eDNA assays must be capable of capturing small amounts of DNA from the environment, as DNA concentrations in the environment can be as low as 0.2 pg/µL (Pilliod et al. 2013), and these experiments showed that the designed primers are sensitive to low concentrations of DNA.

This primer sensitivity came at the expense of specificity as the nested primers amplified both Black-spotted Newt and Eastern Newt DNA. However, Black-spotted Newts and Eastern Newts are only known to co-occur at one historic locality (Welder Wildlife Foundation, Big Lake [San Patricio County]), but neither species has been observed there since the 1960s. The ranges of the two species overlap near the northern edge of the Black-spotted Newt historic range (Mecham 1967, 1968b). Within this area, Eastern Newts have been found in only two counties: San Patricio (mentioned above) and Victoria (Dixon 2013). The San Patricio record represents one Eastern Newt, and the Victoria records indicate that Eastern Newts were most recently found in the county in 1915 (National Museum of Natural History, Smithsonian Institution [USNM] 78503–78507), so the amplification of Eastern Newt DNA from field samples is unlikely. If these primers are used in future studies, Sanger sequencing allows for the differentiation between sites where Black-spotted Newt are present and false positives that amplified Eastern Newt DNA.

The described Epoch extraction protocol combined with an IRK was the most effective extraction method of the ones tested in this study. To the best of our knowledge, this extraction method has not been used in any other eDNA studies. Other commercial kits are commonly used, namely two extraction kits from Qiagen (DNeasy Blood and Tissue Extraction Kit and PowerWater DNA Extraction Kit; Tsuji et al. 2019). In recent years, liquid phase separation methods have increasingly been used in eDNA studies (Tsuji et al. 2019). The three such methodologies tested in this study (chloroform, PC-CTAB, PC-CTAB double extraction) were less effective at capturing dilute DNA. However, Renshaw et al. (2015) found that samples extracted with a phenol-chloroform isoamyl extraction produced a greater copy number than commercial kits. The liquid phase separation methods tested here were significantly cheaper than the commercial kits, however, the PC-CTAB and PC-CTAB double extractions took longer (>6 h) compared to the chloroform and Epoch (ca. 4 h). Further, the liquid separation methods dealt with

potentially harmful chemicals including chloroform (chloroform extraction, PC-CTAB double extraction) and phenol-chloroform and β-mercaptoethanol (PC-CTAB, PC-CTAB double extraction). β- mercaptoethanol breaks down organic compounds, including potential PCR inhibitors such as humic acids (Wilson 1997; Hunter et al. 2019), which are not always removed from commercial DNA extraction kits. For our purposes, the Zymo IRK and NucleoSpin IRK removed potential inhibitors from field samples, however, these are more expensive per sample than chemicals such as β-mercaptoethanol.

Some studies have suggested that EtBr may not be as mutagenic as previously thought and may only be toxic in volumes much beyond what is typically used in the laboratory (Singer et al. 1999; National Toxicology Program 2022). Regardless of the potential toxicity, GelRed stain was found to be much more sensitive than EtBr at detecting PCR-amplified product from dilute DNA samples. In endpoint PCR analyses, using a less sensitive stain such as EtBr could cause false negatives where the target species is incorrectly determined absent from sites that it occupies.

Table 3.1. List of specimens and tissue samples we used to test our Black-spotted Newt (*Notophthalmus meridionalis*) primers against to optimize specificity. Family and species names are provided along with the museum catalog number associated with the sample. Counties where each specimen was collected in Texas, USA are provided for all specimens except a single species (*Rana areolata*: TNHC 14318), which lacks locality information. DRD = Drew R. Davis Field Series; TNHC = Biodiversity Collections, The University of Texas at Austin. Gel-Lane information corresponds to Figure 3.4.

Family	Species	County	Catalog Number	Gel-Lane
Salamandridae	*Notophthalmus meridionalis*	Willacy	TNHC 116644	G-2
Salamandridae	*Notophthalmus meridionalis*	Willacy	TNHC 116645	G-4
Salamandridae	*Notophthalmus meridionalis*	Cameron	DRD 5165	G-6
Salamandridae	*Notophthalmus viridescens*	Harris	TNHC 116646	A-3
Ambystomatidae	*Ambystoma mavortium*	Cameron	TNHC 114655	A-6
Ambystomatidae	*Ambystoma texanum*	Limestone	TNHC 113097	A-5
Sirenidae	*Siren intermedia*	Cameron	TNHC 116624	A-4
Bufonidae	*Anaxyrus debilis*	Jeff Davis	TNHC 67333	F-2
Bufonidae	*Anaxyrus punctatus*	Val Verde	TNHC 116627	F-3
Bufonidae	*Anaxyrus speciosus*	Kenedy	TNHC 112166	B-2
Bufonidae	*Anaxyrus woodhousii*	Austin	TNHC 55521	E-7
Bufonidae	*Incilius nebulifer*	Cameron	TNHC 112149	B-5
Bufonidae	*Rhinella horribilis*	Willacy	TNHC 114653	D-2
Eleutherodactylidae	*Eleutherodactylus cystignathoides*	Cameron	TNHC 116629	F-5
Hylidae	*Acris blanchardi*	La Salle	TNHC 116625	C-4
Hylidae	*Hyla chrysoscelis*	Edwards	TNHC 113477	D-5
Hylidae	*Hyla cinerea*	Matagorda	TNHC 116640	C-5
Hylidae	*Hyla squirella*	Aransas	TNHC 116641	C-7
Hylidae	*Hyla versicolor*	Karnes	TNHC 60516	E-5
Hylidae	*Pseudacris clarkii*	Cameron	TNHC 116647	C-6
Hylidae	*Pseudacris fouquettei*	Liberty	TNHC 65745	E-3
Hylidae	*Pseudacris streckeri*	Travis	TNHC 67424	E-4
Hylidae	*Smilisca baudinii*	Cameron	TNHC 114656	C-2
Leptodactylidae	*Leptodactylus fragilis*	Zapata	TNHC 114657	F-4
Microhylidae	*Gastrophryne carolinensis*	Aransas	TNHC 116632	D-6
Microhylidae	*Gastrophryne olivacea*	Hidalgo	TNHC 112082	B-4
Microhylidae	*Hypopachus variolosus*	Hidalgo	TNHC 112004	B-6
Ranidae	*Rana areolata*	–	TNHC 14318	E-2
Ranidae	*Rana berlandieri*	Cameron	TNHC 112113	B-7
Ranidae	*Rana catesbeiana*	Refugio	TNHC 114658	C-3
Ranidae	*Rana sphenocephala*	Matagorda	TNHC 116648	D-7
Rhinophrynidae	*Rhinophrynus dorsalis*	Starr	TNHC 114654	D-3
Scaphiopodidae	*Scaphiopus couchii*	Cameron	TNHC 112175	B-3
Scaphiopodidae	*Scaphiopus hurteri*	Gonzales	TNHC 116649	D-4
Scaphiopodidae	*Spea bombifrons*	Winkler	TNHC 60528	E-6

Table 3.2. Semi-nested primer set used for in developing an environment DNA (eDNA) assay for the Black-spotted Newt (*Notophthalmus meridionalis*). Primers were designed to amplify a region of the cytochrome c oxidase subunit 1 mitochondrial gene. Melting temperature (T_m), GC content (GC), nucleotide length (nt), and amplicon length are provided for each primer. The underlined sequence (ACACC) is included in both the BSN_CO1_6 and BSN_CO1_7 primer sets.

Primer Set	Primer	T_m (°C)	GC (%)	nt	Amplicon Length
BSN_CO1_6	BSN_CO1_FW6	62.6	52.4	21	181
	BSN_CO1_RV6.1	62.3	57.9	19	
BSN_CO1_7	BSN_CO1_FW7.1	58	47.4	19	122
	BSN_CO1_RV7	58	47.4	19	

Amplified sequence for BSN_CO1_6 and BSN_CO1_7 primer sets

GTAGACCTGAATGTGGACACCCGAGCCTATTTTACATCAGCCACAATAATTATTGC
AATTCCAACAGGAGTAAAAGTATTTAGCTGACTCGCAACAATACACGGAGGATCAA
TTAAGTGAGATGCTGCAATACTATGGGCCTTAGGCTTTATTTTCTTATTTACAGTGG
GAGGGCTTACAG

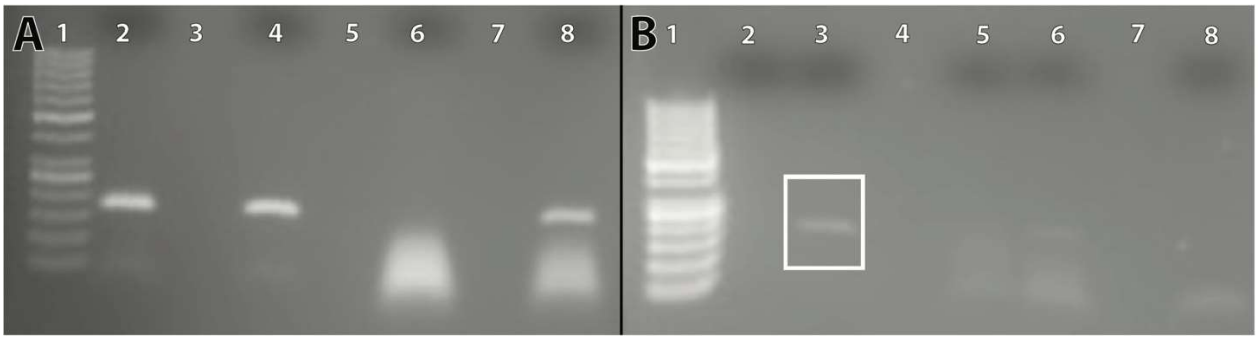

Figure 3.1. Comparison of extraction methods on PCR amplification: A) chloroform extraction; B) PC-CTAB and PC-CTAB double extraction. For gel A, Lane 1 = 50 bp ladder, Lane 2 = GPZ:DI 1:20 chloroform, Lane 4 = GPZ:DI 1:20 chloroform + IRK, Lane 6 = GPZ:F 1:20 chloroform, and Lane 8 = GPZ:F 1:20 chloroform + IRK (Lanes 3, 5, and 7 are empty). When GPZ water was combined with field water, the addition of an IRK following chloroform extraction removed inhibitors that prevented PCR amplification (see gel A, Lane 6 vs. Lane 8). For gel B, Lane 1 = 50 bp ladder, Lane 2 = GPZ:DI 1:20 PC-CTAB, Lane 3 = GPZ:DI 1:20 PC-CTAB double, Lane 5 = GPZ:F 1:20 PC-CTAB modified, Lane 6 = GPZ:F 1:20 PC-CTAB double, Lane 8 = NTC (Lanes 4 and 7 are empty). Note the faint band within the white box for the GPZ:DI 1:20 PC-CTAB double extraction. GPZ = Black-spotted Newt aquarium water from the Gladys Porter Zoo; DI = deionized water; F = water from a field site; IRK = inhibitor removal kit; NTC = no-template control.

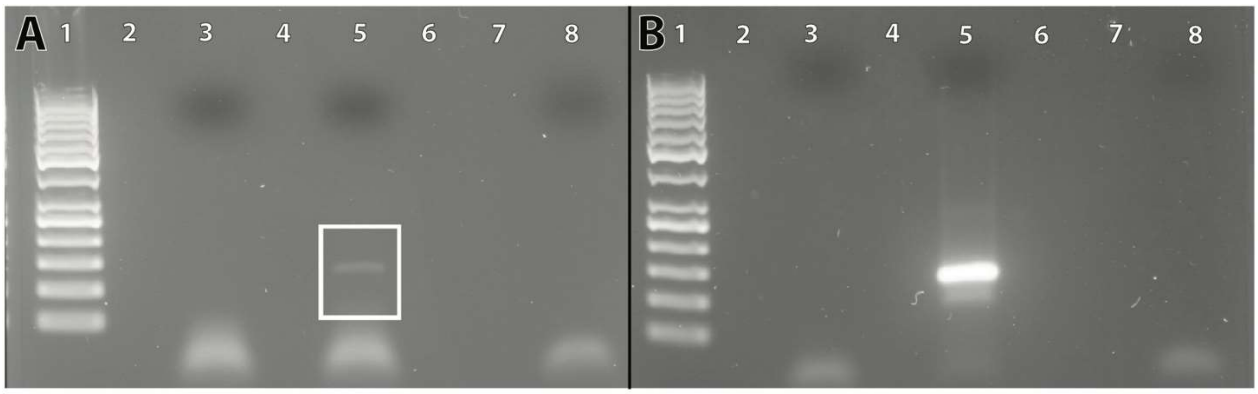

Figure 3.2. Comparison of extraction methods on nested PCR amplification: A) chloroform and chloroform + IRK; B) Epoch and Epoch + IRK. For gel A, Lane 1 = 50 bp ladder, Lane 3 = GPZ:F 1:300 chloroform, Lane 5 = GPZ:F 1:300 chloroform + IRK, and Lane 8 = NTC (Lanes 2, 4, 6 and 7 are empty). Note the faint band only for GPZ:F 1:300 chloroform + IRK (white square). For gel B, Lane 1 = 50 bp ladder, Lane 3 = GPZ:F 1:300 Epoch, Lane 5 = GPZ:F 1:300 Epoch + IRK, and Lane 8 = NTC (Lanes 2, 4, 6, and 7 are empty). There was only amplification when an IRK was used and the Epoch + IRK produced a brighter band than chloroform + IRK. GPZ = Black-spotted Newt aquarium water from the Gladys Porter Zoo; DI = deionized water; F = water from a field site; IRK = inhibitor removal kit; NTC = no-template control.

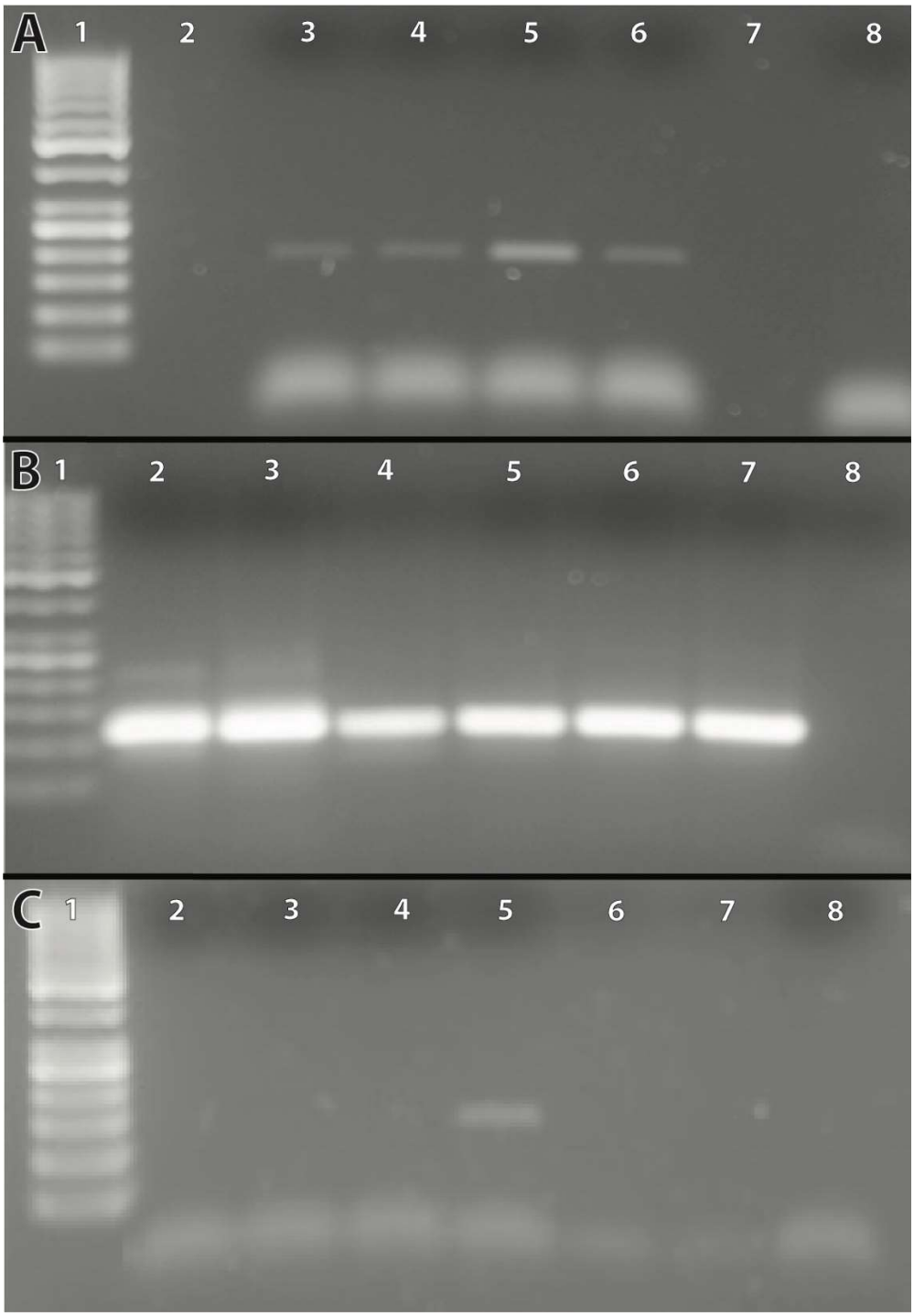

Figure 3.3. Temperature gradients for nested primers using ca. 1 pg/µL Black-spotted Newt tissue: A) BSN_CO1_FW6 + BSN_CO1_RV6.1; B) BSN_CO1_FW7.1 + BSN_CO1_RV7; C) BSN_CO1_FW7.1 + BSN_CO1_RV7. For all gels, Lane 1 = 50 bp ladder and Lane 8 = NTC. In gel A, temperatures are: Lane 3 = 59°C, Lane 4 = 57°C, Lane 5 = 55.5°C (which produced the brightest band), and Lane 6 = 54°C (Lanes 2 and 7 are empty). In gels B and C, temperatures are 56, 55, 54.1, 52.9, 52, and 51°C in Lanes 2–7, respectively. NTC = no-template control.

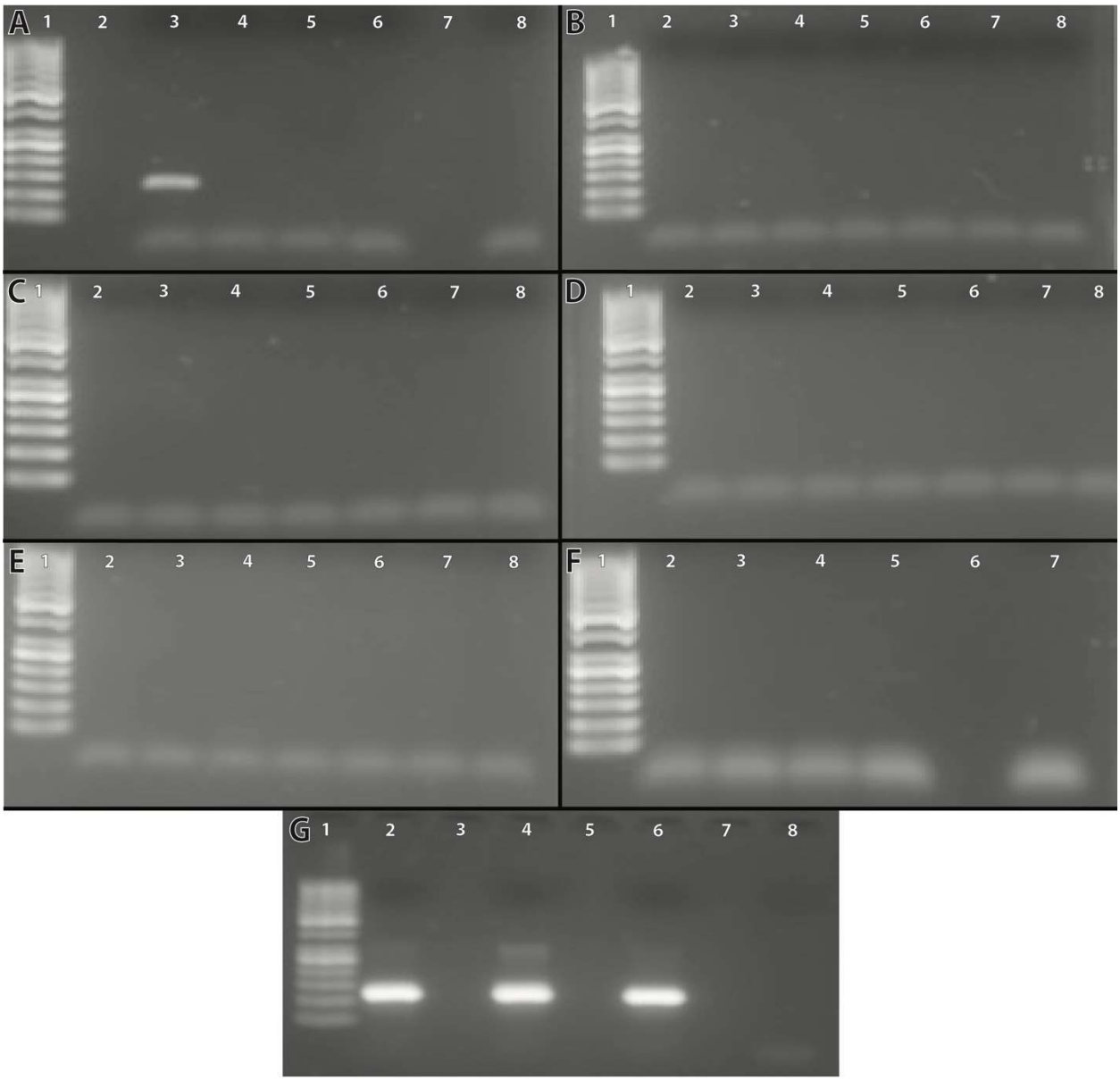

Figure 3.4. Sympatric species test with nested primer set: A) Caudata; B–F) Anura; and G) Black-spotted Newts from three different localities. In all gels, Lane 1 = 50 bp ladder. In gels A–E and G, Lane 8 = NTC; in gel F, Lane 7 = NTC. Complete species information, gel number, and lane number are included in Table 3.1. NTC = no-template control.

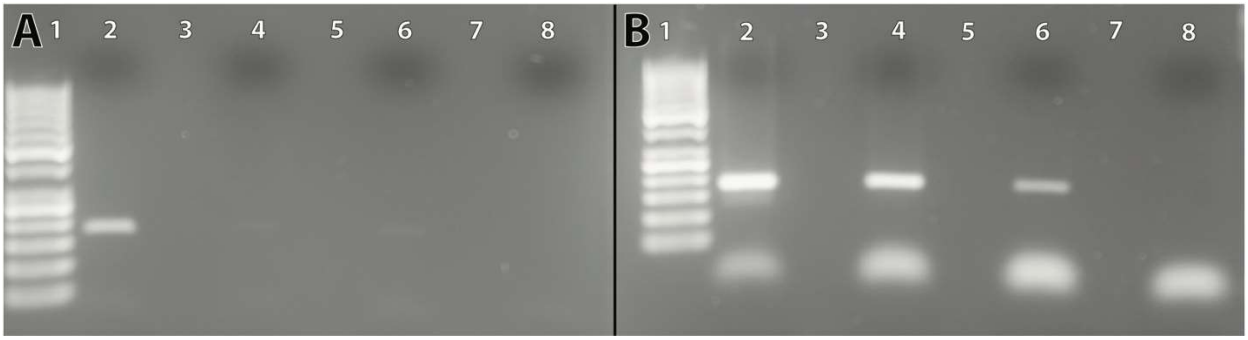

Figure 3.5. Comparison of ethidium bromide stain (A) and Biotium GelRed Nucleic Acid Stain (B) run on a 2% agarose gel run for 40 min at 100 V. In both gels, Lane 1 = 50 bp ladder, Lane 2 = ca. 100 pg/µL Black-spotted Newt tissue, Lane 4 = ca. 10 pg/µL Black-spotted Newt tissue, Lane 6 = ca. 1 pg/µL Black-spotted Newt tissue, and Lane 8 = NTC (Lanes 3, 5, and 7 are empty). NTC = no-template control.

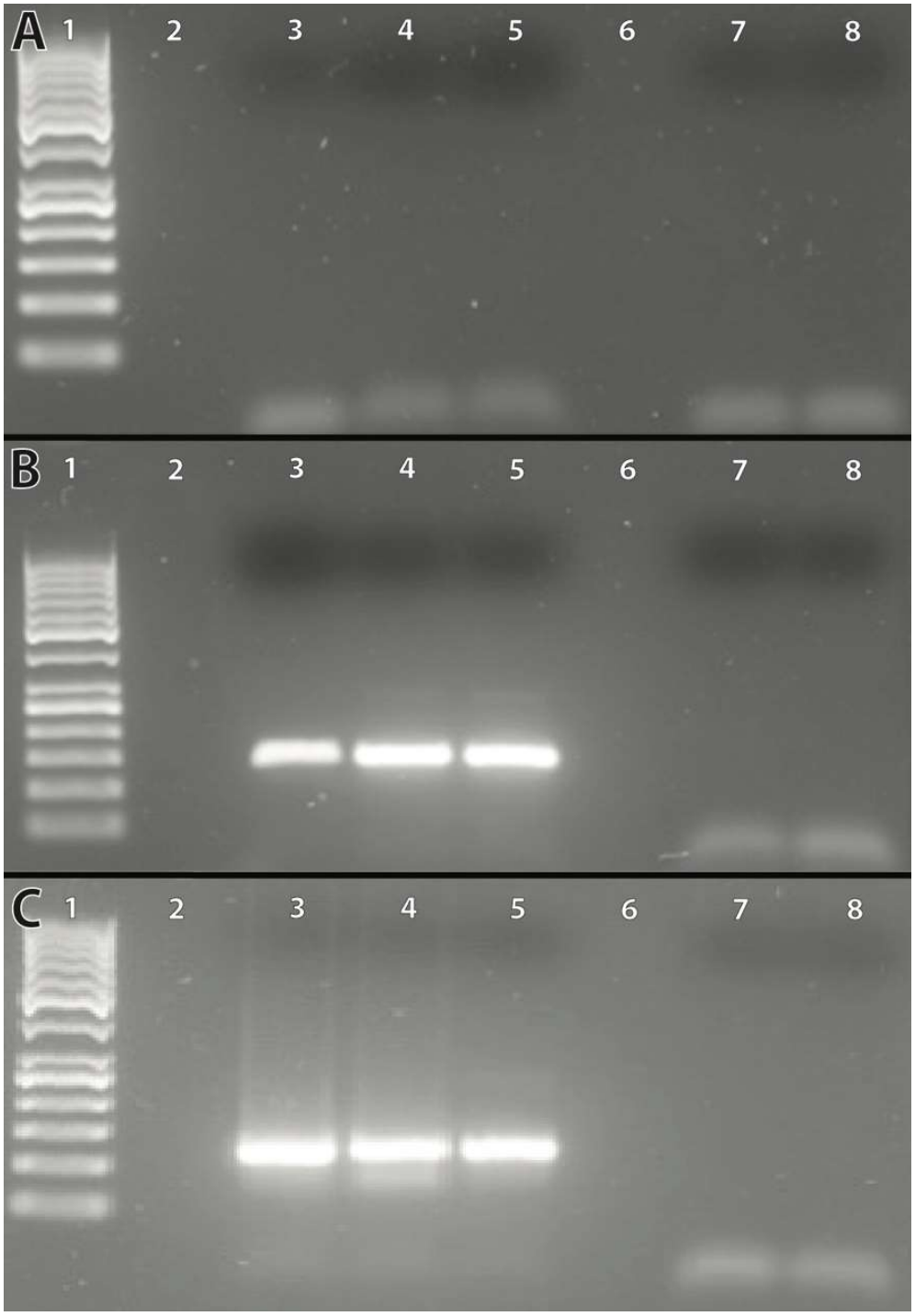

Figure 3.6. Field validation of our Black-spotted Newt (*Notophthalmus meridionalis*) eDNA assay. Field samples from a confirmed newt-positive site (Willacy County) run through initial and nested PCR that were extracted using the Epoch protocol: A) without use of an Inhibitor Removal Kit (IRK); B) with the use of a Zymo IRK; C) with the use of a NucleoSpin IRK. Numbers (1–8) correspond to lanes in the gel, which is the same in all images: 1) 50 bp ladder; 2) empty; 3–5) technical replicates of extracted DNA from field sample; 6) empty; 7) field blank; 8) NTC.

CHAPTER 4

TASK 3. Defining the current distribution of Black-spotted Newts using an environmental DNA (eDNA) assay and traditional methods

OVERVIEW

Chapter 4 focuses on the conducting both eDNA sampling and traditional surveys at 80 sites throughout south Texas for Black-spotted Newts. We detected Black-spotted Newts at 12 localities in total: four localities using eDNA surveys, four localities using traditional methods, and four localities with both methodologies. eDNA detections were obtained from five counties, including one where Black-spotted Newts have never been reported and another in which the species has not been observed since the 1930s. eDNA detections were obtained in all four seasons, generally following moderate to heavy rainfall events. Our results support the increased use of eDNA surveys to detect rare and cryptic amphibians and help to better understand the current distribution of this imperiled species. This chapter addresses Goals 1 (in part), 2 (in part), and 4 of the project. Portions of this chapter were published in Robinson (2021) and Robinson et al. (2022).

METHODS

Sampling Locations.—A total of 80 sites were selected throughout and just beyond the historic range of Black-spotted Newts across south Texas, USA, and were sampled from 2018–2021 (Table 4.1). With Black-spotted Newt activity expected to increase after rainfall (Mecham 1968a), we collected eDNA samples following rainfall events whenever possible. Efforts were made to sample each site twice; however, due to unpredictable rainfall this was not always possible. Sampling locations were chosen by referencing a database of species occurrence records compiled from natural history collections and citizen science observations (see Chapter 2). The selection of sites was constrained due to the lack of publicly accessible lands in Texas (Schmidley et al. 2001), as well as the lack of suitable habitat (Jahrsdoerfer and Leslie 1988). Sampling locations included wetlands, ponds, resacas, roadside ditches, and creeks across 19 counties (Figure 4.1). Included within these sampling sites are 14 "recent" (post-2000) Black-spotted Newt localities, three "historic" (pre-2000) localities, 16 "georeferenced" localities based on historic occurrence records which lack a specific locality, and 47 "other" potential sites within and immediately beyond the current known range of Black-spotted Newts in south Texas (Table 4.1). Potential sites were chosen with a preference for ephemeral water bodies, which lacked large predatory fish and contained aquatic vegetation (Mecham 1968a; Rappole and Klicka 1991).

Field Protocol.—At each site, water was collected from three locations to account for the heterogeneous distribution of eDNA and pooled in a sterilized bucket (Turner et al. 2014; Goldberg et al. 2016). The pooled water was poured over a 47-mm diameter Whatman Grade 4 cellulose filter (25–30 µm pore size) inside of a 250-mL filter cup and pumped through using a hand-operated fluid extractor (as described in Ruppert et al. 2022). Filtration occurred in triplicate; up to 1 L of field-collected water was filtered three times per field site as recommended by Ficetola et al. (2008). The water bodies that Black-spotted Newts occupy are often turbid and suspended sediments can clog the filter. At times we were unable to filter the entire 1-L sample, and the final volume filtered was recorded. Before filtering field-collected water, 1 L of deionized (DI) water was filtered at each field site as a field control (blank). In total, each site visit yielded four filters: one field blank and three field samples. Filters were stored in 2-mL tubes with 700 µL of DNAzol,

a DNA isolation and buffering reagent (Molecular Research Center Inc, Cincinnati, OH, USA). All filtration using the aforementioned equipment occurred on-site for immediate preservation. To prevent contamination among sites, nitrile gloves were worn, the filter cup and the bucket were sprayed with a 3.78% sodium hypochlorite solution (bleach), followed by a 100 g/L sodium thiosulfate solution to inactivate the bleach, and finally rinsed with DI water (Ruppert et al. 2022).

At each sampling location we also conducted a 30-min search for Black-spotted Newts through active dip-netting in the water and by searching under natural and artificial debris surrounding the wetland. Each Black-spotted Newt captured was photographed, swabbed, weighed, and measured. Genetic tissue samples (tail clips) were collected from all individuals, and a single individual from each unique site was collected, vouchered, and deposited at the Biodiversity Collections, The University of Texas at Austin (TNHC). Specimen handling and collection occurred under a Texas Parks and Wildlife Scientific Collecting Permit (SPR-1018-294), and all collecting activities followed an approved IACUC protocol (AUP #18-28, #22-12).

Laboratory Protocol.—eDNA filter extraction occurred following an adapted GenCatch Blood and Tissue Genomic Mini-Prep Kit protocol (Epoch Life Science, Missouri City, TX, USA). The extraction protocol was modified at several steps (no LYS Buffer was added, 10 µL of 10 mg/mL Proteinase-K was used rather than 20 µL, 500 µL of 100% ethanol and EX Buffer were used rather than 200 µL, and the final elution volume was 100 µL). Although inhibition was not explicitly tested, inhibitor removal kits were shown to be essential for our study system (see Chapter 3), and a commercial inhibitor removal kit (Zymo OneStep PCR Inhibitor Removal Kit [Zymo Research, Irvine, CA, USA]) was used following DNA extraction. Primers were designed based on the published mitochondrial genome for Texas Black-spotted Newt available on GenBank (accession numbers: MH367840.1, MH367841.1, MH367842.1, MH367843.1, MH367844.1). Initial and nested primers were designed to amplify a small segment (<200 base pairs [bp]) corresponding to the Black-spotted Newt cytochrome c oxidase subunit 1 (CO1) gene (Tsuji et al. 2019). The initial primers amplified a 181-bp segment (forward: 5′ GTAGACCTGAATGTGGACACC 3′; reverse: 5′ CTGTAAGCCCTCCCTCTGT 3′), and the nested primers amplified a 122-bp segment (forward: 5′ ACACCCGAGCCTATTTTAC 3′; reverse: 5′ GCCCATAGTATTGCAGCAT 3′) within the initial 181-bp segment. Primers were optimized in vitro, with an annealing step temperature gradient and a serial dilution of Black-spotted Newt tissue DNA extract.

PCR was performed using a T100 ThermoCycler (Bio-Rad Laboratories, Hercules, CA, USA). For each reaction, 12.5 µL GoTaq G2 HotStart MasterMix (Promega Corporation, Madison, WI, USA), 0.5 µL of 10 µM forward and reverse primers, 6.5 µL of nuclease-free water, and 5 µL of extracted sample were added to a 0.2-mL PCR tube. To detect potential laboratory contamination or non-specific PCR products, a no-template control (NTC) was run in conjunction with other samples, using 5 µL of nuclease-free water instead of extracted sample. No internal positive control was included in order to avoid potential contamination of samples due to the sensitivity of our nested PCR assay. The product from the initial round of PCR was purified with an Exo-CIP Rapid PCR Cleanup Kit (herein referred to as Exo-CIP; New England Biolabs, Ipswich, MA, USA) prior to use in the nested round. PCR conditions were as follows: 35 cycles of denaturation at 95°C for 30 s, variable annealing temperature for 28 s, and elongation at 72°C for 30 s. The annealing temperature was 55.5°C for the initial primers and 53°C for the nested primers. Following the completion of the nested PCR, 20 µL of the PCR product was run on a 2% agarose gel stained with GelRed Nucleic Acid Stain (Biotium Inc., Hayward, CA, USA) for 40 min at 100 V alongside a 50 bp GeneRuler ladder (Thermo Fisher Scientific, Waltham, MA, USA), and the gel was

visualized using a UVP transilluminator. When samples produced at least two bands of the appropriate size (122 bp), the remaining 5 µL of PCR product from each technical replicate that produced a band of the correct size was pooled and purified using Exo-CIP. Then, 5 µL of purified PCR product and 5 µL of the reverse nested primer were sent to Eurofins Genomics (Louisville, KY, USA) for Sanger sequencing. Sequences >95% identical to published Black-spotted Newt sequences when searched using NCBI Blast (blast.ncbi.nlm.nih.gov/blast.cgi) resulted in a positive species detection. If only one band of the correct size was produced after nested PCR, samples were re-run.

RESULTS

eDNA Sampling.—We detected Black-spotted Newt eDNA in samples from eight sites (Table 4.2; Figure 4.2). These eight sites included: Live Oak County Park, pond SE of parking area (Site 6; Tables 1, 2); Powderhorn WMA, dugout pond near barn at S entrance (Site 11); Willacy County Site #1 (Site 41); Willacy County Site #3 (Site 46); Laguna Atascosa NWR, Kidney Pond (Site 64); Laguna Atascosa NWR, Prairie Trail #2 (Site 68); Cameron County Site #2 (Site 70); and Palo Alto Battlefield National Historic Park, American Tank (Site 74). Black-spotted Newt eDNA was only detected one time (of two visits) at each of these sites (Table 4.2). These detections included four sites in Cameron County (Sites 64, 68, 70, 74), two sites in Willacy County (Sites 41, 46), one site in Live Oak County (Site 6), and one site in Calhoun County (Site 11). Four of these sites are "recent" *N. meridionalis* localities (Sites 41, 46, 70, 74), and one site is a "historic" locality site, with the last detection in 1938 (Site 64). *Notophthalmus meridionalis* has never been observed at the other three sites (Sites 6, 11, 68). Three additional sites did not meet our criteria for a positive eDNA detection because samples from these sites produced just one band of the correct size and zero bands upon subsequent PCR: Powderhorn WMA, midline fence pond (Site 9); Cameron County Site #4 (Site 78); and Cameron County Site #6 (Site 80). However, at two of these three sites (Sites 78, 80), *N. meridionalis* was physically detected, and as a result, both sites are considered *N. meridionalis* positive. The third site (Site 9) should be considered a potentially positive site as it is ca. 4.2 km from a *N. meridionalis*-positive site (Site 11).

Traditional Sampling.—During this study, 21 Black-spotted Newts were found at eight sampling locations using traditional methodologies (Table 4.2; Figure 4.2). Sites where we physically detected *N. meridionalis* include: Willacy County Site #1 (Site 41; Tables 4.1, 4.2); Willacy County Site #3 (Site 46); Hidalgo County Site #1 (Site 52); Cameron County Site #1 (Site 70); Palo Alto Battlefield National Historic Park, American Tank (Site 74); Cameron County Site #4 (Site 78); Cameron County Site #5 (Site 79); and Cameron County Site #6 (Site 80). Individual Black-spotted Newts were detected once at each sampling site, except for Site 46 where two individuals were found on two separate dates. These detections included five sites in Cameron County (Sites 70, 74, 78–80), two sites in Willacy County (Sites 41, 46), and one site in Hidalgo County (Site 52). Of these eight sites, one represents a new specific record of occurrence (Site 79). The most common method in detecting *N. meridionalis* was searching beneath cover objects along the shoreline (n = 11), followed by dip-netting (n = 9), and finally, capturing by hand in the water (n = 1).

Conditions for Positive eDNA Detections.—eDNA detections of Black-spotted Newts were obtained from samples that were collected at various times throughout the year: August (n = 2), February (n = 1), April (n = 1), May (n = 1), June (n = 1), October (n = 1), and December (n = 1;

Table 4.2). Out of our eight eDNA detections, two occurred 17–26 d following heavy precipitation (>10 cm; Brown et al. 2021) from Hurricane Hanna (Sites 68, 74; Table 4.1), five occurred within 8 d following moderate precipitation (2.5–7.6 cm; Sites 6, 11, 41, 64, 70), and one occurred with minimal measurable precipitation in the previous 30 d (<1.3 cm; Site 46). The water turbidity at the time of sample collection from seven of the eight sites with positive eDNA detections was classified as "none" or "light". At the remaining site (Site 70), the turbidity was recorded as "high"; however, a single *N. meridionalis* was observed in the water and the target volume of 3 L (in total) was filtered. At sites where higher levels of turbidity were recorded, the target volume was not often reached, which could have potentially hampered the ability to detect *N. meridionalis* eDNA. In addition, for samples from seven of the eight sites where positive eDNA detections were obtained (Sites 6, 11, 46, 64, 68, 70, 74), the target of 3 L was filtered. For the remaining site (Site 41), 2.55 L was filtered in total; however, eight individual *N. meridionalis* were observed in the water so the concentration of eDNA was likely relatively high.

DISCUSSION

Overall, Black-spotted Newts were detected at 12 sites across five counties (Figure 4.2), and we detected newts with both methodologies at four of these sites. Based on our results, a physical Black-spotted Newt detection did not always correspond with a positive eDNA detection and vice versa. We obtained several eDNA detections without detecting newts through traditional methods, which have proved challenging in the past. In these instances, utilizing the eDNA assay likely expanded the detection window for this species. Additionally, the detections at sites where Black-spotted Newts had not previously been reported can serve to inform future sampling and potentially expand the known range of this species. Our results continue to support the efficacy of eDNA surveys to detect rare or cryptic amphibians (Goldberg et al 2011; McKee et al. 2015; Brozio et al. 2017; Ruppert et al. 2022). The sites where Black-spotted Newts were observed and we failed to obtain a positive eDNA detection are confounding. In these instances, positive eDNA detections were more likely when Black-spotted Newts were captured in the water (2 of 3 sites) than when newts were captured on the land, adjacent to the wetland (1 of 6 sites). The lack of detections when Black-spotted Newts were captured on the land could be due to the observed individuals not recently utilizing the aquatic habitat, or that eDNA concentrations were below detection threshold. Additionally, at two sites we were unable to collect an eDNA sample because the site had no water, and the individuals were observed beneath cover objects near the wetland basin. The discrepancy between traditional and eDNA detections underscores the importance of a dual approach as recommended by Thomsen et al. (2012) in order to minimize false negatives. Using only one methodology, our results would have produced eight (rather than 12) positive detections. Considering the life history of *N. meridionalis*, future monitoring is recommended using both eDNA and traditional methodologies in order to maximize species detection.

We identified one new locality used by *N. meridionalis* through traditional methods (Site 79; Tables 4.1, 4.2) and three new localities through eDNA sampling (Sites 6, 11, 68). Most notable of these new localities are the positive eDNA detections obtained from Live Oak County Park, pond SE of parking area (Site 6), which is the first evidence of *N. meridionalis* occurring in Live Oak County since 1938 (Robinson et al. 2020) and Powderhorn WMA dugout pond near barn at S entrance (Site 11) in Calhoun County, where *N. meridionalis* has never been reported. These detections represent the northernmost records of *N. meridionalis* in recent years, as all verifiable observations since 2000 are limited to the three southernmost counties in Texas (Cameron, Hidalgo, and Willacy). Given that eDNA analyses can occasionally give false-positive results

(Darling and Mahon 2011), future surveys (both traditional and eDNA) are needed to attempt to detect individuals at these locations as well as other nearby sites. Though we cannot completely rule out the possibility of false positives in eDNA detection, we observed no contamination in the field blanks nor NTCs, suggesting no contamination of samples in the field or the laboratory. Additionally, all three technical replicates for these sites resulted in a bright band of the appropriate size and sequencing the PCR product from both sites resulted in a 100% match with published Black-spotted Newt mitochondrial sequences. The other sites that represent new records of occurrence are Laguna Atascosa NWR, Prairie Trail #2 (Site 68), which is ca. 7 km southwest of recent occurrence records of *N. meridionalis* at Laguna Atascosa NWR (Sites 64, 65) and Cameron County Site #5 (Site 79), which is ca. 0.4 km west of from another newt-positive site (Site 80).

Black-spotted Newts were not detected in 14 of the 19 counties sampled, including eight counties with historic records. Nearly half of the sites sampled in this study were in Cameron (n = 20), Hidalgo (n = 9), and Willacy (n = 10) counties. Cameron, Hidalgo, and Willacy counties were disproportionately sampled because Black-spotted Newts have been observed in these counties more recently (post-2000) and in greater abundance than other counties, which was revealed through our species occurrence database (see Chapter 2). Prior to 2000, there had been multiple confirmed observations of *N. meridionalis* from three additional counties: Kenedy, Kleberg, and San Patricio. Efforts were made to sample these counties thoroughly (Kenedy: n = 6 sites; Kleberg: n = 5; San Patricio: n = 7), however, we detected no Black-spotted Newts in any of these three counties, including at known ("historic") sites where previous collections were made. All other counties with historic Black-spotted Newt records are represented by either a single specimen (Aransas, McMullen, Nueces, Victoria) or a single collection event (Duval, Live Oak, Refugio). The other counties sampled (Starr, Brooks, Jim Wells, Bee, Goliad, and Calhoun) had no prior verifiable occurrence records of Black-spotted Newts but were along the periphery of their historic range in Texas and sampled in hope of detecting additional populations. The counties with minimal or no Black-spotted Newt observations were not sampled as thoroughly (spatially), as there was a lack of information available when determining suitable sampling sites. Sampling in Starr County (n = 4 sites) was an exception. Starr County has been included in Black-spotted Newt range maps (e.g., Dixon 2000, 2013), likely based on an erroneously published record (Boundy 1994) or an anecdotal report (Irwin 1993). Given the proximity to historic records in Hidalgo County, future survey efforts should continue in Starr County, particularly along the Rio Grande, in attempt to detect individuals. Future surveys should also focus on Kenedy, Kleberg, and San Patricio counties given the number of historic records and specific localities (e.g., Welder Wildlife Refuge, Big Lake; TAMU-Kingsville CKWRI South Pasture) reported from these counties, as well as Live Oak and Calhoun counties in order to confirm Black-spotted Newt presence. Additionally, samples from Powderhorn WMA, midline fence pond (Site 9) produced one band of the correct size after nested PCR and should be investigated further considering the proximity to another site on Powderhorn WMA where *N. meridionalis* eDNA was detected (Site 11).

Rappole and Klicka (1991) provided a report on Black-spotted Newt distribution and using their results and personal communication from other biologists (i.e., A. Chaney, F. Judd, S. Labuda) they identified seven "metapopulation centers" in south Texas. Among these, we obtained a positive eDNA detection from two sites (Sites 64, 68) within the "Laguna Atascosa National Wildlife Refuge" metapopulation center. A positive eDNA detection and physical detection were obtained from Cameron County Site #4 (Site 78) within the "Matamoros, Mexico–Brownsville" metapopulation center. Additionally, positive eDNA and traditional detections from Cameron County Sites #4 and #5 (Sites 79, 80) would likely fall within this metapopulation center as they

are separated by <3 km. Our results indicate that breeding populations of Black-spotted Newts have persisted within these two areas for 30+ yr. Possibly contributing to the persistence of this species is the conservation focus of the organizations that operate these sites. The remaining metapopulation centers were in Kleberg (n = 4) and Kenedy (n = 1) counties, where we obtained no positive newt detections. These include "Vattmannville, TX", "TAMU-Kingsville CKWRI, South Pasture", "Riviera, TX", "US Hwy 77, 14.7–21.7 mi S of Armstrong, TX", and "FM 772, 1 mi S jct 628." Excluding "TAMU-Kingsville CKWRI, South Pasture", these sites are not operated by conservation-focused groups (roadside ditches and private property). Most notable, Rappole and Klicka (1991) reported that during their study, root-plowing occurred on private property within one of the "Vattmannville, TX" sites that caused "sure death to newts". During our study, many ponds and ditches along "US Hwy 77, 14.7–21.7 mi. S of Armstrong, TX" have been impacted by construction activities, which has caused erosion and siltation at two sampling sites (US Hwy 77, W side, ca. 1.0 rd km N Kenedy/Willacy county line [Site 36]; US Hwy 77, E side, ca. 1.6 rd km N jct La Chata gate #4 [Site 38]). Further, dirt roads running parallel to US Hwy 77 along this stretch of highway in Kenedy County are frequented by U.S. Customs and Border Protection (CBP) vehicles. These vehicles drag tires behind them to monitor foot traffic from illegal immigrants. Tire-dragging and the utilization of these dirt roads could serve as a direct threat to *N. meridionalis* and other wildlife along US Hwy 77. Whether any Black-spotted Newt populations remain at these other metapopulation centers identified by Rappole and Klicka (1991) should continue to be investigated.

The information on the conditions for positive eDNA detections from this study can be used to plan future eDNA sampling for this species and others with similar life histories. Generally, Black-spotted Newt reproduction and activity in the water are tied to rainfall events, which would provide the conditions for a positive eDNA detection (Buxton et al. 2017). Based on our results, eDNA sampling should occur within a few days of light or moderate precipitation events (ca. 1.3–7.6 cm) that cause wetlands to retain a small volume of water. However, for heavy precipitation from hurricanes or tropical storms, the best practice may be to wait for at least 14 d before eDNA sampling, as the target eDNA may be too dilute if immediately sampled. If rainfall events trigger reproduction, waiting at least 14 d may allow eDNA shed from reproductive events, eggs, and larvae to accumulate in high-volume sites. However, high temperatures typically observed during the tropical storm season must be considered as well as limited eDNA persistence in times of high temperatures (Strickler et al. 2015). Increased flow and runoff following heavy rainfall events can dilute eDNA concentrations (Curtis et al. 2021) as well as increase organic matter and suspended sediments, making eDNA detections more difficult to obtain (Buxton et al. 2017; Yaegashi et al. 2020). The water bodies that Black-spotted Newts occupy can be highly turbid, and sampling immediately following heavy rainfall events likely decreases the amount of water that can be filtered due to increased suspended sediment. Filtering larger amounts of water was necessary for our study as ≥85% of the target volume (3 L) was filtered in all eight of our positive eDNA detections. The filter pore size (25–30 µm) used in this study was larger than what is typically used in eDNA studies (Minamoto et al. 2016; Rourke et al. 2021) in order to maximize the volume filtered from the typically turbid water bodies in south Texas. Filtering more water can increase the amount of DNA captured, however, smaller fragments of DNA may not be captured with large filter sizes (Eichmiller et al. 2016). Ruppert et al. (2022) obtained positive detections in 98.2% of samples taken from known Rio Grande Siren (*Siren intermedia texana*) ponds using filters with 25–30 µm pores, lending support to the use of large pore sizes in eDNA assays. Future studies

should continue to investigate the use of larger filter pore sizes considering the success of this assay, particularly in habitats with turbid waters.

The development and implementation of this assay was successful at detecting Black-spotted Newt eDNA from field samples. In total, eDNA samples from 80 sites were analyzed, producing eight positive detections (10%). While not a direct comparison, these results are an improvement from previous efforts where Rappole and Klicka (1991) located Black-spotted Newts at ca. 6% of sites surveyed and Judd (1985) found newts at ca. 1% sites surveyed. Using traditional methodologies, we found *N. meridionalis* at eight sites (10%) including four in which we also obtained positive eDNA detections. Altogether, Black-spotted Newts were detected at 12 of 80 unique localities (15%) spanning five counties in south Texas. Five new Black-spotted Newt localities were reported as part of this study (eDNA: n = 4; traditional methods: n = 1), including one in Live Oak County, which is the first newt detection the county since 1938 and one in Calhoun County where there have been no previous confirmed Black-spotted Newt records. Accurately locating populations of Black-spotted Newts is essential to better understand the current distribution of this species in south Texas, especially considering management and conservation decisions. The results of this study show the efficacy of this eDNA assay in detecting Black-spotted Newts across the landscape under various situations and environmental conditions, and this eDNA assay, in conjunction with traditional methodologies, can be successfully applied to monitor known populations as well to detect Black-spotted Newts at new localities. With proper timing of sampling, this eDNA assay holds the potential to help fill in the current knowledge gaps in the distribution of Black-spotted Newts throughout south Texas.

Table 4.1. List of sites sampled for Black-spotted Newts as part of this study. Descriptive names for private property have been generalized and specific GPS coordinates have been redacted in this table. Sites are classified as "Recent" (those where Black-spotted Newts were detected since 2000), "Historic" (those where Black-spotted Newts were detected before 2000), "Georeferenced" (sites based on historic Black-spotted Newt collection data that lack specific coordinates), or "Other" (potential Black-spotted Newt sites within and just beyond the recognized range of this species in Texas). Site numbers correspond to those listed in Table 4.2 and Figure 4.2.

Site #	County	Site Name	Site Category
1	Victoria	Coleto Creek at US Hwy 77	Georeferenced
2	Victoria	Coleto Creek side channel, ca. 0.5 km SE of US Hwy 77	Georeferenced
3	Goliad	Manahuilla Creek at US Hwy 59	Other
4	Bee	Bee County Site #1	Other
5	Live Oak	Hilbert H. Kopplin Memorial Park	Other
6	Live Oak	Live Oak County Park, pond SE of parking area	Georeferenced
7	McMullen	Hwy 16 bridge over Nueces River	Georeferenced
8	McMullen	ditch along Co Rd 624, ca. 2.6 rd km E jct Nueces River	Other
9	Calhoun	Powderhorn WMA, midline fence pond	Other
10	Calhoun	Powderhorn WMA, Bullrush Pond	Other
11	Calhoun	Powderhorn WMA, dugout pond near barn at S entrance	Other
12	Calhoun	Aransas NWR, Auto Loop Trail, ca. 0.6 rd km SW from observation towers	Other
13	Aransas	Aransas NWR, ca. 0.2 rd km S jct Auto Loop Trail end and main road	Other
14	Refugio	ditch crossing 1st St, ca. 0.1 rd km SW jct Cole	Georeferenced
15	San Patricio	San Patricio County Site #1	Other
16	San Patricio	San Patricio County Site #2	Other
17	San Patricio	San Patricio County Site #3	Historic
18	San Patricio	San Patricio County Site #4	Other
19	San Patricio	San Patricio County Site #5	Other
20	San Patricio	Live Oak Park, pipeline pond	Other
21	San Patricio	Live Oak Park, junkpile pond	Other
22	Jim Wells	dugout pond along TX Hwy 359, SW bridge over Nueces River	Other
23	Nueces	John J. Sablatura Park, flooded field along Agua Dulce Creek	Georeferenced
24	Nueces	Pintas Creek at Co Rd 70	Other
25	Duval	San Diego Creek W of TX Hwy 359	Georeferenced
26	Kleberg	TAMU-Kingsville CKWRI, South Pasture pond	Historic
27	Kleberg	Kleberg County Site #1	Georeferenced
28	Kleberg	west side of Co Rd 1110S, ca. 0.6 rd km N jct Co Rd 2300E	Georeferenced
29	Kleberg	Kleberg County Site #2	Other
30	Kleberg	wetland E of jct of 3rd St and W Poplar Ave (in Riviera, TX)	Georeferenced
31	Kenedy	Kenedy County Site #1	Other
32	Kenedy	Kenedy County Site #2	Other
33	Kenedy	Kenedy County Site #3	Other
34	Kenedy	US Hwy 77, W side, ca. 12.0 rd km N Kenedy/Willacy county line	Georeferenced
35	Kenedy	US Hwy 77, E side, ca. 8.5 rd km N Kenedy/Willacy county line	Georeferenced
36	Kenedy	US Hwy 77, W side, ca. 1.0 rd km N Kenedy/Willacy county line	Georeferenced
37	Brooks	Brooks County Site #1	Other
38	Willacy	US Hwy 77, E side, ca. 1.6 rd km N jct La Chata gate #4	Other
39	Willacy	US Hwy 77, E side, ca. 0.5 rd km S jct La Chata gate #4	Other
40	Willacy	pond along Co Rd 398, ca. 0.7 rd km N jct Bay Ave	Georeferenced
41	Willacy	Willacy County Site #1	Recent
42	Willacy	Willacy County Site #2	Recent
43	Willacy	TX Hwy 186, N side ditch, ca. 1.1 rd km W East Foundation El Sauz Ranch gate near Huesos Tank	Other
44	Willacy	Lower Rio Grande Valley NWR, Willamar Tract, NE pond	Other
45	Willacy	Lower Rio Grande Valley NWR, Willamar Tract, S pond	Other
46	Willacy	Willacy County Site #3	Recent
47	Willacy	Willacy County Site #4	Other
48	Starr	Starr County Site #1	Other
49	Starr	Lower Rio Grande Valley NWR, San Francisco Banco Tract, canal	Other

50	Starr	Lower Rio Grande Valley NWR, San Francisco Banco Tract, concrete spillover	Other
51	Starr	Old Military Hwy, ca. 2.6 rd km ESE jct Co Rd 2360, pond #4	Other
52	Hidalgo	Hidalgo County Site #1	Recent
53	Hidalgo	Hidalgo County Site #2	Recent
54	Hidalgo	Hidalgo County Site #3	Other
55	Hidalgo	ditch along Jesus Flores Rd, ca. 0.4 rd km S jct 12th St	Other
56	Hidalgo	Hidalgo County Site #4	Georeferenced
57	Hidalgo	Hidalgo County Site #5	Other
58	Hidalgo	Hidalgo County Site #6	Other
59	Hidalgo	Lower Rio Grande Valley NWR, Milagro East Tract, resaca	Other
60	Hidalgo	Santa Ana NWR, Willow Lakes	Georeferenced
61	Cameron	Cameron County Site #1	Other
62	Cameron	Laguna Atascosa NWR, Newt Pond	Recent
63	Cameron	Laguna Atascosa NWR, pond ca. 0.2 km SW maintenance shop	Other
64	Cameron	Laguna Atascosa NWR, Kidney Pond	Historic
65	Cameron	Laguna Atascosa NWR, Scum Pond	Recent
66	Cameron	Laguna Atascosa NWR, Prairie Trail, pond #3	Other
67	Cameron	Laguna Atascosa NWR, Prairie Trail, pond #1	Other
68	Cameron	Laguna Atascosa NWR, Prairie Trail, pond #2	Other
69	Cameron	Laguna Atascosa NWR, pond along Buena Vista Dr, ca. 0.4 rd km N jct Co Rd 510	Other
70	Cameron	Cameron County Site #2	Recent
71	Cameron	Laguna Atascosa NWR, TX Hwy 100, crossing 3A pond	Other
72	Cameron	Los Fresnos High School, Agua Negra	Other
73	Cameron	Palo Alto Battlefield National Historic Park, Crescent Tank	Recent
74	Cameron	Palo Alto Battlefield National Historic Park, American Tank	Recent
75	Cameron	Palo Alto Battlefield National Historic Park, dugout pond ca. 0.4 km SE visitor center	Recent
76	Cameron	Resaca de la Palma State Park, resaca near Hunter's Trail	Other
77	Cameron	Cameron County Site #3	Recent
78	Cameron	Cameron County Site #4	Recent
79	Cameron	Cameron County Site #5	Other
80	Cameron	Cameron County Site #6	Recent

Table 4.2. List of sampling sites, Black-spotted Newt (*Notophthalmus meridionalis*) detection results, date(s) sampled, water turbidity, and total volume filtered for each site visit. The "Detection" column indicates Black-spotted Newt sampling results: eDNA detection (eDNA), traditional detection (T), eDNA and traditional detection (Both), or no detection (No). Bold text indicates the date, turbidity, and total volume filtered ("L filtered") when positive eDNA detections were obtained. We were unable to collect eDNA from Site 7 because this site remained dry throughout the study. Volume and/or turbidity data are missing from sites 73, 76 and 78. An asterisk indicates sites where only one band of the correct size was obtained after PCR amplification, and therefore, did not reach the criteria for a full eDNA detection.

Site #	Detection?	Visit 1 Date	Visit 1 Turbidity	Visit 1 L filtered	Visit 2 Date	Visit 2 Turbidity	Visit 2 L filtered
1	No	4-Dec-20	light	3	–	–	–
2	No	30-Mar-20	moderate	0.9	–	–	–
3	No	4-Dec-20	light	3	28-Feb-20	light	1.77
4	No	6-Oct-20	none	3	3-Dec-20	light	3
5	No	29-Jun-20	none	3	–	–	–
6	eDNA	29-Jun-20	none	3	**3-Dec-20**	**light**	**3**
7	No	–	–	–	–	–	–
8	No	8-Nov-18	none	3	–	–	–
9	No*	27-Feb-20	light	3	6-May-21*	none*	3*
10	No	27-Feb-20	light	3	–	–	–
11	eDNA	**27-Feb-20**	**none**	**3**	6-May-21	none	3
12	No	26-Feb-20	light	1.33	6-Aug-20	high	0.75
13	No	26-Feb-20	moderate	3	6-Aug-20	high	1.15
14	No	28-Aug-20	none	3	–	–	–
15	No	30-Jan-20	none	2.6	–	–	–
16	No	31-Jan-20	high	0.15	–	–	–
17	No	29-Jan-20	light	1.18	7-May-21	light	3
18	No	13-Feb-20	none	3	6-Aug-20	light	3
19	No	13-Feb-20	none	3	6-Aug-20	light	3
20	No	7-May-21	high	3	–	–	–
21	No	30-Jan-20	moderate	1.95	–	–	–
22	No	16-Aug-20	light	3	–	–	–
23	No	21-May-20	light	2.55	3-Aug-20	light	3
24	No	21-May-20	light	3	3-Aug-20	light	3
25	No	29-Jun-20	light	3	–	–	–
26	No	24-Jul-20	light	3	27-Aug-20	light	3
27	No	26-Oct-18	none	2.35	12-Jul-20	light	3
28	No	21-Feb-20	high	1.39	–	–	–
29	No	21-Feb-20	light	1.38	18-May-20	light	2.9
30	No	18-May-20	moderate	1.5	3-Aug-20	very high	0.25
31	No	10-Feb-20	light	1.17	–	–	–
32	No	10-Feb-20	light	1.45	18-May-20	very high	0.2
33	No	21-Feb-20	high	2.5	18-May-20	high	1.5
34	No	31-Aug-20	light	2.6	–	–	–
35	No	26-Oct-18	none	2.6	16-Jun-20	none	2.2
36	No	13-Apr-20	light	2.5	28-Jul-20	high	2.5
37	No	20-Jan-20	high	0.25	24-Aug-20	very high	1.5
38	No	9-Apr-20	moderate	2.7	28-Jul-20	light	2.9
39	No	9-Apr-20	moderate	3	–	–	–
40	No	18-Jun-19	high	2.48	9-Apr-20	high	2.6
41	Both	**7-Apr-20**	**light**	**2.55**	14-May-20	high	1.05
42	No	7-Apr-20	moderate	3	28-Jul-20	moderate	3

43	No	27-Jun-19	high	3	14-May-20	light	3
44	No	1-Jun-20	moderate	2.75	18-Aug-20	light	2.75
45	No	1-Jun-20	moderate	1.45	18-Aug-20	none	3
46	Both	18-Jun-19	none	3	**27-Oct-20**	**moderate**	**3**
47	No	20-Nov-18	high	3	18-Jun-19	moderate	3
48	No	2-Feb-19	none	3	3-Nov-20	none	3
49	No	12-May-20	none	3	13-Aug-20	light	3
50	No	12-May-20	light	2.5	–	–	–
51	No	13-Aug-20	light	3	–	–	–
52	T	25-Jun-19	high	1.9	17-Jul-20	high	3
53	No	27-Jul-20	light	2.75	25-Aug-20	light	1.45
54	No	12-Feb-20	none	3	17-Aug-20	high	3
55	No	12-Feb-20	none	3	17-Aug-20	light	3
56	No	12-May-20	light	3	21-Aug-20	none	2.9
57	No	12-May-20	none	3	21-Aug-20	light	3
58	No	23-Oct-19	light	3	21-Aug-20	none	3
59	No	23-Jun-20	light	3	13-Aug-20	light	3
60	No	23-Jun-20	none	3	–	–	–
61	No	12-Feb-20	light	3	24-May-21	light	3
62	No	26-Jun-20	moderate	3	30-Jul-20	light	3
63	No	25-Jun-19	moderate	3	–	–	–
64	eDNA	**19-Jun-19**	**light**	**3**	–	–	–
65	No	26-Jun-20	high	2.2	30-Jul-20	light	3
66	No	26-Jun-20	very high	0.8	23-Aug-20	moderate	3
67	No	11-Oct-19	moderate	3	–	–	–
68	eDNA	26-Jun-20	high	3	**23-Aug-20**	**light**	**3**
69	No	25-Jun-19	moderate	1.65	2-Jun-20	moderate	3
70	Both	27-Jul-20	high	3	**2-May-21**	**high**	**3**
71	No	25-Jun-19	light	3	27-Jul-20	light	3
72	No	11-Sep-19	high	3	–	–	–
73	No	29-Oct-18	–	–	14-Aug-20	none	3
74	Both	2-Nov-18	none	3	**14-Aug-20**	**none**	**3**
75	No	14-Aug-20	light	3	–	–	–
76	No	25-Jan-20	–	0.18	–	–	–
77	No	20-Feb-20	light	3	–	–	–
78	T*	19-Nov-20	light	2.07	4-May-21*	none*	3*
79	T	21-Dec-20	moderate	0.87	–	–	–
80	T*	20-Feb-20	light	3	4-May-21*	light*	2.8*

Figure 4.1. Representative photos of Black-spotted Newts (*Notophthalmus meridionalis*) sampled during this study and their corresponding habitats: A) Adult male (TNHC 116643 [DRD 6320]) from Site 73, Cameron County; B) Adult male (TNHC 116644 [DRD 6610]) from Site 41, Willacy County; C) Adult male (TNHC 116642 [DRD 5813]) from Site 52, Hidalgo County, with a black arrow indicating adjacent agricultural practices. Site numbers correspond to Table 4.1. TNHC = Biodiversity Collections, The University of Texas at Austin; DRD = Drew R. Davis Field Series.

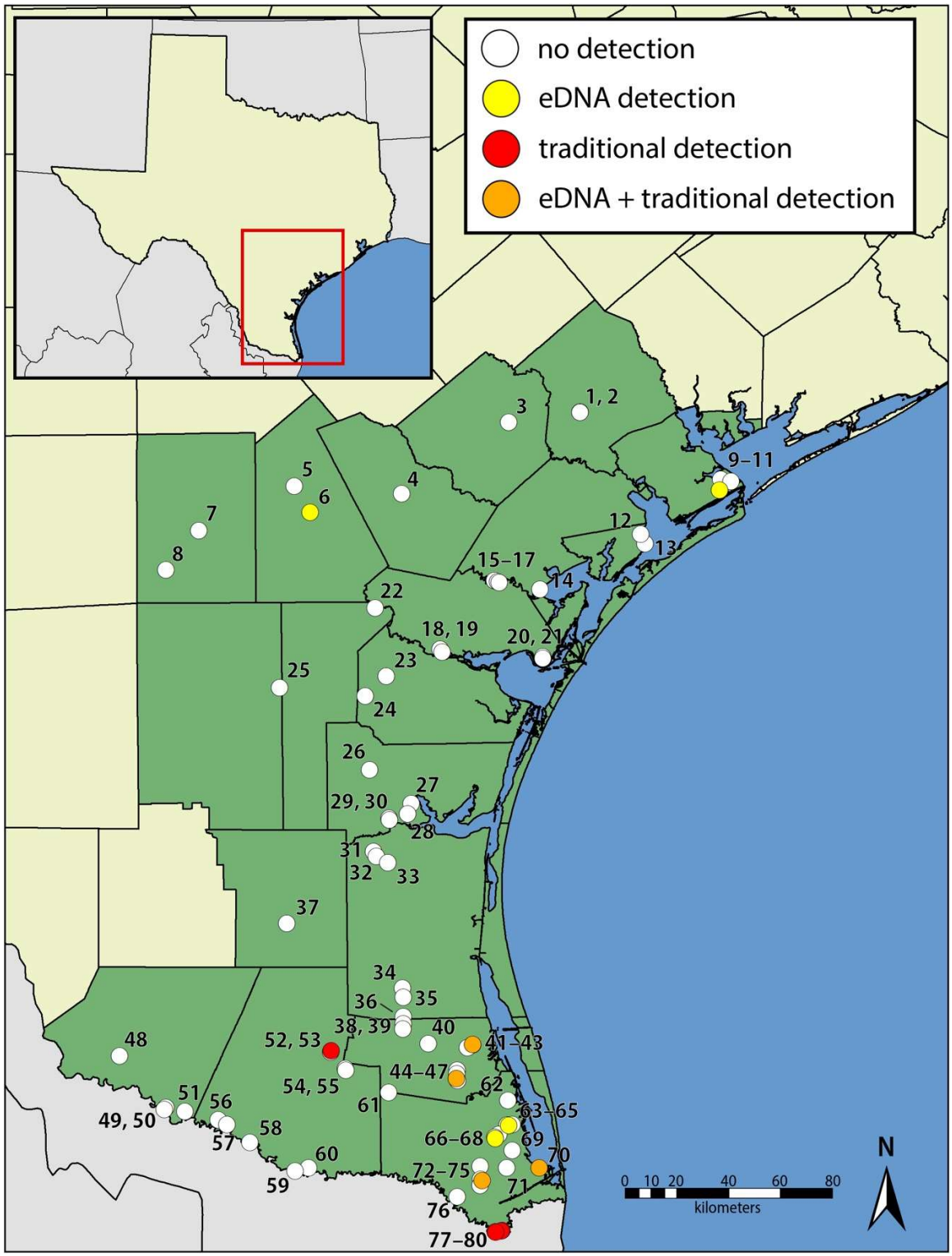

Figure 4.2. Map of 80 sites sampled for Black-spotted Newts (*Notophthalmus meridionalis*) across south Texas, USA. Site numbers correspond to those listed in Table 4.1. Sampled counties (green shading), eDNA detections (yellow), traditional survey detections (red), and both eDNA and traditional survey detections (orange) are shown.

CHAPTER 5

TASK 4. Examining environmental correlates of Black-spotted Newt detection

OVERVIEW

Chapter 5 involves data collected from Chapters 2 and 4 and examines the relationships between environmental habitat variables, soil data, and water quality data between Black-spotted Newt-positive (BSN+) and Black-spotted Newt-negative (BSN-) sites in an attempt to understand if there are characteristics that may drive species presence and what characters help describe suitable habitat this species. Understanding characteristics of the wetlands and surrounding uplands that amphibians utilize as breeding and non-breeding habitat are important to inform conservation efforts. There have been few published studies on Black-spotted Newts, and as a result, many elements of this species' natural history are unknown. The most parsimonious models showed that paved road absence, ephemerality, higher soil copper levels, lower soil sand percentage, and lower water conductivity were associated with Black-spotted Newt presence. This chapter addresses Goal 1 (in part) of the project. Portions of this chapter were published in Robinson (2021) and Robinson et al. (2022).

METHODS

Water Quality and Habitat.—The following parameters were recorded during each sampling trip: water quality, water body characteristics, and surrounding habitat characteristics. Conductivity and dissolved oxygen were recorded using a Hach HQ40D Portable Multi Meter water quality sonde (Hach Company, Loveland, CO, USA). A Hach Pocket Pro Salinity Tester was used to record salinity and Hach water quality strips were used to measure nitrate, nitrite, and ammonia concentrations as well as pH, alkalinity, and hardness. Coarse estimates were made about the water body characteristics including the depth, permanence (permanent/ephemeral), flow (yes/no), connectivity (yes/no), turbidity (none/light/moderate/high/very high), and whether it has been dredged (yes/no). The presence of trees and woody debris were noted, and any observed fish, amphibians, and reptiles were identified to species, though on occasion to the family level. Estimates were made as to the percent cover of emergent, submerged, and floating vegetation. Surrounding land use was recorded from a list of several possible categories (agriculture, rangeland, paved road, developed, undeveloped) in the immediate vicinity of the sampling site.

Soil.— Using a soil auger (AMS, Inc., American Falls, ID, USA), soil was collected from two areas within the site, which were combined for analysis to account for local differences in composition. At sites where water was present, samples were taken near the edge of the water body. At dry sites, samples were taken from the basin of the water body. Samples were taken at the surface as well as 30 and 60 cm below the surface where possible. Samples were dried in a drying oven at 65°C for a minimum of 48 h. Soil samples were sent to Texas A&M AgriLife Extension Service Soil, Water and Forage Testing Laboratory for analysis. The analysis consisted of several parts. Routine Analysis measured conductivity (µmho/cm), pH, as well as the concentration (ppm) of NO_3, P, K, Ca, Mg, Na, and S. Micronutrient Analysis measured the concentration (ppm) of Zn, Fe, Cu, and Mn. Hot Soluble Boron Test measured the concentration of Boron (ppm). Detailed Salinity Test was performed by making a saturated paste of the soil sample with DI water, and then the pH and conductivity were measured directly. Following these

measurements, the water was extracted using a vacuum extractor and Na, Ca, K, and Mg levels were measured using inductively coupled plasma mass spectrometry. Finally, Textural Analysis provided percentages of clay, silt, sand, and organic matter within the soil sample.

Statistical Analysis.—The data gathered from Chapter 4 provided a list of sites where Black-spotted Newts were detected (n = 8) using either eDNA or traditional methodologies. However, because our detections were limited and due to the challenges associated with detecting cryptic species, false negatives may have been present. To account for this, the dataset was supplemented by using confirmed, geo-referenced sites where Black-spotted Newts have been detected in the past 10 years (see Chapter 2) to increase the number of known sites to 16 (BSN+ sites).

Separate binary logistic regression models were constructed for each soil depth (surface, 30 cm, 60 cm) combined with the water quality and habitat data. Independent variables were checked for multicollinearity by generating a Spearman correlation matrix and some highly correlated variables were excluded or replaced where appropriate if $|\rho| \geq 0.7$. Akaike Information Criterion (AIC) was used to select predictor variables, which were chosen by comparing the ΔAIC with the inclusion of the variable versus the null model. Candidate variables were selected if the ΔAIC was > 2 and the model was significant ($p < 0.05$) when compared to the null model. Variables with the lowest AIC were included first in the model. McFadden R^2 values were calculated to show improvement compared to previous models. Variables were then compared between BSN+ and BSN- sites. Mann-Whitney U tests were used for continuous variables and averages are reported ± 1 SD. Chi-squared tests were used for categorical variables.

RESULTS

Final Models.—The most parsimonious model incorporating water quality, habitat, and surface soil data included four variables: sand percentage, paved road presence, average conductivity, and ephemerality (McFadden $R^2 = 0.531$; Table 5.1). The most parsimonious model incorporating water quality, habitat and 30 cm soil data included four variables: copper concentration, paved road presence, ephemerality, and average conductivity (McFadden $R^2 = 0.694$; Table 5.2). The most parsimonious model incorporating water quality, habitat and 60 cm soil data included four variables: copper concentration, paved road presence, average conductivity, and ephemerality (McFadden $R^2 = 0.615$; Table 5.3).

Water Quality and Habitat.—Variables that differed significantly between BSN+ and BSN- sites included: dissolved oxygen, paved road presence, ephemerality, whether the site was dredged, and amphibian presence/absence. All other factors were not significantly different between BSN+ and BSN- sites. The water bodies at BSN+ sites had significantly lower levels of dissolved oxygen (4.99 mg/L ± 2.13) compared to BSN- sites (7.13 mg/L ± 3.70; $p = 0.030$; Figure 5.1). All 16 BSN+ sites were not in the immediate vicinity of paved roads, while 17 of the 45 BSN- sites (ca. 38%) were nearby to paved roads, and this difference was significant ($p = 0.004$; Table 5.4). Additionally, all 16 BSN+ sites were ephemeral, while 10 of the 45 BSN- sites (ca. 22%) were permanent water bodies, and this difference was significant ($p = 0.039$; Table 5.4). Amphibian presence at the time of sampling differed significantly ($p = 0.047$; Table 5.4) between BSN+ (15/16 sites; ca. 94%) and BSN- sites (31/45 sites; ca. 69%). At BSN+ sites, the amphibians observed at the time of sampling included: Rio Grande Leopard Frog (*Rana berlandieri*; n = 6 sites; Figure 5.2A), Gulf Coast Toad (*Incilius nebulifer*; n = 5 sites; Figure 5.2B), Couch's Spadefoot (*Scaphiopus couchii*; n = 3 sites; Figure 5.2C), Western Narrow-mouthed Toad (*Gastrophryne*

olivacea; n = 2 sites; Figure 5.2D), Texas Toad (*Anaxyrus speciosus*; n = 1 site; Figure 5.2E), Sheep Frog (*Hypopachus variolosus*; n = 1 site; Figure 5.2F), and Rio Grande Siren (*Siren intermedia texana*; n = 1 site). In addition, unidentified tadpoles and metamorphic bufonids were observed at four sites, which were likely either *I. nebulifer* or *A. speciosus*, and *R. berlandieri* eggs were observed at one site. The most observed amphibian species at BSN+ sites were also observed at several BSN- sites: *R. berlandieri* (n = 9 sites) and *I. nebulifer* (n = 7). Further, BSN+ sites were more often not dredged (9/16 sites; ca. 56%) and BSN- sites were more often dredged (32/45 sites; ca. 71%), which was significant (p = 0.050; Table 5.4).

Notable differences between BSN+ and BSN- sites that were not significant included: average conductivity, fish presence, and vegetation cover. Average conductivity at BSN+ sites (536.70 µS/cm ± 495.34) was lower than BSN- sites (1569.29 µS/cm ± 2486.29), although this difference was not significant (p = 0.131). There was no significant difference (p = 0.360) between fish presence at BSN+ (4/16 sites; 25%) and BSN- sites (17/45 sites; ca. 38%). However, the only fish identified at BSN+ sites were Western Mosquitofish (*Gambusia affinis*; Poeciliidae). Slightly larger fish belonging to the families Cyprinodontidae, Centrarchidae, and Fundulidae were observed at several BSN- sites. There were no significant differences in aquatic vegetation cover between BSN+ and BSN- sites. Although submerged and or emergent vegetation covered at least 20% of the water body (ca. 96%) of the time when eDNA samples were taken at BSN+ sites.

Soil.— Soil samples were taken all sites included within this study, with the exception of one site which had a concrete basin (TNC Southmost Preserve, Siren Pond). We were unable to collect soil at 30 or 60 cm at another site due to border wall construction activities (Lower Rio Grande Valley NWR, San Francisco Banco Tract, canal). We were also unable to collect soil at 60 cm from three additional sites: US Hwy 77, W side, ca. 1.0 rd km N Kenedy/Willacy county line; US Hwy 77, E side, ca. 1.6 rd km N jct La Chata gate #4; and Cameron County Site #2 due to difficulties reaching the 60 cm depth.

The soil variables that differed significantly between BSN+ and BSN- sites at the surface were: copper concentration, phosphorous concentration, magnesium concentration, nitrogen concentration, manganese concentration, potassium concentration, iron concentration, sand percentage, clay percentage, and organic matter percentage (Figures 5.3, 5.4). The average surface cooper concentration was significantly higher ($p < 0.001$) at BSN+ sites (2.11 ppm ± 1.19) compared to BSN- sites (0.88 ppm ± 0.77). The average surface phosphorous concentration was significantly higher (p = 0.005) at BSN+ sites (61.64 ppm ± 37.34) compared to BSN- sites (33.43 ppm ± 20.04). The average surface magnesium concentration was significantly higher (p = 0.002) at BSN+ sites (768.21 ppm ± 484.63) compared to BSN- sites (399.92 ppm ± 323.05). The average surface nitrogen concentration was significantly higher (p = 0.016) at BSN+ sites (27.29 ppm ± 27.98) compared to BSN- sites (12.85 ppm ± 14.30). The average surface manganese concentration was significantly higher (p = 0.024) at BSN+ sites (11.74 ppm ± 7.42) compared to BSN- sites (7.40 ppm ± 5.27). The average surface potassium concentration was significantly higher (p = 0.026) at BSN+ sites (668.79 ppm ± 249.84) compared to BSN- sites (486.28 ppm ± 289.45). The average surface iron concentration was significantly higher (p = 0.003) at BSN+ sites (36.96 ppm ± 29.53) compared to BSN- sites (20.61 ppm ± 22.93). The average surface clay percentage was significantly higher ($p < 0.001$) at BSN+ sites (43.47 ± 18.13) compared to BSN- sites (23.96 ± 16.48) and the average surface sand percentage was significantly lower ($p < 0.001$) at BSN+ sites (34.07 ± 17.82) compared to BSN- sites (59.70 ± 23.16). Finally, average surface organic matter

percentage was significantly lower ($p = 0.004$) at BSN+ sites (7.69 ± 5.12) compared to BSN- sites (4.10 ± 3.172).

The soil variables that differed significantly between BSN+ and BSN- sites at 30 cm were: copper concentration, iron concentration, potassium concentration, manganese concentration, magnesium concentration, zinc concentration, phosphorous concentration, clay percentage, sand percentage, and organic matter percentage (Figures 5.5, 5.6). The average 30 cm cooper concentration was significantly higher ($p < 0.001$) at BSN+ sites (1.70 ppm ± 1.08) compared to BSN- sites (0.60 ppm ± 0.36). The average 30 cm iron concentration was significantly higher ($p < 0.001$) at BSN+ sites (23.74 ppm ± 20.30) compared to BSN- sites (10.20 ppm ± 6.69). The average 30 cm potassium concentration was significantly higher ($p < 0.001$) at BSN+ sites (591.00 ppm ± 194.10) compared to BSN- sites (340.53 ppm ± 230.16). The average 30 cm manganese concentration was significantly higher ($p < 0.001$) at BSN+ sites (7.35 ppm ± 8.94) compared to BSN- sites (3.37 ppm ± 3.8). The average 30 cm magnesium concentration was significantly higher ($p = 0.001$) at BSN+ sites (791.60 ppm ± 399.50) compared to BSN- sites (415.044 ppm ± 316.91). The average 30 cm zinc concentration was significantly higher ($p = 0.003$) at BSN+ sites (0.73 ppm ± 0.75) compared to BSN- sites (0.31 ppm ± 0.51). The average 30 cm phosphorous concentration was significantly higher ($p = 0.024$) at BSN+ sites (30.53 ppm ± 32.14) compared to BSN- sites (14.93 ppm ± 25.02). The average 30 cm clay percentage was significantly higher ($p < 0.001$) at BSN+ sites (47.20 ± 15.93) compared to BSN- sites (27.311 ± 18.40). The average 30 cm sand percentage was significantly lower ($p = 0.002$) at BSN+ sites (30.87 ± 19.88) compared to BSN- sites (57.18 ± 26.40). The average 30 cm organic matter percentage was significantly higher ($p = 0.001$) at BSN+ sites (1.53 ± 0.87) compared to BSN- sites (0.76 ± 0.67).

The variables that differed significantly between BSN+ and BSN- sites at 60 cm include: copper concentration, zinc concentration, magnesium concentration, potassium concentration, , iron concentration, boron concentration, phosphorous concentration, clay percentage, sand percentage, and organic matter percentage (Figures 5.7, 5.8). The average 60 cm cooper concentration was significantly higher ($p < 0.001$) at BSN+ sites (1.43 ppm ± 1.04) compared to BSN- sites (0.49 ppm ± 0.29). The average 60 cm zinc concentration was significantly higher ($p < 0.001$) at BSN+ sites (0.70 ppm ± 1.06) compared to BSN- sites (0.11 ppm ± 0.15). The average 60 cm magnesium concentration was significantly higher ($p < 0.001$) at BSN+ sites (827.50 ppm ± 438.49) compared to BSN- sites (427.28 ppm ± 303.43). The average 60 cm potassium concentration was significantly higher ($p = 0.002$) at BSN+ sites (518.86 ppm ± 213.49) compared to BSN- sites (310.88 ppm ± 205.78). The average 60 cm iron concentration was significantly higher ($p = 0.006$) at BSN+ sites (18.32 ppm ± 17.96) compared to BSN- sites (7.97 ppm ± 7.27). The average 60 cm boron concentration was significantly higher ($p = 0.007$) at BSN+ sites (2.098 ppm ± 1.26) compared to BSN- sites (1.21 ppm ± 1.48). The average 60 cm phosphorous concentration was significantly higher ($p = 0.023$) at BSN+ sites (36.93 ppm ± 52.10) compared to BSN- sites (11.84 ppm ± 25.84). The average 60 cm clay percentage was significantly higher ($p < 0.001$) at BSN+ sites (44.85 ± 17.29) compared to BSN- sites (26.19 ± 15.40). The average 60 cm sand percentage was significantly lower ($p = 0.002$) at BSN+ sites (31.36 ± 22.94) compared to BSN- sites (57.67 ± 23.85). Finally, the average 60 cm organic matter percentage was significantly higher ($p = 0.001$) at BSN+ sites (1.27 ± 1.08) compared to BSN- sites (0.47 ± 0.45).

At the surface, copper concentration was highly correlated to clay percentage ($\rho = 0.75$) and sand percentage ($\rho = -0.74$), so copper was removed for analysis for the logistic regression model incorporating the soil surface data. At 30 cm clay percentage was highly correlated to potassium concentration ($\rho = 0.82$), and magnesium concentration ($\rho = 0.74$), so magnesium and potassium

were removed for analysis for the logistic regression model incorporating the soil 30 cm data. At 60 cm clay percentage was highly correlated to potassium concentration ($\rho = 0.74$), so potassium was removed for analysis for the logistic regression model incorporated the soil 60 cm data. Clay percentage and sand percentage were highly negatively correlated at the surface ($\rho = -0.91$), at 30 cm ($\rho = -0.91$), and at 60 cm ($\rho = -0.87$), however both clay percentage and sand percentage were included for analysis.

The textural analysis revealed that BSN+ sites were classified as clay (n = 8), silty clay loam (n = 5), or clay loam (n = 2). In this study, the BSN+ sites were not classified as any of the other categories (loam, sand, sandy loam, silty clay, silty loam, sandy clay, or sandy clay loam).

DISCUSSION

All sites where Black-spotted Newts have been detected recently were ephemeral, which is consistent with what has been reported by Mecham (1968a) and Rappole and Klicka (1991). The lack of recent Black-spotted Newt records from permanent sites likely explains why BSN+ sites had significantly lower levels of dissolved oxygen compared to BSN- sites, as higher levels of dissolved oxygen are associated with larger, more permanent water bodies (Colburn 2004). In addition, higher levels of dissolved oxygen are needed to support larger fish species (Dean and Richardson 1999). In this case, the significantly higher levels of dissolved oxygen in BSN- sites may represent permanent ponds that are not suitable for Black-spotted Newts. In this study, no Black-spotted Newt detections were obtained from the 10 permanent water bodies sampled. Permanent water bodies should not be the focus of future surveys, with the exception of La Joya and Walker Lakes in Hidalgo County, where Black-spotted Newts has been observed on multiple occasions (TNHC 6116–6141; Mayborn Museum Complex, Strecker Museum, Baylor University [SMBU] 15125–15141; Carnegie Museum of Natural History [CM] 25838–25840, 62295–62296, AMNH 182322; LSUMZ 6827–6830).

Mecham (1968a) reported that Black-spotted Newts can be found in roadside ditches, and Rappole and Klicka (1991) identified a stretch of US Hwy 77 in Kenedy County as a "metapopulation center". However, the absence of nearby paved roads was a shared characteristic among all sites in which Black-spotted Newts have been detected in recent years. Several sampling sites (n = 5) were classified as roadside ditches, but no positive detections of newts were obtained through traditional methods or eDNA. Many ponds and ditches along this stretch have since been impacted by construction activities, which has caused erosion and siltation at two sampling sites (US Hwy 77, W side, ca. 1.0 rd km N Kenedy/Willacy county line; US Hwy 77, E side, ca. 1.6 rd km N jct La Chata gate #4). Further, dirt roads running parallel to US Hwy 77 along this stretch of highway in Kenedy County are frequented by Customs and Border Patrol (CBP) vehicles. These vehicles drag tires behind them to monitor foot traffic from illegal immigrants. Tire-dragging and the utilization of these dirt roads could serve as a direct threat to Black-spotted Newts and other wildlife along US Hwy 77. Roadside ditches along US Hwy 77 in Kenedy County, particularly those unimpacted by construction and adjacent CBP roads, should continue to be investigated. Although the absence of paved roads was the only surrounding land use category that differed significantly between BSN+ and BSN- sites, the absence of nearby development was recorded at eleven of the sixteen sites where Black-spotted Newts have been detected in recent years, while, rangeland (n = 3), row-crops (n = 2), and residential/developed (n = 1) were less common. Unfortunately, very few remaining tracts of undeveloped land exist in south Texas (Jahrsdoerfer and Leslie 1988), so working with ranches and other private landowners will be essential for the conservation of this species.

In the 30 cm and 60 cm logistic regression models it was shown that higher concentrations of copper in the soil can help predict Black-spotted Newt presence. Copper levels at BSN+ sites were significantly higher compared to BSN- sites across all soil depths (surface, 30 cm, 60 cm), and nine of the ten highest copper (ppm) concentrations were reported at the 30 cm depth from BSN+ sites. The average levels of copper at BSN+ sites ranged from 1.45 ppm ± 1.075 at 60 cm to 2.04 ppm ± 1.178 at the surface, which are at or are slightly below the normal levels of copper in the soil, which reportedly range from 2–250 ppm (Dorsey et al. 2004). The average levels of copper at BSN- sites ranged from 0.49 ppm ± 0.29 at 60 cm to 0.88 ppm ± 0.78 at the surface. Copper levels below 1.0 ppm in the soil can be indicative of a copper deficiency (Solberg et al. 1999).

Clay soils have a higher nutrient holding capability compared to loamy and sandy soils (Gatiboni 2022), therefore the differences in some nutrient and micronutrient levels (including copper) between BSN+ and BSN- sites could be attributed to a higher percentage of clay found at BSN+ sites. Additionally, the soil composition is likely a more biologically meaningful predictor than copper concentration. It has previously been reported that Black-spotted Newts occupy ponds with Edroy and Tiocano clay soils (Rappole and Klicka 1991), and the results of this study reaffirm this assertion as BSN+ sites had a significantly higher percentages of clay and significantly lower percentages of sand compared to BSN- sites. At BSN+ sites, the minimum clay percentage was 6% at the surface, 26% at 30 cm, and 21% at 60 cm, while the maximum percentage of sand was 67% at the surface, 68% at 30 cm, and 72% at 60 cm. These minimum and maximum values could serve as indicators of potentially suitable habitat. Waudby and Petit (2017) reported that cracks within clay soils moderate temperature and humidity in desert environments and because Black-spotted Newts are thought to remain at breeding sites when they dry, such refugia and clay soils are likely required for individuals to persist at a given site. This is in contrast to the congeneric Striped Newt (*N. perstriatus*) and Eastern Newt (*N. viridescens*), which migrate away from ephemeral breeding ponds when they dry (Gill 1978; Dodd 1993).

BSN+ sites had a significantly higher average percentage of organic matter compared to BSN- sites at all three depths (surface, 30 cm, and 60 cm), which is consistent with the finding that organic carbon content at the surface contributed significantly in a constrictive Maxent model for Black-spotted Newt distribution (Bare 2018). Higher organic matter in the soils could be advantageous for Black-spotted Newts because organic matter is an important food sources for many invertebrates (Nadkarni and Longino 1990), which are common prey items (Rappole and Klicka 1991). In addition, Van Meter et al. (2016) found that higher levels of organic matter significantly decreased the bioaccumulation of pesticides in American Toads (*Anaxyrus americanus*), thus low soil organic matter concentrations could increase the risk of pesticide exposure in Black-spotted Newts, particularly in agricultural and developed areas.

Although the presence/absence of amphibians was significant between BSN+ and BSN- sites there were no clear species associations, as many species were observed at both BSN+ and BSN- sites. Both Judd (1985) and Rappole and Klicka (1991) reported an association between Black-spotted Newts and Lesser Sirens (*S. intermedia*), and, although sirens were only observed at one site during our sampling, there are records of sirens at three other BSN+ sites (Palo Alto National Battlefield, Crescent Tank [Drew R. Davis Field Series (DRD) 5131]; Cameron County Site #2 [TNHC 116624]; Cameron County Site #4 [TNHC 116993–116997]) and anecdotal evidence from Cameron County Site #3 (M. Pons, pers. comm). Characterizing the amphibian community assemblages at BSN+ sites using eDNA metabarcoding may provide more information on Black-spotted Newt community associations.

While there was no significant difference between fish presence at BSN+ and BSN- sites, fish were absent from the majority of water bodies where Black-spotted Newts have been detected recently when eDNA samples were taken (ca. 82%). These results support the previously established perception that these newts do not co-occur with larger, potentially predatory fish (Judd 1985; Rappole and Klicka 1991). Sites with minimal vegetation are likely unsuitable because, aquatic vegetation, in some form, is needed for Black-spotted Newts to successfully lay eggs and likely provides for larvae cover from predators. In addition, submergent vegetation had been linked to higher invertebrate diversity (Dvořák 1987), which are common prey items for Black-spotted Newts (Rappole and Klicka 1991).

The average level of conductivity was a significant predictor variable in each of the three logistic regression models. The average conductivity at BSN+ sites was lower than BSN- sites. These results are consistent with the anecdotal evidence from Rappole and Klicka (1991), who did not find Black-spotted Newts in saline water bodies. However, Wittig and Brown (1997) showed that Eastern Newts have a greater sodium tolerance than many other amphibians, and Lee and Kent (2020) observed an Eastern Newt swimming in the Chesapeake Bay, seemingly unimpacted by the saline environment. The maximum conductivity at BSN+ sites was 2073 µS/cm; conductivity in water bodies significantly greater than this value may not be suitable for Black-spotted Newts, but future laboratory tests are required to better understand what levels of conductivity are within a suitable range for this species.

Taken together, many of the BSN- sites may not be suitable due to their soil composition, permanence, proximity to paved roads, conductivity, or absence of aquatic vegetation. Table 5.5 lists the sampling sites included in this study along with variables that were associated with Black-spotted Newt presence/absence and Table 5.6 lists minimum and maximum values for a selection of continuous variables. Sites that have low levels of clay (< 20%) and high percentages of sand (> 75%) at 30 and 60 cm are likely not suitable for Black-spotted Newts. In addition, all BSN+ sites were ephemeral and paved roads were absent from the immediate vicinity of the water body. Black-spotted Newts were not found in water bodies with high levels of conductivity (> 2500 µS/cm) or those that lacked sufficient submerged or emergent vegetation (< 20%). These variables should continue to be investigated but can serve to inform future *N. meridionalis* sampling localities.

Table 5.1. Logistic regression model assessed with AIC ranking criteria to determine water, habitat, and soil (surface) variables that predict Black-spotted Newt presence in south Texas, USA.

					Wald Test		Model Evaluation	
Model	**Predictor**	**β**	**Robust SE**	**Odds Ratio**	**Wald $\chi 2$**	**p**	**McFadden R^2**	**p**
null	Intercept	-1.099	0.298	0.333	13.578	< 0.001		
1	Intercept	1.789	0.829	5.985	4.208	0.031	0.231	< 0.001
	Sand %	-0.063	0.020	0.939	9.819	0.002		
2	Intercept	1.965	0.843	7.135	4.786	0.02	0.354	0.004
	Sand %	-0.057	0.018	0.945	8.354	0.002		
	Paved Road?	-18.394	0.496	1.027e -8	6.197e -5	< 0.001		
3	Intercept	3.151	1.069	23.362	6.654	0.003	0.444	0.014
	Sand %	-0.063	0.02	0.939	8.205	0.002		
	Paved Road?	-18.298	0.531	1.131e -8	6.567e -5	< 0.001		
	Conductivity	-0.001	0.001	0.999	2.496	0.025		
4	Intercept	-15.999	1.154	1.126e -7	1.226e -5	< 0.001	0.531	0.015
	Sand %	-0.071	0.025	0.932	7.846	0.004		
	Paved Road?	-19.422	0.579	3.672e -9	2.863e -5	< 0.001		
	Conductivity	-0.001	0.000	0.999	2.445	0.021		
	Ephemeral?	19.799	0.842	3.968e +8	1.877e -5	< 0.001		

Table 5.2. Logistic regression model assessed with AIC ranking criteria to determine water, habitat, and soil (30 cm) variables that predict Black-spotted Newt presence in south Texas, USA.

					Wald Test		Model Evaluation	
Model	**Predictor**	**β**	**Robust SE**	**Odds Ratio**	**Wald χ2**	**p**	**McFadden R^2**	**p**
null	Intercept	-1.076	0.299	0.341	12.955	< 0.001		
1	Intercept	-4.192	1.030	0.015	16.500	< 0.001	0.392	< 0.001
	Copper ppm	3.300	0.925	27.099	10.914	< 0.001		
2	Intercept	-3.536	0.953	0.029	12.125	< 0.001	0.510	0.005
	Copper ppm	3.217	0.978	24.956	9.250	0.001		
	Paved Road?	-18.478	0.552	9.438e -9	5.778e -5	< 0.001		
3	Intercept	-25.421	2.021	9.119e -12	2.951e -5	< 0.001	0.617	0.008
	Copper ppm	4.599	1.194	99.403	7.159	< 0.001		
	Paved Road?	-19.723	0.594	2.719e -9	2.668e -5	< 0.001		
	Ephemeral?	21.150	1.181	1.532e +9	2.043e -5	< 0.001		
4	Intercept	-26.482	2.679	3.156e -12	3.577e -5	< 0.001	0.694	0.023
	Copper ppm	5.719	1.664	304.597	6.604	< 0.001		
	Paved Road?	-19.461	0.725	3.532e -9	2.881e -5	< 0.001		
	Ephemeral?	22.665	1.748	6.971e +9	2.620e -5	< 0.001		
	Conductivity	-0.002	0.001	0.998	2.403	0.018		

Table 5.3. Logistic regression model assessed with AIC ranking criteria to determine water, habitat, and soil (60 cm) variables that predict Black-spotted Newt presence in south Texas, USA.

					Wald Test		Model Evaluation	
Model	**Predictor**	**β**	**Robust SE**	**Odds Ratio**	**Wald $\chi 2$**	**p**	**McFadden R^2**	**p**
null	Intercept	-1.099	0.309	0.333	12.673	< 0.001		
1	Intercept	-3.683	0.830	0.025	17.696	< 0.001	0.363	< 0.001
	Copper ppm	3.355	0.845	28.638	10.746	< 0.001		
2	Intercept	-3.227	0.847	0.040	12.094	< 0.001	0.473	0.008
	Copper ppm	3.398	0.918	29.905	8.509	< 0.001		
	Paved Road?	-18.524	0.658	9.023e -9	5.198e -5	< 0.001		
3	Intercept	-2.438	0.957	0.087	5.936	0.011	0.547	0.031
	Copper ppm	3.739	1.162	42.076	7.448	0.001		
	Paved Road?	-18.362	0.644	1.061e -8	5.454e -5	< 0.001		
	Conductivity	-0.001	0.001	0.999	2.542	0.032		
4	Intercept	-22.215	1.811	2.251e -10	2.084e -5	< 0.001	0.615	0.039
	Copper ppm	4.338	1.550	76.541	6.262	0.005		
	Paved Road?	-19.609	0.798	3.047e -9	2.484e -5	< 0.001		
	Conductivity	-0.002	0.001	0.998	2.421	0.019		
	Ephemeral?	19.788	1.346	3.923e +8	1.653e -5	< 0.001		

Table 5.4. Contingency tables for binary predictor variables: A) proximity to paved road; B) if the wetland was ephemeral; C) if other amphibians were detected; and D) if the wetland was dredged.

A)

Paved Road?	Recent Detection? NO	YES	Total
NO	28	16	44
YES	17	0	17
Total	45	16	61

Chi-Squared test p-value = 0.004

B)

Ephemeral?	Recent Detection? NO	YES	Total
NO	10	0	10
YES	35	16	51
Total	45	16	61

Chi-Squared test p-value = 0.039

C)

Amphibians?	Recent Detection? NO	YES	Total
NO	14	1	15
YES	31	15	46
Total	45	16	61

Chi-Squared test p-value = 0.047

D)

Dredged?	Recent Detection? NO	YES	Total
NO	13	9	22
YES	32	7	39
Total	45	16	61

Chi-Squared test p-value = 0.050

Table 5.5. List of sampling sites and a selection of variables associated with Black-spotted Newt presence/absence. Maximum conductivity is measured in µS/cm. Maximum rooted vegetation (Max. Rooted Veg. %) is the maximum value of summed of submerged and emergent vegetation percentages from each sampling site. Descriptive names for private property have been generalized and specific GPS coordinates have been redacted in this table.

Site #	County	Site Name	Paved Roads?	Ephemeral?	Clay % 30 cm	Sand % 30 cm	Max. Conductivity	Max. Rooted Veg. %
1	Victoria	Coleto Creek at US Hwy 77	Y	N	0	100	776	45
2	Goliad	Manahuilla Creek at US Hwy 59	Y	Y	1	97	2640	35
3	Bee	Bee County Site #1	N	Y	17	75	123.6	95
4	Live Oak	Live Oak County Park, pond SE of parking area	N	Y	37	36	211.4	80
5	McMullen	Hwy 16 bridge over Nueces River	Y	Y	51	33	-	-
6	Aransas	Aransas NWR, ca. 0.2 rd km S jct Auto Loop Trail end and main road	N	Y	18	76	183.4	15
7	Calhoun	Aransas NWR, Auto Loop Trail, ca. 0.6 rd km SW from observation towers	N	Y	11	83	2500	20
8	San Patricio	San Patricio County Site #1	N	Y	0	100	1647	80
9	San Patricio	San Patricio County Site #2	N	Y	35	39	445	5
10	San Patricio	San Patricio County Site #3	N	N	37	33	585	50
11	Refugio	ditch crossing 1st St, ca. 0.1 rd km SW jct Cole	Y	Y	45	35	7470	30
12	Jim Wells	dugout pond along TX Hwy 359, SW bridge over Nueces River	Y	N	39	42	502	10
13	San Patricio	San Patricio County Site #4	N	Y	49	29	26200	60
14	San Patricio	San Patricio County Site #5	N	Y	53	31	2900	100
15	Nueces	John J. Sablatura Park, flooded field along Agua Dulce Creek	Y	Y	27	56	347	70
16	Duval	San Diego Creek W of TX Hwy 359	Y	Y	31	54	215.3	15
17	Nueces	Pintas Creek at Co Rd 70	Y	Y	37	49	610	60
18	Kleberg	TAMU-Kingsville CKWRI, South Pasture pond	N	Y	61	25	222	95
19	Kleberg	Kleberg County Site #1	N	Y	35	52	154.3	40
20	Kleberg	Kleberg County Site #2	Y	Y	21	74	296	60
21	Kleberg	Kleberg County Site #3	Y	Y	11	80	649	95
22	Kenedy	Kenedy County Site #1	N	N	3	90	1920	0

23	Kenedy	Kenedy County Site #2	N	N	32	59	298	0
24	Kenedy	Kenedy County Site #3	N	N	4	92	2197	0
25	Brooks	Brooks County Site #1	N	N	0	94	1926	5
26	Kenedy	US Hwy 77, W side, ca. 12.0 rd km N Kenedy/Willacy county line	Y	Y	12	82	426	70
27	Kenedy	US Hwy 77, E side, ca. 8.5 rd km N Kenedy/Willacy county line	Y	Y	13	82	140.2	40
28	Kenedy	US Hwy 77, W side, ca. 1.0 rd km N Kenedy/Willacy county line	Y	Y	18	80	131.8	100
29	Willacy	US Hwy 77, E side, ca. 1.6 rd km N jct La Chata gate #4	Y	Y	1	98	249	80
30	Willacy	pond along Co Rd 398, ca. 0.7 rd km N jct Bay Ave	N	Y	13	80	149.2	30
31	Willacy	Willacy County Site #1	N	Y	26	68	221	80
32	Willacy	Willacy County Site #2	N	Y	48	43	213.4	90
33	Willacy	TX Hwy 186, N side ditch, ca. 1.1 rd km W East Foundation El Sauz Ranch gate near Huesos Tank	Y	Y	23	65	187.4	100
34	Hidalgo	Hidalgo County Site #1	N	Y	52	38	466	50
35	Hidalgo	Hidalgo County Site #2	N	Y	27	60	196.8	50
36	Starr	Starr County Site #1	N	N	9	39	310	100
37	Hidalgo	ravine along W side of irrigation canal along 12th St, ca. 0.3 rd km W jct Jesus Flores Rd	N	Y	20	67	4370	40
38	Hidalgo	ditch along Jesus Flores Rd, ca. 0.4 rd km S jct 12th St	N	Y	14	72	1680	75
39	Willacy	Lower Rio Grande Valley NWR, Willamar Tract, NE pond	N	Y	39	48	292	100
40	Willacy	Lower Rio Grande Valley NWR, Willamar Tract, S pond	N	Y	33	58	367	60
41	Willacy	Willacy County Site #3	N	Y	31	57	298	80
42	Willacy	Willacy County Site #4	N	Y	29	57	202.5	60
43	Cameron	Laguna Atascosa NWR, Newt Pond	N	Y	38	42	1131	55
44	Starr	Lower Rio Grande Valley NWR, San Francisco Banco Tract, canal	N	N	-	-	1516	70
45	Starr	Old Military Hwy, ca. 2.6 rd km ESE jct Co Rd 2360, pond #4	Y	Y	56	18	1256	40
46	Hidalgo	Hidalgo County Site #3	N	Y	17	41	7080	85
47	Hidalgo	Hidalgo County Site #4	N	Y	45	31	9220	15
48	Cameron	Laguna Atascosa NWR, Scum Pond	N	Y	62	18	312	55

49	Cameron	Laguna Atascosa NWR, Prairie Trail, pond #3	N	Y	35	53	1447	30
50	Cameron	Laguna Atascosa NWR, Prairie Trail, pond #2	N	Y	71	13	1809	70
51	Hidalgo	Hidalgo County Site #5	N	Y	41	5	1181	55
52	Cameron	Laguna Atascosa NWR, pond along Buena Vista Dr, ca. 0.4 rd km N jct Co Rd 510	Y	Y	51	26	6960	20
53	Hidalgo	Santa Ana NWR, Willow Lakes	N	N	65	11	742	90
54	Cameron	Laguna Atascosa NWR, TX Hwy 100, crossing 3A pond	Y	Y	55	18	1964	60
55	Cameron	Cameron County Site #1	N	Y	37	20	469	90
56	Cameron	Lower Rio Grande Valley NWR, Milagro East Tract, resaca	N	Y	22	44	1789	70
57	Cameron	Palo Alto National Battlefield, Crescent Tank	N	Y	72	4	502	90
58	Cameron	Palo Alto National Battlefield, American Tank	N	Y	58	19	184.7	35
59	Cameron	Palo Alto National Battlefield, dugout pond ca. 0.4 km SE visitor center	N	Y	33	18	492	90
60	Cameron	Cameron County Site #2	N	Y	67	9	1462	20
61	Cameron	Cameron County Site #3	N	Y	-	-	556	50
62	Cameron	Cameron County Site #4	N	Y	49	18	2073	80

Table 5.6. Minimum and maximum values for a selection of water quality and soil variables between Black-spotted Newt positive (BSN+) and negative (BSN-) sites.

	BSN+		BSN-	
Variable	**Min**	**Max**	**Min**	**Max**
Avg. Dissolved Oxygen (mg/mL)	0.54	12.81	0.43	20.44
Avg. Conductivity (µS /cm)	51.6	2073	49.4	26200
pH	6	9	6	9
Water Temperature (°C)	13.2	36.4	10.2	37.4
Surface Copper (ppm)	0.83	5.14	0.05	4.77
Surface Sand %	13	67	13	100
Surface Clay %	6	75	0	57
Surface Org. Matter %	2.18	20.95	0.06	13.08
30 cm Copper (ppm)	0.45	4.27	0.03	1.61
30 cm Sand %	4	68	5	100
30 cm Clay %	26	72	0	65
30 cm Org. Matter %	0.39	3.61	0.03	2.56
60 cm Copper (ppm)	0.3	4.1	0.03	1.25
60 cm Sand %	3	72	4	100
60 cm Clay %	21	71	0	59
60 cm Org. Matter %	0.26	3.91	0.04	2.41

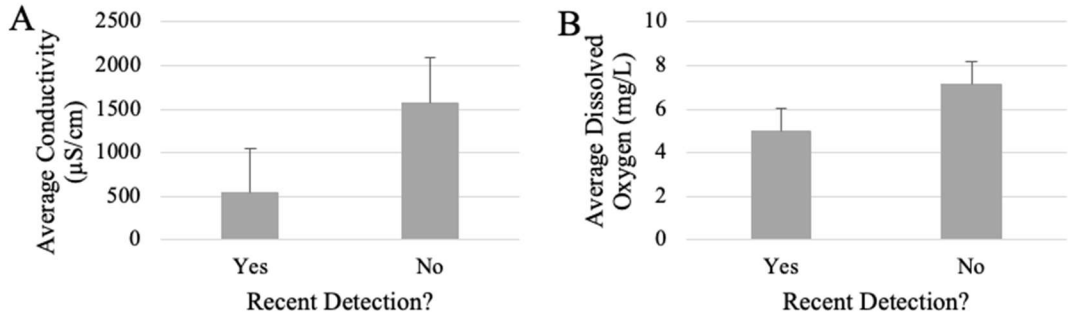

Figure 5.1. Differences in average conductivity (p = 0.131) (A) and average dissolved oxygen (p = 0.030) (B) between BSN+ and BSN- sites. Graphs are shown + 1 SE.

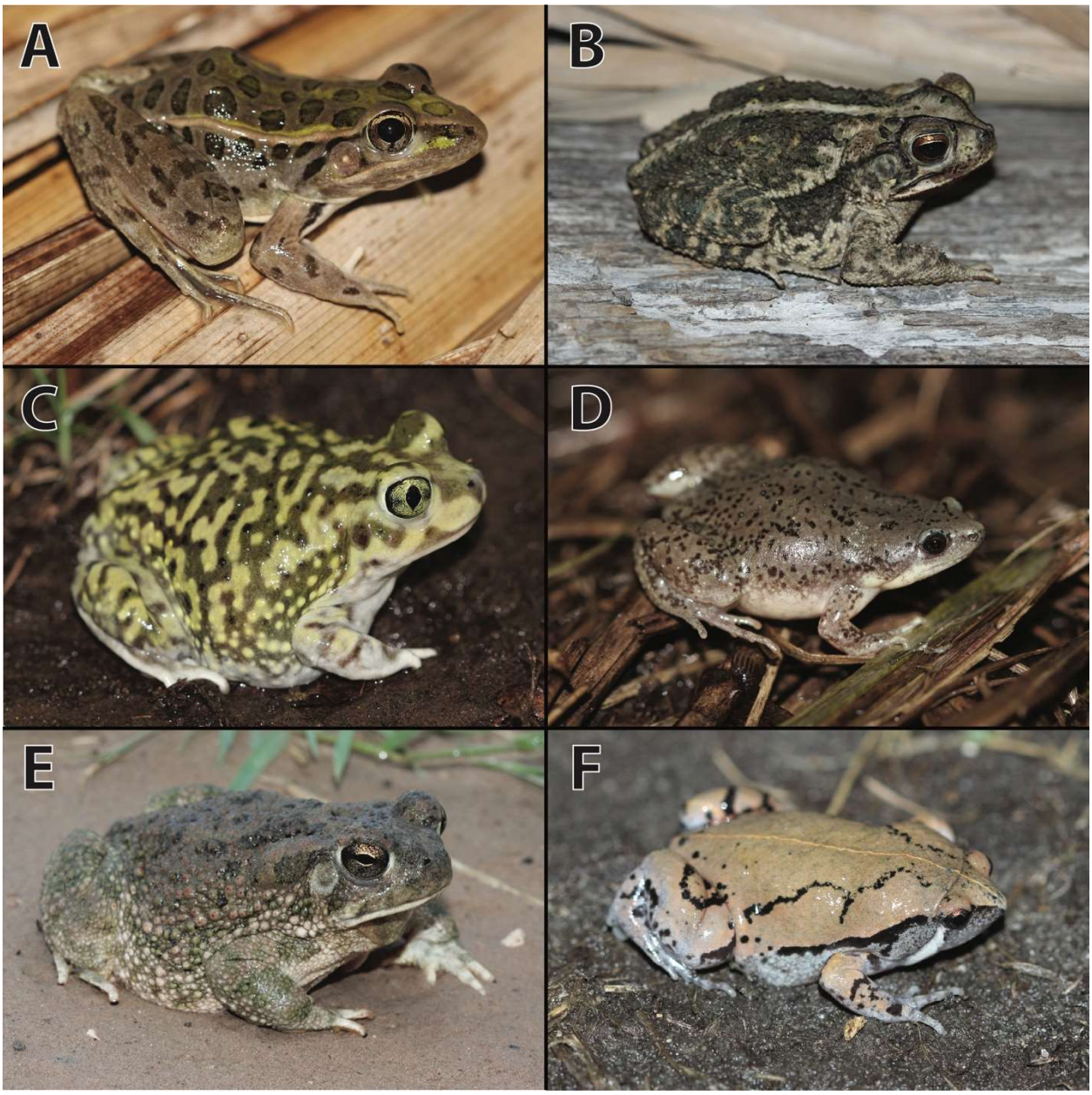

Figure 5.2. Selection of amphibians observed sympatric with Black-spotted Newts: A) Rio Grande Leopard Frog (*Rana berlandieri*); B) Gulf Coast Toad (*Incilius nebulifer*); C) Couch's Spadefoot (*Scaphiopus couchii*); D) Western Narrow-mouthed Frog (*Gastrophryne olivacea*); E) Texas Toad (*Anaxyrus speciosus*); and F) Sheep Frog (*Hypopachus variolosus*). All photos by DRD.

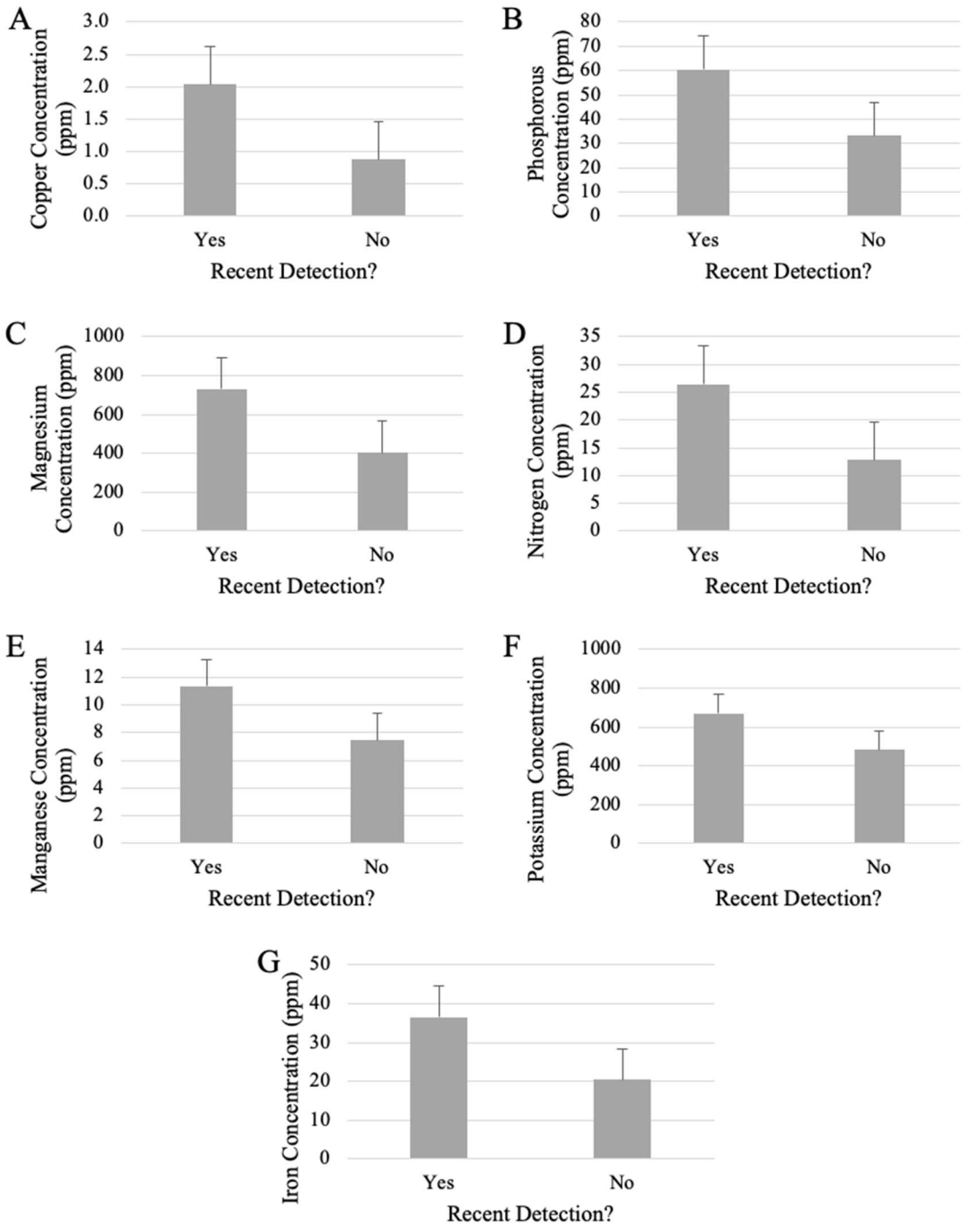

Figure 5.3. Differences in surface soil characteristics between BSN+ and BSN- sites: A) copper concentration ($p < 0.001$); B) phosphorous concentration ($p = 0.005$); C) magnesium concentration ($p = 0.002$); D) nitrogen concentration ($p = 0.016$); E) manganese concentration ($p = 0.024$); F) potassium concentration ($p = 0.026$), and G) iron concentration ($p = 0.003$). All means are + 1 SE.

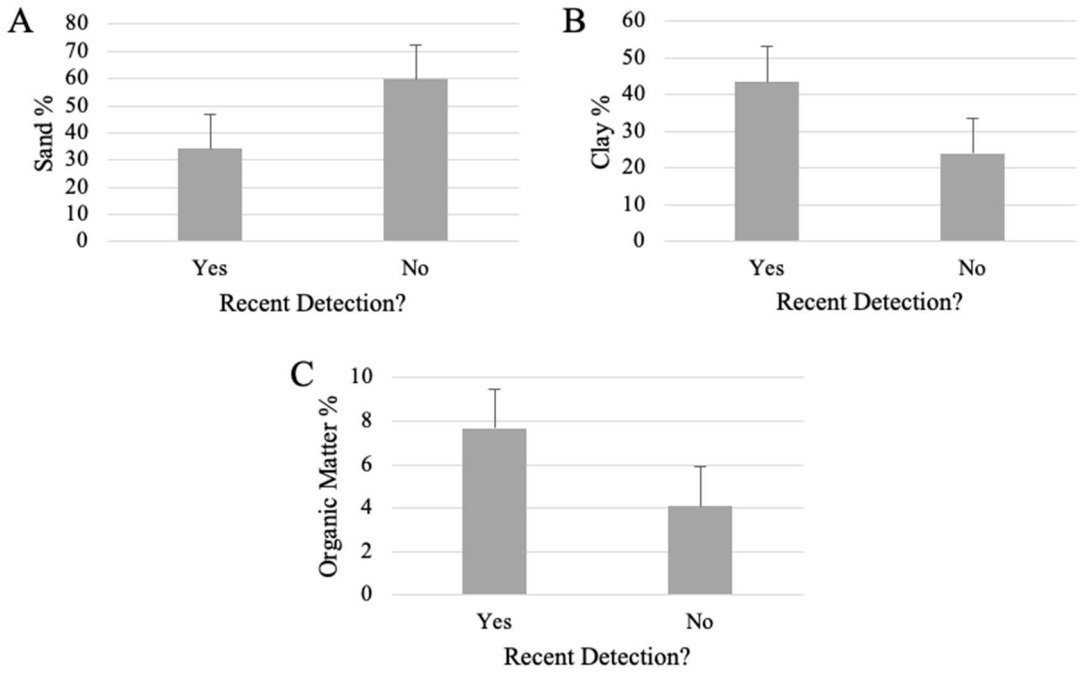

Figure 5.4. Differences in surface soil characteristics between BSN+ and BSN- sites: A) sand percentage ($p < 0.001$); B) clay percentage ($p < 0.001$); and C) organic matter percentage ($p = 0.004$). All means are + 1 SE.

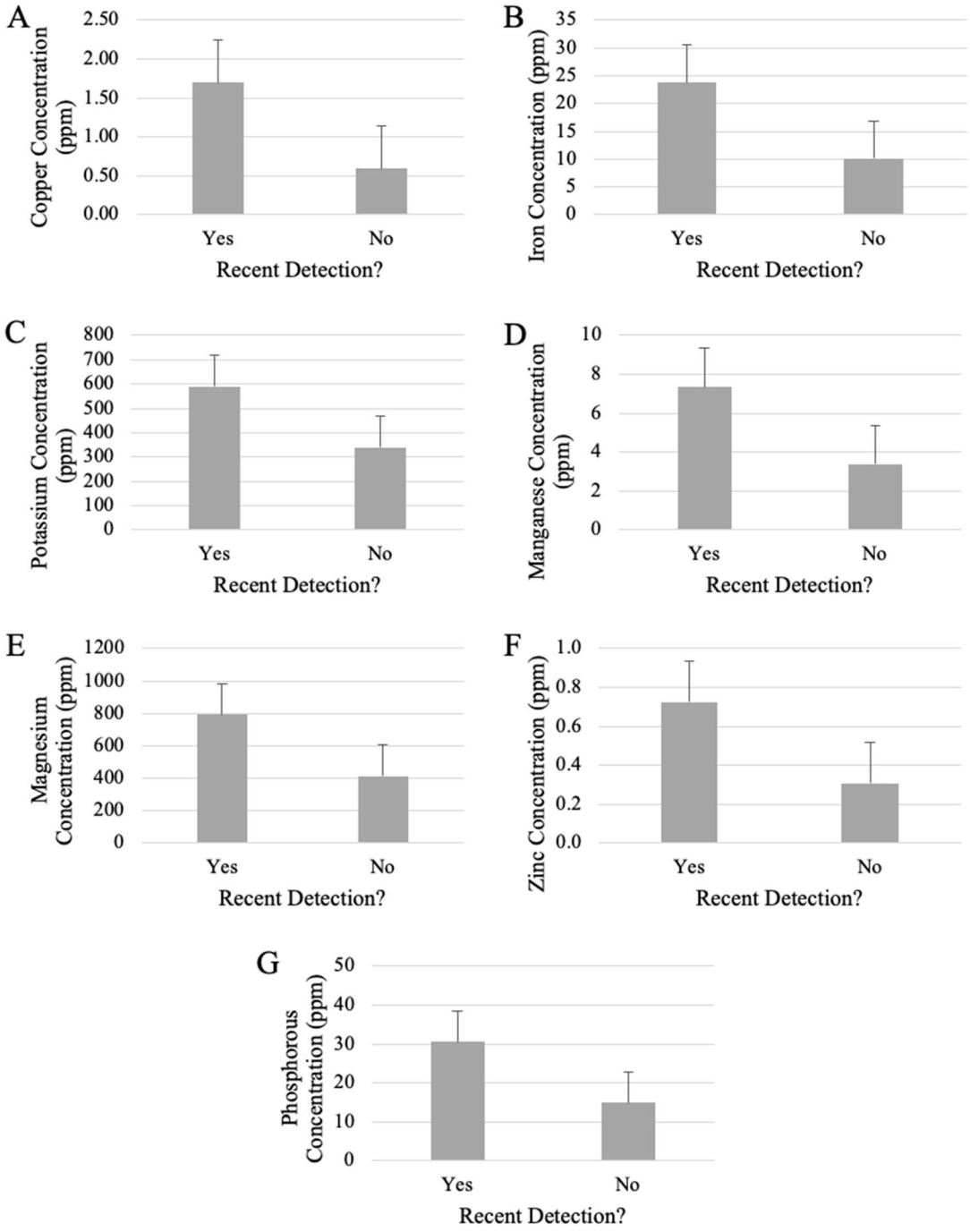

Figure 5.5. Differences in 30 cm soil characteristics between BSN+ and BSN- sites: A) copper concentration ($p < 0.001$); B) iron concentration ($p < 0.001$); C) potassium concentration ($p < 0.001$); D) manganese concentration ($p < 0.001$); E) magnesium concentration ($p = 0.001$); F) zinc concentration ($p = 0.003$); and G) phosphorous concentration ($p = 0.024$). All means are + 1 SE.

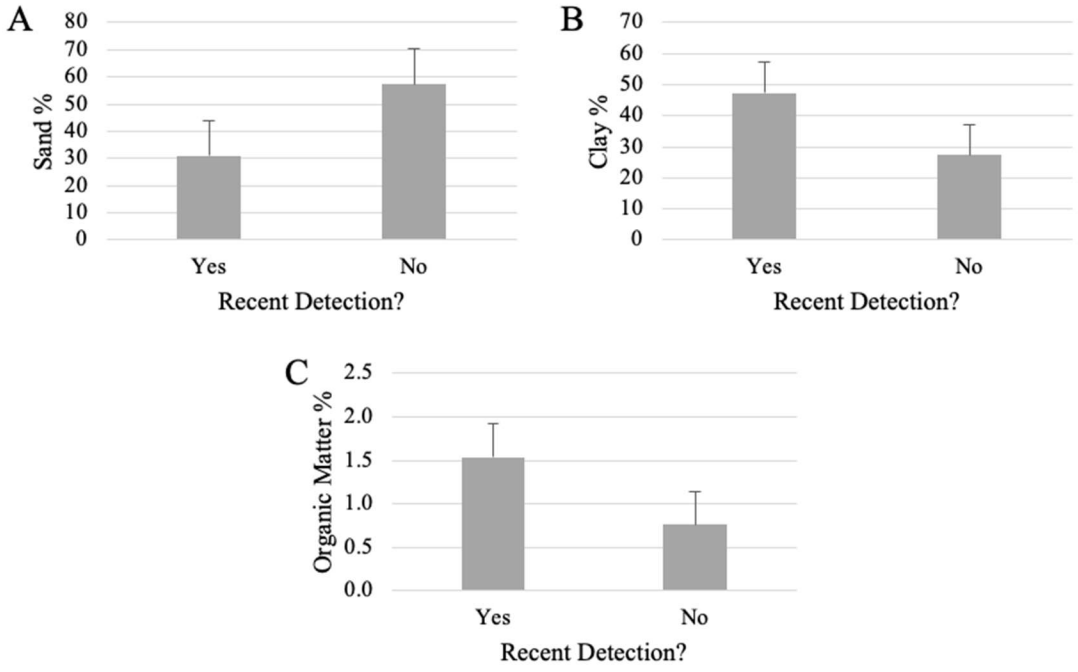

Figure 5.6. Differences in 30 cm soil characteristics between BSN+ and BSN- sites: A) sand percentage ($p = 0.002$); B) clay percentage ($p < 0.001$); and C) organic matter percentage ($p = 0.004$). All means are + 1 SE.

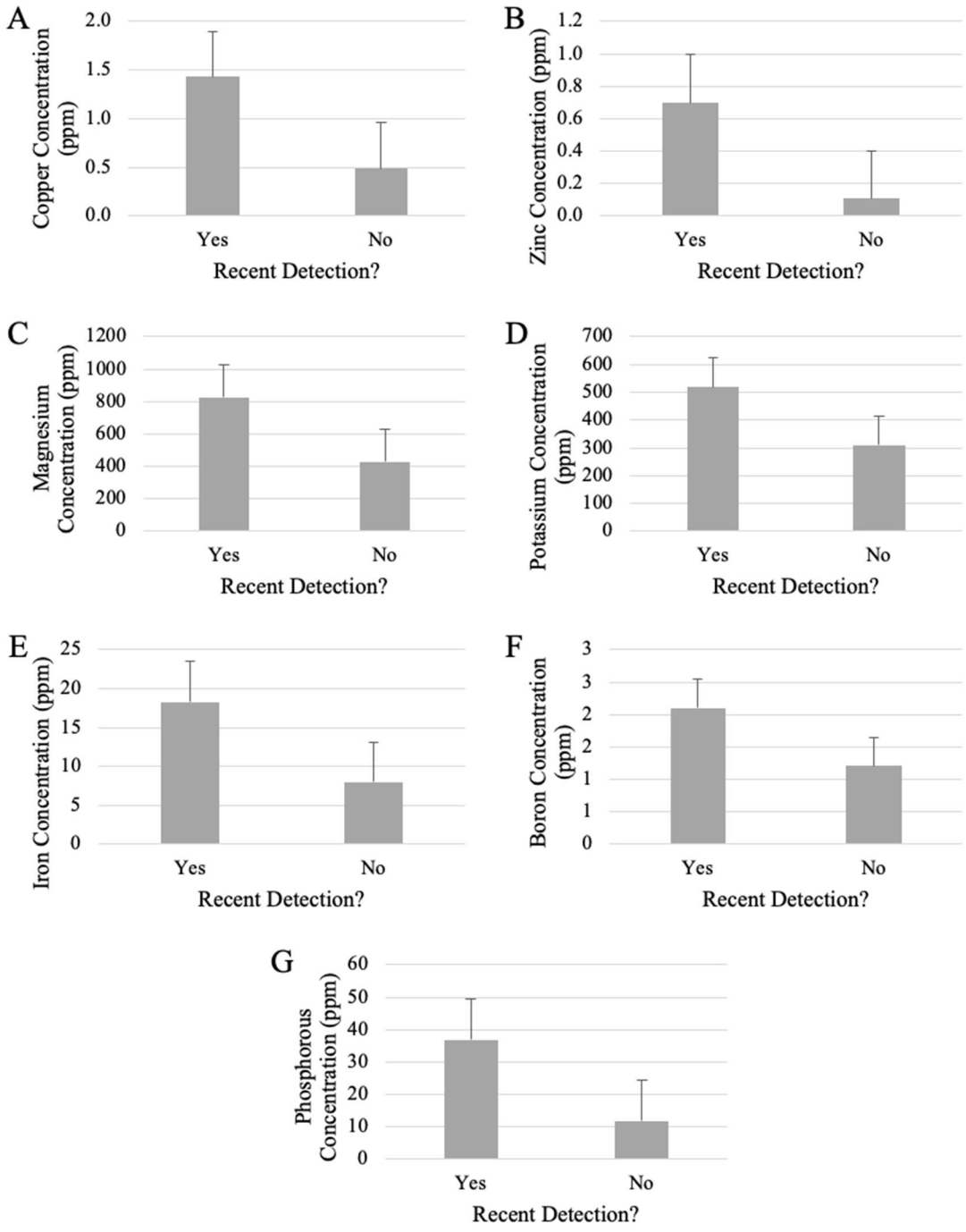

Figure 5.7. Differences in 60 cm soil characteristics between BSN+ and BSN- sites: A) copper concentration ($p < 0.001$); B) zinc concentration ($p < 0.001$); C) magnesium concentration ($p < 0.001$); D) potassium concentration ($p = 0.002$); E) iron concentration ($p = 0.006$); F) boron concentration ($p = 0.007$); and G) phosphorous concentration ($p = 0.023$). All means are + 1 SE.

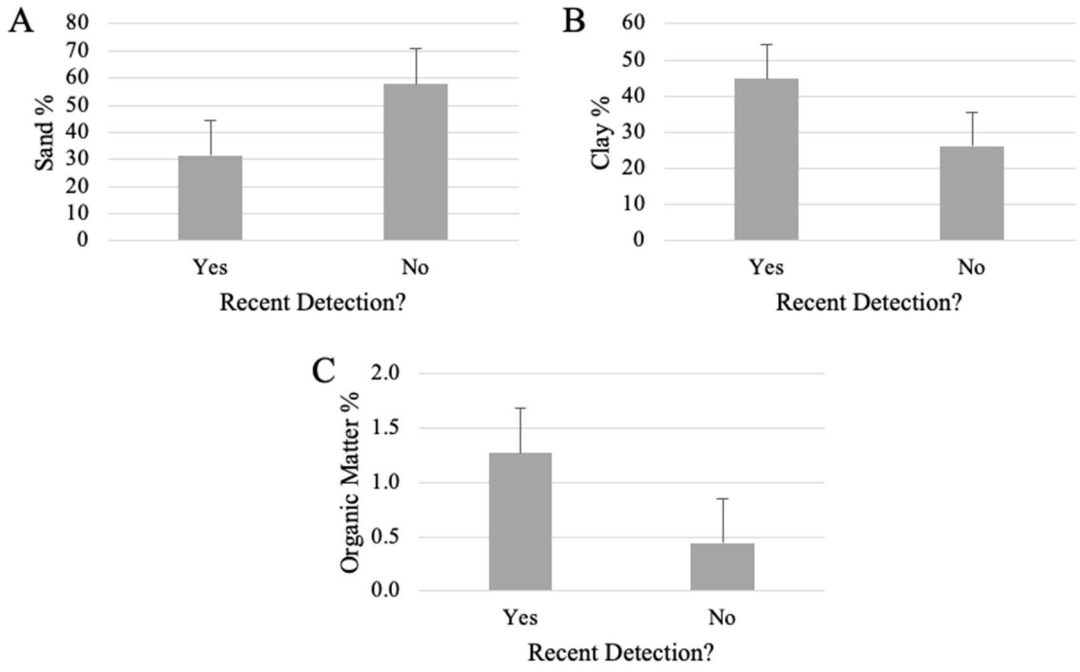

Figure 5.8. Differences in 60 cm soil characteristics between BSN+ and BSN- sites: A) sand percentage ($p = 0.001$); B) clay percentage ($p < 0.001$); and C) organic matter percentage ($p = 0.002$). All means are + 1 SE.

CHAPTER 6

TASK 5. Developing a metabarcoding assay to detect south Texas amphibians and a comparison with single-species assays

OVERVIEW

Chapter 6 involves the development, validation, and testing of an eDNA metabarcoding assay for south Texas amphibians, including the Black-spotted Newt. Our assay was developed following Valentini et al. (2016) and validated with 33 species of regional amphibians. We also amplified eDNA of amphibians from 24 sites across south Texas to characterize local amphibian communities and compared these results to amphibian detections from traditional methods. Additionally, we compared this metabarcoding approach to targeted (single-species) eDNA assays in the detection of two imperiled species that different in their abundance and ecology, the Black-spotted Newt and the Lesser Siren. We successfully validated the metabarcoding with 32 of the 33 tested species and detected 13 species and two genera, significantly more amphibian taxonomic units than detected with traditional methods. The targeted eDNA assay detected Black-spotted Newts at ten sites (41.7%); the eDNA metabarcoding assay had a much lower number of detections at only one site (4.2%). The targeted eDNA assay detected Lesser Sirens at 16 sites (66.7%), and the eDNA metabarcoding assay had detections at 15 sites (62.5%). In sum, our data suggest that while eDNA metabarcoding can detect more amphibians than traditional methods alone, metabarcoding performed poorly at detecting the Black-spotted Newt, a rare species across the landscape, compared to a targeted (single-species) assay. This chapter addresses Goals 1 (in part), 2 (in part), and 4 (in part) of the project. Portions of this chapter were published in Collins (2022).

METHODS

Study Area.—We sampled 24 unique wetlands, generally following rain events, from 2020–2021 (Table 6.1). Sites were chosen based on being previously identified as potential Black-spotted Newt habitat by Bare (2018) and Robinson et al. (2022).

Amphibian Species Validated and Tissue Extraction.—According to a review of the literature (Dixon 2013), we determined that 33 amphibian species may occur in our sampled sites across the study area. Tissue samples for these 33 amphibian species were collected from sampled amphibians across this region or loaned from the Biodiversity Collections, The University of Texas at Austin (TNHC); extracts from of each tissue samples were tested to validate the eDNA metabarcoding assay (Table 6.2). We extracted tissue subsamples (ca. 30 mg of tissue [liver]) using GenCatch Genomic DNA Extraction Kits (Epoch Life Sciences, Missouri City, TX, USA) following the manufacturer's tissue protocol. All tissue extracts were stored at -20°C until testing.

eDNA Collection and Amphibian Surveys.—Field sample collection followed previous protocols from Ruppert et al. (2022) and Robinson et al. (2022). In summary, water was collected from 3–4 locations from within a sampled wetland, taking care to minimize sediment disturbance and capture, to form a composite sample of the entire site. Once the composite sample was collected, it was brought back to the filtering equipment. To prevent contamination, all the equipment required for sample collection and water filtration was sterilized with 50% bleach, allowed to sit for 1 min, sprayed with 10% sodium thiosulfate, and was rinsed with DI water. Water filtration equipment included a 250-mL filter cup (MilliporeSigma, Darmstadt, Germany)

connected to a fluid evacuator (Mityvac, St. Louis, MO, USA) that pulled water through the filter and a plastic pitcher used for pouring the samples. Filters used for field sampling were 47-mm diameter Grade 4 (25 µm pore size) Whatman cellulose filters (GE Healthcare, Chicago, IL, USA).

Prior to filtering the field eDNA samples for each site, 1 L of DI water was filtered as a field negative control to test if the field equipment was sterile. Following the field negative control, three 1-L field sample replicates from the composite water sample were filtered through the same apparatus. The field negative controls and field samples were each stored in a individual labeled 1.5-mL microcentrifuge tube prefilled with 700 µL of DNAzol (Molecular Research Center Inc, Cincinnati, OH, USA). Fresh gloves were used for each site sampled.

A visual encounter survey was conducted throughout each site alongside the collection of the eDNA sample. Amphibians, reptiles, and fish found during the visual encounter survey were noted and identified to the lowest taxonomic level possible. Our visual encounter survey methods followed those from previous studies (Judd 1985; Rappole and Klicka 1991; Mazerolle et al. 2007; Heyer et al. 2014). Surveys were conducted in a circular fashion around the water body and lasted for 30 min or less depending on the number of surveyors and consisted of 2–3 individuals either sweeping a dipnet through the water or searching under cover objects along the shore.

eDNA Extraction.—Field samples and field controls were extracted using a GenCatch Genomic DNA Extraction Kit (Epoch Life Sciences, Missouri City, TX, USA) following a modified protocol from Robinson et al. (2022; see Chapter 2). Following sample collection, the filter was left in DNAzol at room temperature for at least 3 d. After 3 d, the centrifuge tubes containing the used filters and DNAzol were placed on a heat block at 55°C for 30 min. Then each centrifuge tube was vortexed for 30 s and centrifuged at 2400 rcf for 1 min. The filters were then squeezed into their centrifuge tube with clean forceps to collect any remaining DNAzol out of the filter prior to discarding the filters; new gloves were used for each sample during this step to prevent contamination among sites. DNAzol from each field sample was pooled and combined into a 5 mL centrifuge tube. Then 600 µL of DNAzol was pipetted out of the pooled field sample and placed into a fresh centrifuge tube; the remaining DNAzol from the pooled field sample was stored at room temperature as an archived sample. We added 10 µL of RNAase A to the 600 µL of DNAzol, and the solution was incubated at 37°C for 10 min. After the solution sat at room temperature for 1 min, 10 µL of proteinase-K was added. The solution was then vortexed and incubated at room temperature for 1 h, vortexing every 10–15 min during the incubation. After incubation, 500 µL of EX buffer was added and the solution was vortexed and incubated at 70°C for 20 min. During that incubation, 50 µL of sample elution buffer (EB) was preheated to 70°C. Following the 20 min incubation, the solution sat at room temperature for 5 min. Then 500 µL of 100% ethanol was added to the solution and the solution was vortexed prior to the solution being passed through a GenCatch column and centrifuged at 5800 rcf for 2 min. This centrifugation step was repeated 2–3 times more until the entire volume of the solution passed through the GenCatch column. The column was rinsed by the addition of 500 µL of WS buffer, centrifugation at 5800 rcf for 2 min, addition of 500 µL WS buffer, and centrifugation for 2 min at 18000 rcf. The column was then moved into a new 1.5 mL microcentrifuge tube and 50 µL of heated sample elution buffer was passed through the column. The DNA was then eluted by centrifuging the solution at 18000 rcf for 2 min, after which 50 µL of nuclease-free water was pipetted onto the column, and any remaining DNA was eluted by centrifuging the solution at 18000 rcf for 2 min. Either a Zymo OneStep PCR Inhibitor Removal Kit (Zymo Research, Irvine, CA, USA) or a NucleoSpin Inhibitor

Removal Kit (Macherey-Nagel, Düren, DEU) was used following the manufacturer's protocol to remove potential inhibitors. The DNA extract was stored at -20°C until used in PCR.

Metabarcoding Primer Validation.—The Batrachia primer set (Table 6.3) from Valentini et al. (2016), that amplified a portion of the 12s rRNA region, was tested against tissue samples of amphibians native to the study area (Table 6.2). PCR was conducted using a T100 ThermoCycler (Bio-Rad Laboratories, Hercules, CA, USA). Temperature gradients were used to determine annealing temperatures for PCR protocols. Two PCR protocols were validated; the "original" PCR protocol: 2 min at 95°C, then 40 cycles of 20 s at 95°C, 30 s at 55°C and 30 s at 72°C followed by 7 min at 72°C and a 4 min hold at 4°C. The other PCR protocol was the "optimized" PCR protocol: 2 min at 95°C, then 35 cycles of 20 s at 95°C, 20 s at 50°C and 10 s at 72°C followed by 7 min at 72°C and a 4 min hold at 4°C. Tissue extracts used for validation were diluted down to 1 ng/µL (Valentini et al. 2016). The PCR mixture for the validating species consisted of GoTaq G2 HotStart MasterMix (Promega Corporation, Madison, WI, USA), molecular grade water, 0.2 µM final concentration forward and reverse primers, 4 µM final concentration of human blocker (Valentini et al. 2016) and then 1 µL of template was added to the mixture. A no-template control (NTC) consisting of the same reagent mixture with 1 µL of molecular grade water, added in place of DNA, was run with each PCR cycle to test for contamination of lab reagents. Total PCR reaction volumes were 50 µL.

Gel electrophoresis was used to visualize each PCR product; a 2% agarose gel (40 mL 1× TBE + 800 mg agarose) with 2–4 µL of GelRed Stain (Biotium Inc., Hayward, CA, USA) was made and run at 100 volts for 40 min. Gels were then viewed in a UVP transilluminator (Figure 6.1). PCR products were purified using Monarch PCR Purification Kits (New England Biolabs, Ipswich, MA, USA) following the manufacturer's protocol. PCR products were quantified using a QUBIT 2.0 fluorometer (Thermo Fisher Scientific, Waltham, MA, USA) and samples with measurable DNA concentrations were sent for Sanger sequencing at Eurofins Genomics (Louisville, KY, USA) with 5 µL of 10 µM forward primer and 5 µL of purified PCR product. The resulting sequences were compared to sequences available on GenBank, with either the 'megablast' or 'blastn' algorthims found on NCBI BLAST (blast.ncbi.nlm.nih.gov/blast.cgi). Purified PCR products that matched their respective species had a DNA concentration between 0.1–1.0 ng/µL of DNA. Due to the conserved nature of the 12s rRNA region some BLAST searches were limited to the respective species.

eDNA Metabarcoding.—The two validated PCR protocols were used with 50-µL reactions on extracted field eDNA samples. The only difference in the PCR mixture from the in-vitro validation PCR mixture was that the template volume for field samples was increased to 10 µL (1–30 ng/µL of DNA). Field negative controls and NTCs were tested alongside field samples and received the same 10 µL volume of extract or molecular grade water as with field samples. All PCR products were visualized on 2% agarose gel electrophoresis with a UVP transilluminator and purified using Monarch PCR Purification Kits. Field samples were split into two next-generation sequencing (NGS) runs but the detections from each run were combined for analysis so that all possible data generated could be used for analysis (Table 6.4). All NGS was conducted at the Harvard Biopolymers Facility (www.genome.med.harvard.edu). The initial run was a preliminary run and sequenced using a Miseq Nano platform with an expected sequencing depth of 100,000 reads per library. Only the "optimized" PCR protocol was used to amplify samples in the initial NGS run. The second run was sequenced with a Miseq V3 platform with an expected read depth of 330,000

reads per library, with the main goal of collecting more data on more sites. Both the "original" and "optimized" PCR protocols were used in the second NGS run. For both NGS runs all samples were diluted to a standardized concentration before being sent off for sequencing. Once the samples were received at the Harvard Biopolymers Facility, the DNA quality and fragment size were examined using an Agilent 4200 TapeStation instrument, with a corresponding Agilent TapeStation HSD1000 assay. Following confirmation of DNA quality and fragment size, samples for each run were moved to library prep for their respective sequencing platforms.

OBITools3 (Boyer et al. 2016; www.git.metabarcoding.org/obitools/obitools3) and Geneious Prime (v2022.0.1; www.geneious.com/prime/) were used to analyze NGS data. Sequences were compared to a local in-silico generated reference database with a 97% match requirement. The local in-silico reference database was created using OBITools3 following an existing tutorial (www.git.metabarcoding.org/obitools/obitools3/-/wikis/Wolf-tutorial-with-the-OBITools3) with modifications to commands so that the reference database would be specific to the Batrachia primers. Other primer specific modifications to the OBITools3 pipeline were done as needed (Appendix B). Sequences were matched to the family, genus, or species level in OBITools3 based on the 97% match requirement. Sequences not identified by OBITools3 were exported to Geneious Prime and were compared to sequences on GenBank using either the 'megablast' or 'blastn' algorithms for further examination. If a sequence was assigned to a taxonomic unit that did not have a distribution within the study area it was examined further to determine if the sequence matched an organism with a possible distribution in the study area. The sequence was removed from further analysis if it was not able to be matched with a species native to the study area. Positive detections from 'megablast' and 'blastn' had a percent match ranging from 90–96%. Ten reads per taxonomic unit was chosen as an initial threshold for a positive detection based on read numbers per Valentini et al. (2016). In three instances, a positive detection was also considered when a sample, that was amplified with replicates, had a low number of reads assigned to a taxonomic unit in each replicate (i.e, 1–3 reads per replicate) as the detection was shown to be repeatable and previous literature has also considered low read numbers as a positive detection (e.g., Klymus et al. 2017).

Comparison of eDNA Metabarcoding and Targeted eDNA Assays.—Targeted (single-species) eDNA assays designed for both the Black-spotted Newt and Lesser Siren (*Siren intermedia*) were used to evaluate the sensitivity of the eDNA metabarcoding assay by comparing the number of each of these two species in each methodology. Both species are potentially found across the sites we sampled, but perceived abundances of both species vary markedly. Previous data (Chapter 2, 4) and personal observations suggest that the Black-spotted Newt is a rare species across the landscape, has low abundance, and the species is not an obligate aquatic species. Conversely, the Lesser Siren can be quite high in abundance within and among sites, and is fully aquatic. Comparing metabarcoding and targeted eDNA assays for these two species provided a robust comparison between the strengths of each method. Targeted assays for Black-spotted Newts are described in Chapter 4, Robinson (2021), and Robinson et al. (2022) and we slightly modified the single-species PCR methods described for Rio Grande Sirens in Ruppert et al. (2022) using a lower number of cycles in both the initial and nested rounds. As described in these published studies, we amplified DNA using two rounds of PCR, ran products on an agarose gel, and mailed purified products to Eurofins Genomics (Louisville, KY, USA) for Sanger sequencing.

The detection threshold using the targeted, single-species assays, occurred with successful amplification of at least one technical replicate of a field sample with no amplification in the field

control or NTC. Additionally, replicates with amplified target-species DNA were purified and sent for Sanger sequencing at Eurofins Genomics (Louisville, KY, USA). Sanger sequencing for both species consisted of submitting 5 µL of purified PCR product and 5 µL primer, and Sanger sequences were be compared with published sequence data on GenBank using NCBI BLAST (blast.ncbi.nlm.nih.gov/blast.cgi) and needed to match the appropriate species data with >95% similarity.

Statistical Analyses.—For eDNA metabarcoding, the number of reads assigned to each taxonomic unit in each sample was summed together for each site. Read numbers were then transformed into presence/absence for comparison to field surveys presence/absence data. Bar plots were then used to visualize the amphibian and non-amphibian detections of each method. The number of sites a taxonomic unit was detected at using eDNA metabarcoding and traditional surveys were totaled for comparison. Due to the varied resolution of detections between each method (e.g., a family-level detection from the traditional visual encounter survey vs. a species-level detection from eDNA metabarcoding) a weighted scale was applied to all species-, genus-, and family-level detections so that a formal test of differences between eDNA metabarcoding and traditional survey methods could be conducted. Species-level detections were given a score of three, genus-level detections were given a score of two, and family-level detections were given a score if one. Lower taxonomic detections were given higher weights because they offer more information than higher-level taxonomic detections. To test whether one method or another detected more amphibian taxonomic units per site, the weighted detections for each site using eDNA metabarcoding and traditional visual encounter survey were respectively totaled. A Kolmogorov-Smirnov test (Kolmogorov 1933) and Levene's test (Levene 1960) for homoscedasticity were used to determine normality and homoscedasticity for the comparison of taxonomic units detected between eDNA metabarcoding and traditional survey methods. The data for that comparison were non-normally distributed ($p < 0.05$), but homoscedastic ($p = 0.634$), and a Mann-Whitney U test (Mann and Whitney 1947; Wilcoxon 1945) test was then conducted. All statistical analyses were conducted in SPSS (v28.0.00, IBM; Levesque 2007) and Primer e (v7, Quest Research Limited; Clarke and Gorley 2006).

RESULTS

Primer Validation.—Tissue extracts of all 33 tested amphibian species (Table 6.2) successfully amplified and tissue extracts of 32 species were successfully Sanger sequenced; only *Rana areolata* was not able to be Sanger sequenced.

Amphibian Diversity from Field Surveys vs. Metabarcoding.—From the eDNA metabarcoding assay, 13 unique amphibian species and two genera (*Rana*, *Anaxyrus*) were detected (Table 6.5). From traditional survey methods alone, nine unique amphibian species, four genera and three families were detected (Table 6.5). eDNA metabarcoding detected all species, genera, and families more often at most sites compared to traditional visual surveys with the exception of *Notophthalmus meridionalis*, *Rana berlandieri*, *R. catesbeiana*, and *Hypopachus variolosus*, which were detected more often with traditional survey methods (Table 6.5). Two sites (Laguna Atascosa NWR, Newt Pond, Cameron County; Laguna Atascosa NWR, Prairie Trail, pond #2, Cameron County; Table 6.6) had no amphibian detections through eDNA metabarcoding and three sites (Laguna Atascosa NWR, Kidney Pond, Cameron County; US Hwy 77, W side, ca. 1.0 rd km N Kenedy/Willacy county line, Kenedy County; Old Military Hwy, pond #4, Starr County; Table

6.6). eDNA metabarcoding provided more amphibian species- and genus-level detections for almost all sites (Table 6.6). In contrast, the traditional survey tended to provide mostly family- and genus-level detections (Table 6.6). There was a high amount of variation in the number of amphibian taxonomic units detected at each site using eDNA metabarcoding and traditional survey methods by themselves. eDNA metabarcoding (weighted average ± 1SE = 9.42 ± 1.23) detected significantly more amphibian taxonomic units compared to traditional survey methods (5.83 ± 1.06; Mann-Whitney U = 397.50, p = 0.02).

Although the eDNA metabarcoding assay was not validated on taxa outside of amphibians, it was able to detect a variety of non-amphibian taxa in field samples (Table 6.7). eDNA metabarcoding was able to provide more species- and genus-level detections for non-target taxa compared to traditional survey methods (Table 6.7). In many sites, non-target taxa represented most of the taxonomic units detected using eDNA metabarcoding. Twelve fish species, four fish genera, and the groups Oreochromini and Stethaprioninae were detected using eDNA metabarcoding (Table 6.7). Six reptile species and the group Testudinoidea were detected using eDNA metabarcoding (Table 6.7). Using traditional visual encounter surveys, one species and three genera and one family (Centrarchidae) of fish were detected as were six species and two genera of reptiles (Table 6.7).

Comparison of eDNA Metabarcoding and Single-species eDNA Assays.—The targeted eDNA assay detected Black-spotted Newts at ten sites (41.7%), and the eDNA metabarcoding assay had a much lower number of detections, with a detection at only one site (4.2%; Table 6.8). The targeted eDNA assay detected Lesser Sirens at 16 sites (66.7%), and the eDNA metabarcoding assay had detections at 15 sites (62.5%; Table 6.8).

DISCUSSION

The eDNA metabarcoding assay detected significantly more amphibian taxonomic units compared to traditional survey methods with an almost twice as high a weighted average detection per site compared to traditional survey methods. Most literature suggests that eDNA metabarcoding is as sensitive or more sensitive than traditional survey methods (e.g., Lacoursière-Roussel et al. 2016; Hallam et al. 2021; Sakata et al. 2021, 2022; Ruppert et al. 2022). As predicted, our data suggest that eDNA metabarcoding is more sensitive than visual encounter surveys based on the significantly higher number of amphibian taxonomic units detected by eDNA metabarcoding methods. However, we also observed variation in amphibian taxonomic units recorded at each site using both methods. While out in the field it can be difficult to identify some tadpoles and metamorphic amphibians down to the species, and as a result, there were more family- and genus-level detections in our field surveys. These results highlight an advantage of eDNA metabarcoding, as detections are based off genetic similarity rather than morphology (Grosjean et al. 2015). Incorporating other methods, such as call surveys, trapping, or pit fall traps, could have made for a more robust traditional survey and resulted in additional amphibian detections (Todd et al. 2007; Sasso et al. 2017).

In some samples, non-amphibian species accounted for the majority of detections and some amphibians could have been missed due to the ability of this primer set to amplify non-amphibian taxa. The biphasic lifestyle of most amphibians means they are not always in the aquatic environment, so amphibian eDNA concentrations may be lower relative to obligate-aquatic taxa. For example, a previous study that used a microfluidic metagenomic eDNA approach to assessing aquatic biodiversity in a tributary in the Oregon Coastal Range found only 0.80% of total

sequences were amphibian, while the rest of the sequences were attributed to other aquatic organisms (Hauck et al. 2019). In our study, a high number of non-amphibian detections were observed, thus amphibian DNA may be less abundant relative to other aquatic taxa, such as fish, and a consistent representation of amphibians using eDNA may be difficult without primers that have higher specificity for amphibians. The variation in amphibian taxonomic units detected and the inability to obtain certain species-level detections (e.g., *Rana berlanderi, R. catesbeiana, Hypopachus variolosus*) using eDNA metabarcoding suggests the need for primer refinement. This also suggest that pairing eDNA metabarcoding with other methods, such as traditional surveys and targeted eDNA assays, are needed for a comprehensive community assessment in order to avoid missed detections (Coghlan et al. 2021; Wikston 2021). Pairing eDNA and traditional survey data is beneficial because the data can be compared, and the effectiveness of each method can be compared (Wikston 2021). The unexpected detections of non-amphibian taxa do suggest a broader application of this primer set for larger community assemblage analyses at these sites, supporting the use of eDNA metabarcoding methods for diverse community assemblages as suggested by others (Klymus et al. 2017; Bylemans et al. 2019; Roffler et al. 2021). The variety of taxa detected in this study emphasizes the importance of ephemeral ponds for wildlife in south Texas as previous studies suggested (Jahrsdoerfer and Leslie 1988; Fulbright et al. 1990; Duran 2021).

This metabarcoding assay also provided information on amphibian community assemblages for each site and detected more species (13/33 amphibian species reported for the region) than traditional survey methods (9/33 species), further supporting the idea that eDNA metabarcoding is more sensitive at detecting amphibian species than traditional survey methods. The lack of detection of the other 20 potential amphibian species could have been due to a number of factors such as favoring ephemeral ponds, timing of the survey, or overall DNA abundance. Additionally, though data exists recording 33 species of amphibians from the counties we sampled, it is important to note that these species are not universally expected to be present at every site. Regular sampling throughout the year may also help to increase amphibian detections as many amphibians found within the study area are active at different times throughout the year (Tipton et al. 2012) and most of the samples used in this study came from May–September (n = 29) with fewer from October–February (n = 7). Some of the winter-breeding amphibian species (e.g., *R. berlandieri*) may have been underrepresented in eDNA samples. DNA degradation rates and aquatic DNA abundance within these ephemeral ponds should be investigated further to better examine whether or not these factors play a role in the detection of certain species.

Our results support the growing evidence that many metabarcoding primer sets can have miss detections of certain taxa based on primer match and not just based on biomass (Harper et al. 2018; Nester et al. 2020; Schenekar et al. 2020; Gold et al. 2021). Although, the eDNA metabarcoding assay was validated on most tissue extracts (32/33 species), there were three troublesome species (*Gastrophryne carolinensis*, *Hypopachus variolosus*, *Rana areolata*) species that required the redesign from the "original" protocol to the "optimized" protocol, In this study, the Batrachia primer set had a lower affinity, or a blind spot, for *H. variolosus*, *G. carolinensis*, *R. areolata* as tissue extracts of each species were difficult to amplify and Sanger sequence. *Rana berlanderi* was also a species that was only able to get a genus-level match during the validation phase even though there is published data on the 12s rRNA region for the species. Both *R. berlanderi* and *R. catesbeiana*, which are larger-bodied abundant species, were species that were detected more often using the traditional visual encounter survey compared to eDNA metabarcoding, indicating that the Batrachia primer set may have a lower affinity for these species as well. The Batrachia primer set obtained a number of genus-level detections of *Rana*, however the number of detections was

still less than the traditional visual encounter survey. The difficulty of obtaining species-level detections for some species agrees with a previous study that had a similar issue with the primer set not being able to differentiate some species of gobies and rockfishes at the species level (Gold et al. 2021).

For the detection of the Black-spotted Newt, the single-species assay detected the species at more sites than the metabarcoding method which matches with a growing body of literature that targeted eDNA assays are more effective at detecting rare, small-bodied species compared to eDNA metabarcoding assays (Harper et al. 2018; Bylemans et al. 2019; Nester et al. 2020; Gold et al. 2021). Although eDNA metabarcoding assay detected more species than traditional survey methods, eDNA metabarcoding was less efficient at specifically detecting the Black-spotted Newt in field samples (4.2% of sites) compared to the visual encounter survey (12.5% of sites). Robinson et al. (2022) likewise had a low, but identical, detection of Black-spotted Newts with both traditional surveys and a species-specific eDNA assay (see Chapter 4). Using only traditional survey methods, Judd (1985) found Black-spotted Newts at two of 221 sites (0.9%) and Rappole and Klicka (1991) found Black-spotted Newts at seven of 114 sites (6%). This study detected Black-spotted Newts at a higher percentage of sites from traditional survey methods and the single-species (targeted) eDNA assay relative to Judd (1985), Rappole and Klicka (1991), and Robinson et al. (2022). The higher detection percentage was most likely due to surveying a smaller number of sites compared to Robinson et al. (2022) and only incorporating sites previously identified as Black-spotted Newt habitat, or potential habitat, from the results of Robinson et al. (2022). The results of the present study suggest that eDNA metabarcoding may be less efficient than single-species eDNA assays and traditional survey methods at detecting some rare and cryptic species such as the Black-spotted Newt. As found in Robinson et al. (2022), the combination of multiple survey methods can complement increase species detections, and we recommend the continued use of multiple methodologies.

Previous eDNA studies on rare, cryptic taxa have considered amplification of 1/3, 1/6, or even 1/12 technical replicates as potential positives (Harper et al. 2018; Bylemans et al. 2019). Our requirement of at least 1/3 replicated amplifying and sequencing correctly matches that used in previous studies. These lower detection thresholds could help to identify sites that have smaller populations of Black-spotted Newts, sites where the optimum sampling window for eDNA has been missed, or sites where eDNA has become dilute or degraded (Goldberg et al. 2016; Harper et al. 2018). Future studies could use this lower threshold and incorporate repeated sampling to confirm Black-spotted Newt presence, and future studies should continue to examine how long Black-spotted Newt eDNA persists in a water body so that the effectiveness of eDNA sampling may be increased. For the Black-spotted Newt, our data suggest that the targeted eDNA assay outperformed eDNA metabarcoding with the goal of generating species detections, however, we found a similar number of detections of the Lesser Siren through both the targeted eDNA assay and eDNA metabarcoding. These differing results between these two species likely is attributed to aspects of their abundance and ecology: the Black-spotted Newt is rare across the landscape, small, bi-phasic, and not an obligate aquatic species, while the Lesser Siren occurs in higher abundance, is significantly larger, and is an obligate aquatic species. These results are in line with other studies who have suggested that target eDNA assay outperform metabarcoding methods, and as a result, we suggested that future eDNA surveys for the Black-spotted Newt use a targeted assay.

Table 6.1. Information on sites sampled, number of samples tested using eDNA metabarcoding methods, sampling dates, and wetland type (ephemeral or permanent). Descriptive names for private property have been generalized and specific GPS coordinates have been redacted in this table.

County	Site Name	# of Samples	Date(s)	Ephemeral or Permanent
Bee	Bee County Site #1	1	4 Oct 2020	Ephemeral
Calhoun	Powderhorn WMA, Bullrush Pond	1	27 Feb 2020	Permanent
Calhoun	Powderhorn WMA, dugout pond near barn at S entrance	3	6 May 2021, 10 June 2021, 30 June 2021	Ephemeral
Calhoun	Powderhorn WMA, midline fence pond	3	6 May 2021, 10 June 2021, 30 June 2021	Ephemeral
Cameron	Laguna Atascosa NWR, Kidney Pond	1	26 May 2021	Permanent
Cameron	Laguna Atascosa NWR, Newt Pond	1	26 May 2021	Ephemeral
Cameron	Laguna Atascosa NWR, Prairie Trail, pond #2	1	23 Aug 2020	Ephemeral
Cameron	Laguna Atascosa NWR, Scum Pond	1	26 May 2021	Ephemeral
Cameron	Cameron County Site #1	2	2 Sept 2020, 2 May 2021	Ephemeral
Cameron	Cameron County Site #2	1	9 Nov 2020	Ephemeral
Cameron	Cameron County Site #3	1	4 May 2021	Ephemeral
Cameron	Cameron County Site #4	1	4 May 2021	Ephemeral
Hidalgo	Hidalgo County Site #1	2	27 July 2020, 7 June 2021	Ephemeral
Hidalgo	Hidalgo County Site #2	1	7 June 2021	Ephemeral
Kenedy	US Hwy 77, W side, ca. 1.0 rd km N Kenedy/Willacy county line	2	31 Aug 2020, 8 June 2021	Ephemeral
Kleberg	TAMU-Kingsville CKWRI, South Pasture pond	2	28 May 2021, 8 June 2021	Ephemeral
Live Oak	Live Oak County Park, pond SE of parking area	2	3 Dec 2020, 30 June 2021	Ephemeral
Nueces	Pintas Creek at Co Rd 70	1	8 June 2021	Ephemeral
San Patricio	San Patricio County Site #1	1	7 May 2021	Ephemeral
San Patricio	San Patricio County Site #2	4	29 Jan 2020, 7 May 2021, 11 June 2021, 1 July 2021	Ephemeral
Starr	Old Military Hwy, pond #4	1	24 June 2021	Ephemeral
Starr	Old Military Hwy, pond #5	1	9 June 2021	Ephemeral
Starr	Lower Rio Grande Valley NWR, Milagro East resaca	1	13 Aug 2020	Ephemeral
Willacy	Willacy County Site #1	1	27 Oct 2020	Ephemeral

Table 6.2. List of amphibian species validated for use with the eDNA metabarcoding methods. Family and species names are provided along with the museum catalog number associated with the sample. Counties where each specimen was collected in Texas, USA are provided for all specimens except a single species (*Rana areolata*: TNHC 14318), which lacks locality information. DRD = Drew R. Davis Field Series; TNHC = Biodiversity Collections, The University of Texas at Austin.

Family	Species	County	Catalog Number
Salamandridae	*Notophthalmus meridionalis*	Cameron	DRD 5165
Salamandridae	*Notophthalmus viridescens*	Harris	TNHC 116646
Ambystomatidae	*Ambystoma mavortium*	Cameron	TNHC 114655
Ambystomatidae	*Ambystoma texanum*	Limestone	TNHC 113097
Sirenidae	*Siren intermedia texana*	Cameron	TNHC 116624
Bufonidae	*Anaxyrus debilis*	Jeff Davis	TNHC 67333
Bufonidae	*Anaxyrus punctatus*	Val Verde	TNHC 116627
Bufonidae	*Anaxyrus speciosus*	Kenedy	TNHC 112166
Bufonidae	*Anaxyrus woodhousii*	Austin	TNHC 55521
Bufonidae	*Incilius nebulifer*	Hidalgo	TNHC 116991
Bufonidae	*Rhinella horribilis*	Willacy	TNHC 114653
Eleutherodactylidae	*Eleutherodactylus cystignathoides*	Cameron	TNHC 116629
Hylidae	*Acris blanchardi*	La Salle	TNHC 116625
Hylidae	*Hyla chrysoscelis*	Edwards	TNHC 113477
Hylidae	*Hyla cinerea*	Matagorda	TNHC 116640
Hylidae	*Hyla squirella*	Aransas	TNHC 116641
Hylidae	*Hyla versicolor*	Karnes	TNHC 60516
Hylidae	*Pseudacris clarkii*	Cameron	TNHC 116647
Hylidae	*Pseudacris fouquettei*	Liberty	TNHC 65745
Hylidae	*Pseudacris streckeri*	Travis	TNHC 67424
Hylidae	*Smilisca baudinii*	Cameron	TNHC 114656
Leptodactylidae	*Leptodactylus fragilis*	Zapata	TNHC 114657
Microhylidae	*Gastrophryne carolinensis*	Aransas	TNHC 116632
Microhylidae	*Gastrophryne olivacea*	Hidalgo	TNHC 112082
Microhylidae	*Hypopachus variolosus*	Willacy	TNHC 116990
Ranidae	*Rana areolata*	–	TNHC 14318
Ranidae	*Rana berlandieri*	Cameron	TNHC 112113
Ranidae	*Rana catesbeiana*	Refugio	TNHC 114658
Ranidae	*Rana sphenocephala*	Matagorda	TNHC 116648
Rhinophrynidae	*Rhinophrynus dorsalis*	Starr	TNHC 114654
Scaphiopodidae	*Scaphiopus couchii*	Cameron	TNHC 112175
Scaphiopodidae	*Scaphiopus hurteri*	Gonzales	TNHC 116649
Scaphiopodidae	*Spea bombifrons*	Winkler	TNHC 60528

Table 6.3. Batrachia primers and human blocker used from Valentini et al. (2016).

ID	Sequence	Fragment Size
Batrachia FW	ACACCGCCCGTCACCCT	90bp
Batrachia RV	GTAYACTTACCATGTTACGACTT	90bp
human blocker	TCACCCTCCTCAAGTATACTTCAAAGGCA [SpC3]	N/A

Table 6.4. All field samples tested using eDNA metabarcoding methods. Number of technical replicates per sample and PCR protocol used is shown. Descriptive names for private property have been generalized.

Sample	Date	Technical Replicates	PCR Protocol
Bee County Site #1	4 Oct 2020	1	Optimized
Powderhorn WMA, Bullrush Pond	27 Feb 2020	1	Original
Powderhorn WMA, dugout pond near barn at S entrance	6 May 2021	1	Original
Powderhorn WMA, dugout pond near barn at S entrance	10 June 2021	2	Original
Powderhorn WMA, dugout pond near barn at S entrance	30 June 2021	1	Original
Powderhorn WMA, midline fence pond	6 May2021	1	Original
Powderhorn WMA, midline fence pond	10 June 2021	1	Original
Powderhorn WMA, midline fence pond	30 June 2021	1	Original
Laguna Atascosa NWR, Kidney Pond	26 May 2021	1	Original
Laguna Atascosa NWR, Newt Pond	26 May 2021	1	Original
Laguna Atascosa NWR, Prairie Trail, pond #2	23 Aug 2020	1	Optimized
Laguna Atascosa NWR, Scum Pond	26 May 2021	2	1 Original, 1 Optimized
Cameron County Site #1	2 Sept 2020	2	Optimized
Cameron County Site #1	2 May 2021	2	1 Original, 1 Optimized
Cameron County Site #2	9 Nov 2020	2	Optimized
Cameron County Site #3	4 May 2021	1	Original
Cameron County Site #4	4 May 2021	1	Original
Hidalgo County Site #1	27 July 2020	1	Optimized
Hidalgo County Site #1	7 June 2021	3	2 Original, 1 Optimized
Hidalgo County Site #2	7 June 2021	2	Original
US Hwy 77, W side, ca. 1.0 rd km N Kenedy/Willacy county line	31 Aug 2020	1	Optimized
US Hwy 77, W side, ca. 1.0 rd km N Kenedy/Willacy county line	8 June 2021	1	Original
TAMU-Kingsville CKWRI, South Pasture pond	26 May 2021	1	Original
TAMU-Kingsville CKWRI, South Pasture pond	8 June 2021	1	Original
Live Oak County Park, pond SE of parking area	3 Dec 2020	1	Optimized
Live Oak County Park, pond SE of parking area	30 June 2021	1	Original
Pintas Creek at Co Rd 70	8 June 2021	3	2 Original, 1 Optimized
San Patricio County Site #1	7 May 2021	1	Original
San Patricio County Site #2	29 Jan 2020	1	Optimized
San Patricio County Site #2	7 May 2021	1	Original
San Patricio County Site #2	11 June 2021	1	Original
San Patricio County Site #2	1 July 2021	1	Original
Old Military Hwy, pond #4	24 June 2021	2	Original
Old Military Hwy, pond #5	9 June 2021	1	Original
Lower Rio Grande Valley NWR, Milagro East resaca	13 Aug 2020	1	Optimized
Willacy County Site #1	27 Oct 2020	2	Optimized

Table 6.5. Amphibian species, genera, and families detected using eDNA metabarcoding and traditional survey methods across 24 sampled sites.

Species/Genus/Family	# sites detected: eDNA metabarcoding	# sites detected: Traditional
Notophthalmus meridionalis	1	3
Siren intermedia texana	15	1
Anaxurus speciosus	3	2
Anaxyrus sp.	8	2
Incilius nebulifer	16	7
Rhinella horribilis	2	0
Bufonidae	16	8
Hyla cinerea	3	0
Hyla squirella	2	2
Smilisca baudinii	1	1
Hylidae	6	5
Gastrophryne olivacea	14	0
Gastrophryne sp.	14	5
Hypopachus variolosus	0	3
Microhylidae	14	7
Rana berlandieri	0	6
Rana catesbeiana	0	1
Rana sphenocephala	4	0
Rana sp.	9	12
Scaphiopus couchii	5	0
Scaphiopus hurterii	1	0
Scaphiopus sp.	6	2
Spea bombifrons	1	0

Table 6.6. Number of amphibian taxonomic units detected using eDNA metabarcoding and traditional survey methods across 24 sampled sites. Descriptive names for private property have been generalized.

Site Name	# sites detected: eDNA metabarcoding	# sites detected: Traditional
Bee County Site #1	2	7
Powderhorn WMA, Bullrush Pond	2	1
Powderhorn WMA, dugout pond near barn at S entrance	5	6
Powderhorn WMA, midline fence pond	7	5
Laguna Atascosa NWR, Kidney Pond	3	0
Laguna Atascosa NWR, Newt Pond	0	1
Laguna Atascosa NWR, Prairie Trail, pond #2	0	1
Laguna Atascosa NWR, Scum Pond	3	1
Cameron County Site #1	5	8
Cameron County Site #2	3	1
Cameron County Site #3	1	1
Cameron County Site #4	2	2
Hidalgo County Site #1	7	3
Hidalgo County Site #2	2	1
US Hwy 77, W side, ca. 1.0 rd km N Kenedy/Willacy county line	3	0
TAMU-Kingsville CKWRI, South Pasture pond	1	2
Live Oak County Park, pond SE of parking area	5	7
Pintas Creek at Co Rd 70	3	2
San Patricio County Site #1	7	2
San Patricio County Site #2	6	4
Old Military Hwy, pond #4	3	0
Old Military Hwy, pond #5	2	1
Lower Rio Grande Valley NWR, Milagro East resaca	2	5
Willacy County Site #1	5	6

Table 6.7. Non-amphibian species, genera, and families detected using eDNA metabarcoding and traditional survey methods across 24 sampled sites.

Taxonomic Unit	Group	# sites detected: eDNA metabarcoding	# sites detected: Traditional
Atractosteus sp.	Fish	1	0
Lepisosteus sp.	Fish	1	0
Gambusia affinis	Fish	15	2
Gambusia holbrooki	Fish	7	0
Gambusia sp.	Fish	22	8
Poecilia formosa	Fish	6	0
Poecilia latipinna	Fish	13	0
Poecilia mexicana	Fish	2	0
Poecilia sp.	Fish	19	3
Fundulus grandis	Fish	1	0
Fundulus sp.	Fish	1	2
Herichtys cyanoguttatus	Fish	2	0
Dormitator maculatus	Fish	3	0
Lepomis cyanellus	Fish	6	0
Cyrpinodon variegatus	Fish	7	0
Ameiurus sp.	Fish	1	0
Oreochromis sp.	Fish	3	0
Oreochromini sp.	Fish	5	0
Lepomis macrochirus	Fish	2	0
Menidia beryllina	Fish	1	0
Stethaprioninae	Fish	3	0
Trachemys scripta	Reptile	1	0
Kinosternon sp.	Reptile	0	1
Testudinoidea sp.	Reptile	3	0
Alligator mississippiensis	Reptile	0	1
Holbrookia propinqua	Reptile	0	1
Scincilla sp.	Reptile	0	2
Coluber constrictor	Reptile	1	0
Regina grahamii	Reptile	1	0
Thamnophis marcianus	Reptile	2	0
Thamnophis proximus	Reptile	2	1
Thamnophis saurita	Reptile	0	2
Thamnophis sp.	Reptile	5	4
Agkistrodon piscivorus	Reptile	0	1
Crotalus atrox	Reptile	1	0

Table 6.8. Black-spotted Newt and Lesser Siren detections at all 24 sites comparing eDNA detected using both single-species assays and metabarcoding methods. Descriptive names for private property have been generalized.

	Black-spotted Newt		Lesser Siren	
Site Name	**Single-species**	**Metabarcoding**	**Single-species**	**Metabarcoding**
Bee County Site #1	–	–	+	+
Powderhorn WMA, Bullrush Pond	–	–	–	+
Powderhorn WMA, dugout pond near barn at S entrance	–	–	+	+
Powderhorn WMA, midline fence pond	+	–	+	+
Laguna Atascosa NWR, Kidney Pond	–	–	+	–
Laguna Atascosa NWR, Newt Pond	+	–	–	–
Laguna Atascosa NWR, Prairie Trail, pond #2	+	–	–	–
Laguna Atascosa NWR, Scum Pond	+	–	+	+
Cameron County Site #1	+	+	+	+
Cameron County Site #2	–	–	+	+
Cameron County Site #3	+	–	+	+
Cameron County Site #4	+	–	+	+
Hidalgo County Site #1	–	–	+	+
Hidalgo County Site #2	–	–	–	–
US Hwy 77, W side, ca. 1.0 rd km N Kenedy/Willacy county line	–	–	+	+
TAMU-Kingsville CKWRI, South Pasture pond	–	–	–	+
Live Oak County Park, pond SE of parking area	+	–	+	–
Pintas Creek at Co Rd 70	–	–	+	–
San Patricio County Site #1	–	–	+	+
San Patricio County Site #2	–	–	+	+
Old Military Hwy, pond #4	+	–	–	–
Old Military Hwy, pond #5	–	–	–	–
Lower Rio Grande Valley NWR, Milagro East resaca	–	–	–	–
Willacy County Site #1	+	–	+	+

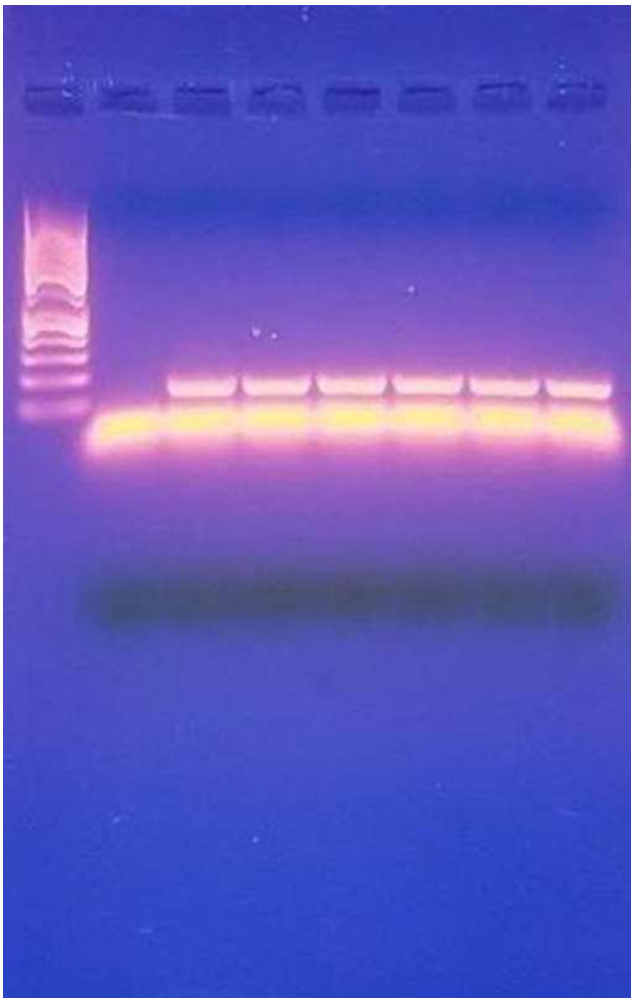

Figure 6.1. Example of visualized PCR product. The length of PCR-amplified tissue extracts when using the Batrachia primer set (Valentini et al. 2016) are 90 bp. The large smear below the DNA band is excess primer which is visible when using GelRed Stain (see Chapter 2). L to R: 50 bp ladder, NTC, *Siren intermedia texana*, *Notophthalmus meridionalis*, *Rhinophrynus dorsalis*, *Anaxyrus speciosus*, *Smilisca baudinii*, and *Incilius nebulifer*. NTC = no-template control.

CHAPTER 7

TASK 6. Developing Black-spotted Newt habitat suitability models under current and future scenarios

OVERVIEW

Chapter 7 discusses the creation of both current and future Black-spotted Newt habitat suitability models. Previously, Bare (2018) created a habitat suitability model for both the Texas Black-spotted Newt using 32 training points. However, due to new Black-spotted Newt detections, updated environmental variables, and evidence suggesting the importance of wetland ephemerality, we sought to generate an updated current habitat suitability model for the Texas Black-spotted Newt. We combined bioclimatic, soil, and wetland data to model the current distribution of suitable habitat for the Texas Black-spotted Newt. Additionally, we projected this new model to explore how habitat suitability would change under varying climate change scenarios. Future habitat suitability models include two emissions scenarios (SSP2-4.5, SSP3-7.0) and two time periods (2061–2080, 2081–2100) that were created using three different general circulation models (ACCESS-ESM1.5, CanESM5.0.3, MIROC6). From each unique combination of emission scenario, time period, and circulation model, both a continuous and binary model was created. Binary models for each circulation model at a given emission scenario and time period were combined to result in a single consensus model, resulting in a total of four consensus models. Consensus models were then used to calculate the amount of suitable habitat that was gained, lost, and remained stable. This chapter addresses Goals 1 (in part), 5, and 6 (in part) of the project.

METHODS

Study Area.—We delineated the study area by creating a rectangle surrounding all occurrence records, with limits set to the nearest integer degree that was at least one degree from the nearest occurrence in each cardinal direction. This resulted in a rectangle bounded by 100°W as the western boundary, 95°W as the eastern boundary, 30°N as the northern boundary, and 22°N as the southern boundary. This area encompassed the known historical range of the Texas Black-spotted Newt, including the zone of intergradation with the Mexican Black-spotted Newt (*N. m. kallerti*) in southern Tamaulipas, Mexico (Mecham 1968b), and land areas to the north and west of known occurrences that allowed for potential dispersal under future climate scenarios.

Training Points.—We began with a set of previously selected Texas Black-spotted Newt training points used by Bare (2018) created from a database of newt occurrences compiled from natural history museum collections, community science platforms, and recent survey efforts. Bare (2018) selected these training points using methods outlined by Andersen and Beauvais (2013), in which records are excluded on the basis of site duplication, geographical error, and the level of detail in locality descriptions. We cross-referenced the training points used by Bare (2018) with occurrence records in our newly created Black-spotted Newt occurrence database (see Chapter 2) to examine similarities and differences in geographic coordinates between sources. Due to discrepancies in coordinates for many localities in the Bare (2018) training points, we updated the geographic coordinates and their associated errors using GEOLocate (www.geo-locate.org). We also removed duplicate and unverifiable records from the training points used by Bare (2018). We also added records from our new Black-spotted Newt occurrence database with errors <8000 m (following Anderson and Beauvis 2013) that were unknowingly excluded from the Bare (2018)

training points and occurrence records generated from recent eDNA sampling (Robinson 2021; Robinson et al. 2022; Collins 2022).

A key assumption of Maxent modeling is that occurrence data are a product of uniform sampling across the study area (Phillips et al. 2006). In our case, as is common with many occurrence datasets, records were compiled from multiple sources representing different survey efforts and community science observations and, as a result, they contain spatial bias toward roadways, areas of relatively high population density, and publicly accessible lands. The spatial autocorrelation of occurrence data can create bias in environmental predictors, resulting in a model that is overfit to the environmental biases and unable to accurately predict independent occurrence records used to evaluate model performance (Peterson et al. 2011; Boria et al. 2014). With biased datasets, the proximity of records used for model training and evaluation can artificially increase metrics of predictive performance (Veloz 2009; Hijmans 2012). To reduce the spatial bias present in our dataset while retaining as many records as possible, we spatially rarefied our training points at a distance of 5 km using the Spatially Rarefy Occurrence Data for SDMs tool of SDMToolbox v2.5 in ArcGIS 10.6.1 (Veloz 2009; Kramer-Schadt et al. 2013; Boria et al. 2014; Brown 2014). Additionally, training points which lacked corresponding soil data were excluded from the final data set. In total, we used 35 occurrence records as training points for modeling (Table 7.1).

Environmental Variables.—We considered 24 predictor variables for inclusion in the final model that represented climate, soil, topography, and wetland attributes (Table 7.2). To represent the influence of climatic conditions on Black-spotted Newt habitat, we obtained bioclimatic variables derived from temperature and precipitation data from WorldClim (v2.1) for the years 1970–2000 at a 30 arc-second (ca. 1 km) spatial resolution (Fick and Hijmans 2017). Several soil characteristics were included that were associated with Black-spotted Newt presence including clay, sand, and organic matter contents (Rappole and Klicka 1991; Robinson 2021). We obtained raster data of clay content (g/kg), sand content (g/kg), and soil organic carbon (dg/kg) from SoilGrids250m v2 using the mean value at a depth of 5–15 cm for each metric at a spatial resolution of 250 m (Poggio et al. 2021). A direct measurement of organic matter was unavailable, and soil organic carbon was used as a proxy since the two characteristics are related across biomes by a near-constant factor (Schulte and Hopkins 1996) and a significant relationship between organic matter and organic carbon contents in clay soils of a similar semi-arid environment has been described (Sakin 2012). Elevation was included as a predictor variable because of its ability to improve model precision even when its explanatory power is relatively low (Hof et al. 2012). We obtained SRTM digital elevation rasters of the study region at a 1 arc-second resolution (ca. 30 m) from USGS Earth Explorer (USGS 2000).

Since Black-spotted Newt presence was significantly correlated with the ephemerality of freshwater bodies or basins where they are found (Robinson et al. 2022), we derived a variable representing wetland ephemerality using data from the U.S. National Wetland Inventory (USFWS 2020) and from a Mexican wetland inventory conducted using a similar wetland classification scheme from Ducks Unlimited de México (DUMAC). The distance Black-spotted Newts travel from ponds has not been directly studied, but they are often found under cover items and in burrows and fissures near dry wetland basins (Judd 1985; Rappole and Klicka 1991; Bare 2018). A congener, the Eastern Newt (*N. viridescens*) has been observed traveling up to 800 m from natal ponds during non-migration periods (Healy 1975a; Healy 1975b; Gill 1978; Rinehart et al. 2009). To account for the movement of Black-spotted Newts into suitable habitat surrounding wetlands where they are found, a buffer of 500 m was placed around each wetland. Using the U.S. National

Wetland Inventory classification scheme (Cowardin et al. 1979), each unique wetland type was identified as ephemeral if the natural water regime resulted in fresh water covering the substrate for only a portion of the year under typical conditions (i.e., not during years of extreme drought). All other wetland types were classified as non-ephemeral. We converted this reclassified shapefile to a raster layer with the following categories: ephemeral wetland (3), non-ephemeral wetland (2), non-wetland (1).

We used ArcGIS 10.6.1 to create the ephemerality raster and to uniformly format the environmental rasters. We resampled bioclimatic and soil raster layers to 1 arc-second (ca. 30 m) to match the finest resolution predictor variable, while maintaining the original values assigned to an area by dividing a given cell into smaller cells with the same value. We chose to use a 1 arc-second resolution to maintain the detail in the elevation layer since even small depressions have the potential to serve as ephemeral habitat for Black-spotted Newts following rainfall events.

Without a thorough understanding of all habitat requirements for Black-spotted Newts, we chose to reduce the number of predictor variables to create a more accurate model than would likely result from using the entire set of predictor variables (Low et al. 2021). To determine which variables to retain for our final model, we first used all 24 variables to generate a set of 35 models made with different combinations of regularization multipliers (0.5, 1, 1.5, 2, 3, 4, 5) and feature classes (L, LQ, LQH, H, LQHP). We used geographically structured k-fold cross validation (spatial jackknifing) using three spatially segregated groups to test model predictive performance. Using geographically independent training and test datasets allowed us to use all 35 presence records as training points in model calibration and tested the model's ability to predict suitable habitat in areas that are geographically separated from training localities, an important consideration when sampling bias is present and model transferability is necessary (Merow et al. 2013; Araújo et al. 2019; Low et al. 2021). We ranked the relative performance of models using the omission rate on the 10^{th} Percentile Training Presence threshold (Anderson et al. 2003; Radosavljevic and Anderson 2014) and, if models had the same omission rate, they were secondarily ranked using the area under the receiver operating characteristic curve (AUC; Radosavljevic and Anderson 2014). The highest-performing model, abbreviated MaxVar, was used for variable reduction.

Although Maxent can perform well with highly correlated predictor variables, the variables selected for use in the model may not be the most biologically meaningful and using all predictor variables can result in an overly complex model (Elith et al. 2011; Merow et al. 2013). We assessed the collinearity of predictors by calculating Pearson correlation coefficients (r) across the entire study extent for all pairs of quantifiable variables (Dormann et al. 2013) and identified variable pairs with $r \geq |0.8|$ as highly correlated (Elith et al. 2011; Andersen and Beauvais 2013; Syfert et al. 2013; Warren et al. 2014). Since we lacked a comprehensive biological understanding of habitat requirements for Black-spotted Newts, we determined which variable in highly correlated pairs to retain based on the percent contributions to MaxVar (Andersen and Beauvais 2013; Warren et al. 2014; Groff et al. 2014). We retained the variable with the highest contribution to MaxVar and discarded any highly correlated variables. We repeated this process with the next highest contributing variable until all variables had been retained or discarded. We then removed variables having both percent contribution and permutation importance <3%. The following six variables were retained for use in the final models: bio02, bio14, bio18, clay, elevation, ephemerality. These variables contributed 96.4% to MaxVar. We used SDMToolbox v2.5 (Brown 2014) to create Maxent models, calculate and rank omission rates and AUC values, and calculate Pearson correlation coefficients for use in the variable reduction process.

Modeling Approach and Evaluation.—When using a biased set of occurrences, if background points are selected from areas far from occurrence records, the potential for environmental bias between background and training samples and the likelihood of model overfitting to this bias both increase (Phillips et al. 2009; Anderson and Raza 2010; Peterson et al. 2011; Radosavljevic and Anderson 2014). Using areas far from known occurrences for background selection can also produce models that struggle to detect minor changes in habitat suitability when relatively small environmental differences exist across the study extent (VanDerWal et al. 2009). Limiting the area of background selection to within a given distance of occurrence records can improve model sensitivity (Barbet-Massin et al. 2012). Instead of randomly selecting a background sample from the entire study extent, we used SDMToolbox v2.5 (Brown 2014) to create a minimum convex polygon around the occurrence records using a 25-km buffer to account for potential dispersal from these localities (Merow et al. 2013), while mirroring the bias in occurrence data (Phillips et al. 2009) to improve predictive performance. We used this bias file to create MaxVar and the final model used to show current and future distributions of suitable habitat.

We created the final model, MaxFinal, following the same procedure used to create MaxVar. We tuned the model to select optimal feature class combinations and regularization multipliers with the reduced set of predictor variables (Merow et al. 2013; Warren et al. 2014; Araújo et al. 2019; Low et al. 2021). We tested the same five feature class combinations (L, LQ, LQH, H, LQHP) and eight regularization multipliers (1, 1.5, 2, 2.5, 3, 3.5, 4, 5), using spatial jackknifing with three groups to calculate the omission rate on the 10th Percentile Training Presence threshold and AUC for each model created. As with MaxVar, we chose MaxFinal by selecting the model with the highest omission rate and, secondarily, the highest AUC. We used the 10th Percentile Training Presence threshold to create a binary raster representing the distribution of suitable habitat within the study region (Radosavljevic and Anderson 2014).

We then projected MaxFinal to create distributions of suitable habitat for Black-spotted Newts at two times in the future and under two climate change scenarios. The Sixth Assessment Report (AR6) of the Intergovernmental Panel on Climate Change (IPCC) analyzed the climate response to five different scenarios of future human development known as Shared Socioeconomic Pathways (SSPs; IPCC 2021). The underlying socioeconomic assumptions of the SSPs were associated with different levels of greenhouse gas emissions that range from reaching net zero emissions by the middle of the 21st century under SSP1-1.9 to an approximate doubling of emissions from current levels in the same time frame under SSP5-8.5 (IPCC 2021). To limit warming to 2°C or below by 2100, as depicted by the two lowest emissions SSPs, immediate action must be taken to rapidly reduce greenhouse gas emissions (IPCC 2022). Because of the drastic actions required to achieve the outcomes depicted by the more optimistic SSPs, we chose to use SSP2-4.5 (SSP2 hereafter) and SSP3-7.0 (SSP3 hereafter) to represent different potential emissions trajectories for the time periods 2061–2080 (2070 hereafter) and 2081–2100 (2090 hereafter; Harris et al. 2014). SSP2 represents an intermediate emissions scenario in which social, economic, and technological trends remain relatively consistent into the future and the increase in average global surface temperature from 2081–2100 relative to 1850–1900 is predicted to be between 2.1°C and 3.5°C (Riahi et al. 2017; Arias et al. 2021). SSP3 represents a high emissions scenario in which regional issues take precedence over international cooperation and the average global surface temperature from 2081–2100 is predicted to increase by 2.8–4.6°C relative to the reference period (Riahi et al. 2017; Arias et al. 2021).

We used the following general circulation models (GCMs) to create continuous and binary distributions for each of the four combinations of SSP and time period (SSP2-2070, SSP2-2090, SSP3-2070, SSP3-2090): CanESM5.0.3 (Swart et al. 2019), ACCESS-ESM1.5 (Ziehn et al. 2020), MIROC6 (Tatebe et al. 2019). Each GCM was admitted to the Coupled Model Intercomparison Project Phase 6 (CMIP6), which has facilitated the development of more comprehensive earth system models (Li et al. 2021) and requires models to meet exacting standards of consistency with past and present observations (Harris et al. 2014). CMIP6 models have different equilibrium climate sensitivities (ECS) that create a range of plausible future climates for a given emissions scenario and time period due to different rates and magnitudes of temperature change (Wehner 2020). We selected GCMs with low (MIROC6 ECS=2.6), intermediate (ACCESS-ESM1.5 ECS=3.9), and high (CanESM5 ECS=5.6) climate sensitivities (Hausfather 2019) to capture the uncertainty in projected climates for each SSP and time period (Harris et al. 2014). We downloaded rasters of future bioclimatic variables at a 30 arc-second resolution from WorldClim (v2.1) (Fick and Hijmans 2017). We formatted the bioclimatic rasters to have the same 30-m spatial resolution used for MaxFull, but the spatial extent was expanded to 32°N to account for potential northward dispersal. We created continuous and binary distributions using the 10th Percentile Training Presence threshold for all projections.

Geospatial Analyses.—We reclassified the continuous distributions of habitat suitability for current and projected models into 13 approximately equal intervals to highlight areas of higher suitability for survey efforts and to visualize changes in distribution under different emissions scenarios. We created ensemble models to depict the level of agreement in suitability between the three GCM projections for each SSP and year combination by summing the binary rasters. The resulting ensemble models had cell values ranging from 0–3, corresponding to the number of models that identified a given cell as suitable habitat, where a value of zero indicated the cell was identified as unsuitable by all GCMs and a value of three indicated the cell was identified as suitable habitat by all GCMs. Using these ensemble models, we created a binary consensus model by retaining cells identified as suitable by a majority of GCMs (cell values ≥2) and reclassifying all other cells as unsuitable. We used SDMToolbox v2.5 (Brown 2014) to calculate areas of contraction (suitable in current, unsuitable in future), expansion (unsuitable in current, suitable in future), no suitability (unsuitable in current and future), and continued suitability (suitable in current and future; Brown and Yoder 2015) under each future scenario using the current binary thresholded raster and the binary consensus rasters. We calculated centroid changes in the distribution of suitable habitat between current and future binary rasters and between the 2070 and 2090 binary rasters for each future scenario using SDMToolbox. These calculations produced vectors that depicted the magnitude and direction of shifts in the habitat distributions.

RESULTS

The following six variables were retained for use in the final models: bio02, bio14, bio18, clay, dem, ephemerality (Table 7.2). These variables contributed 96.4% to MaxVar. Through variable reduction and model tuning we created a model of the current distribution of suitable habitat, MaxFinal, using linear, quadratic, hinge, and product features and a regularization multiplier of two (Figure 7.1). MaxFinal had an omission error of 14.29% and an AUC of 0.8111. The range of potential distributions of suitable habitat under each of the four combinations of future climate change scenario and year (SSP2/2070, SSP2/2090, SSP3/2070, SSP3/2090) are visualized in the three models created using GCMs with different climate sensitivities (Figures 7.2–7.5). The

accompanying ensemble models displayed the level of agreement between GCMs in the binary distribution of suitable habitat for each scenario and year combination (Figures 7.6–7.9). The area of suitable habitat under SSP2 decreases by 136.25 km^2 in 2070 but increases by 1168.42 km^2 in 2090 compared to the current area of suitable habitat (Table 7.3). Under SSP3, the area of suitable habitat increases in 2070 and 2090 compared to the current area, with an expected increase of 6065.67 and 5000.71 km^2 of suitable habitat in 2070 and 2090, respectively. The greatest area of suitable habitat is present under SSP3 in 2070 (47993.51 km^2; Table 7.3).

The centroid of the current distribution of suitable habitat was calculated to fall in southwestern Willacy County, Texas (26.381869, -97.505354). Under SSP2, the centroid of the habitat distribution moves southward by 2070 then shifts northwest by 2090, resulting in an overall southwest shift of ca. 4.7 km from current to 2090 (Figure 7.10). Under SSP3, the centroid of the habitat distribution moves southwest by 2070 then south-southeast until 2090, resulting in a southwestern shift of ca. 15.2 km compared to the current centroid (Figure 7.10).

DISCUSSION

Current Habitat Suitability Model.—In the current habitat distribution model, MaxFinal, the largest patches of the highest suitability habitat are in Kleberg, Kenedy, Willacy, Hidalgo, and Cameron counties in Texas and the municipalities of Matamoros and San Fernando in Tamaulipas (Figure 7.1). Smaller areas of high suitability are found in southeastern Nueces County and along the Rio Grande in Starr County. The suitability of habitat generally decreases moving northeast from Corpus Christi Bay along the coastline. Additionally, habitat suitability is generally low along coastal Tamaulipas south of the Municipality of San Fernando, but increases in along the border with Veracruz. We were surprised to find potential low suitability habitat extending inland along the Nueces River into LaSalle County, which we attribute to two training points occurring along the drainage.

Current habitat suitability varies among the seven Texas metapopulation centers described by Rappole and Klicka (1991) and appears to coincide with our data on Black-spotted Newt detections, despite not accounting for this in the model. The model generally returned lower estimates of suitability around the five metapopulation centers found in Kleberg and Kenedy counties (1: Vattmannville; 2: CKWRI South Pasture; 3: Riviera; 4: FM 772, 1.0 mi S jct 628; and 5: US Hwy 77, 14.7–21.7 mi S Armstrong [herein, "US Hwy 77") compared to the two metapopulation centers in Cameron County (6: Laguna Atascosa NWR; 7: Brownville–Matamoros) despite including occurrences from all these areas as training points. Despite survey efforts by Bare (2018), Robinson et al. (2022), and Collins (2022), there have been no recent detections of Black-spotted Newts in Kenedy and Kleberg counties where relatively lower habitat suitability is estimated by the model. In contrast, the Laguna Atascosa NWR and Brownsville–Matamoros metapopulation centers, where most of the highest suitability habitat is located, contain recent Black-spotted Newt detections, both with eDNA and traditional sampling. Within the Laguna Atascosa NWR and Brownsville–Matamoros metapopulation centers, our recent survey work has resulted in both continued detections of Black-spotted Newts in historic localities (though not all historic localities sampled), but also new localities.

In Kleberg County, the CKWRI South Pasture metapopulation center is found in a narrow corridor of moderately suitable habitat (ca. 0.72) characterized by heavy fragmentation with low suitability to the north and south, and deteriorating suitability when moving west. The other three metapopulation centers are in an area of more continuous and higher suitability habitat ranging from ca. 0.82–0.90, but suitability decreases moving north and west from these areas, and they are

bounded by Baffin Bay to the south and east. In Kenedy County, the US Hwy 77 metapopulation center is found in habitat with suitability increasing from north to south from ca. 0.68 to 0.86 into a patch of higher suitability habitat to the east of US Hwy 77 along the border with Willacy County.

In Cameron County, the Laguna Atascosa NWR metapopulation center is characterized by a large area of nearly continuous high suitability habitat (>0.97 in most areas) with patches and corridors of slightly less suitable habitat (ca. 0.80–0.86). The Brownville–Matamoros metapopulation center also contains large areas of continuous and high suitability habitat, but suitability drops dramatically and fragmentation increases moving toward the Brownsville city center. While Brownsville is surrounded by patches of high suitability habitat, habitat surrounding Matamoros is estimated to be much lower with only a few very small patches of moderate suitability habitat within and directly surrounding the urban area. Along the Rio Grande, habitat suitability increases, and the size of high suitability habitat patches increases moving east toward the Gulf of Mexico.

The current habitat distribution model places the core of suitable Black-spotted Newt habitat in Willacy, Hidalgo, and Cameron counties, the only counties where newts have been physically detected (e.g., vouchered or photographed) since 2000 (see Chapter 2), with other large areas of high-suitability habitat in Kenedy and Kleberg counties. Despite the high degree of estimated suitability in these counties, large patches of cool colors in this greater matrix represent unsuitable habitat and correspond with human population centers and areas of urban development (Figure 7.1). This trend is most apparent in southern Hidalgo County, where a large blue patch with narrow corridors extending east and west from the center represents the McAllen–Edinburg–Mission metropolitan area and US IH-2. Additionally, a similar trend exists for the Brownsville–Matamoros metropolitan area, where Matamoros is a nearly continuous blue patch while Brownsville is a more fragmented blue patch north of the Rio Grande. Other developments and population centers estimated as very low suitability habitat that are distinguishable within the surrounding matrix of habitat include: Harlingen and US IH-69E in Cameron County, Raymondville in Willacy County, Kingsville in Kleberg County, and Robstown and Corpus Christi in Nueces County.

Future Habitat Suitability Models.—Future climate projections of MaxFull indicate the potential for important changes within the habitat core. Under SSP2, the core of the binary distribution (Figures 7.6B, 7.7B) remains relatively stable over time. In 2070, small areas of suitable habitat are lost along the inland edge of the distribution from Kleberg County southwest through Starr County. Similar contractions occur in the municipalities of Reynosa and Camargo. Contractions occur in the interior of the distribution in central Kenedy County, northeastern Kleberg County, and in Hidalgo County around the McAllen–Edinburg–Mission metropolitan area and extending east along US IH-2 toward Cameron County. Suitable habitat is gained along the edge of the distribution in Jackson, Victoria, Refugio, San Patricio, and Zapata counties and from southern Rio Bravo Municipality to northern Veracruz. By 2090, many areas of contraction have been restored and even converted to gains resulting in net expansion along the inland edge of the distribution from Jackson County south into Starr County (Figure 7.7B). Additional patches of suitable habitat appear in Zapata County. The interior contractions found in Kenedy and Hidalgo counties remain unchanged. Within the unchanged core of suitable habitat, the GCM models reveal the potential for a slight decrease in overall suitability by 2090 (Figure 7.3). This is particularly apparent in the slight deterioration of current moderate-quality habitat in Kenedy, Willacy, Cameron, and Hidalgo counties and in northern Tamaulipas predicted by ACCESS-ESM1.5 and

CanESM5.0.3. This results in a decrease in the quality of habitat surrounding the highest suitability patches.

Under SSP3, the dominant mode of change in suitable habitat is that of expansion. Similar to the expansion under SSP2, gains are mostly seen along the inland edges of the distribution with the largest areas of gain in Nueces, Jim Wells, Brooks, and Hidalgo counties, and in Reynosa, Rio Bravo, Mendez, San Fernando, and Soto la Marina municipalities by 2070 (Figure 7.8B). In 2090, the magnitude of the gains is much smaller compared to the gains predicted in 2070 (Figure 7.9B). The large areas of predicted gains in Jim Wells and Nueces counties are completely absent, most of the expansion predicted in Brooks, Hidalgo, and Starr counties are absent, and new areas of habitat loss are visible. A similar trend occurs in the municipalities adjacent to Starr County and in the Municipality of Reynosa. Despite the gains displayed in 2070, by 2090, suitable habitat is lost around the Nueces River in Live Oak and McMullen counties. Additional expansion of habitat in 2090 occurs in Jackson, Victoria, Goliad, Refugio, and Bee counties and in southern Tamaulipas, Soto la Marina, and Abasolo municipalities (Figures 7.9B). The individual GCM models reveal that most of the habitat gained on the edges of the distribution is of relatively low suitability (Figures 7.4, 7.5). By 2090, all GCMs predict at least some improvement in the overall suitability of habitat in Kleberg, Kenedy, Willacy, Cameron, and Hidalgo counties. MIROC6 predicts minor improvements in suitability but little outward expansion (Figure 7.5C), ACCESS-ESM1.5 predicts low suitability habitat converting to moderate suitability habitat and an inland expansion of moderate habitat (Figure 7.5B), and CanESM5.0.3 predicts an overall inland expansion of suitable habitat with highly suitable habitat covering almost all of Cameron and Willacy counties, most of Hidalgo and Kenedy counties, and larger expanses of Star and Kleberg counties (Figure 7.5A). CanESM5.0.3 also predicts the expansion of moderate and high suitability habitat in northern Tamaulipas, including areas surrounding Matamoros.

Land Use Change.—The impact of urbanization on the suitability of habitat is evident in the current and future distributions without being explicitly included as a predictor variable in the models, indicating some degree of difference in bioclimatic, soil, elevation, or wetland variables between urban and non-urban environments. The current model and future projections all place the most high-suitability habitat for the Texas Black-spotted Newt in Hidalgo, Cameron, and Willacy counties and, under SSP3, even predict improved suitability in these counties. However, Cameron and Hidalgo counties also contain the most pronounced areas of low-suitability habitat that correspond to high human population density and, along with Starr and Willacy counties, are predicted to experience continued population growth through the first half of the 21st Century (Stubbs et al. 2003). The rapidly growing population is accompanied by the conversion of native habitat and agricultural land to urban land cover (Ellard and Patrick 1988; Huang and Fipps 2011; Pena 2012; Lombardi et al. 2020) and correlates with an increase in paved roads, drainage of ponds and low-lying areas, and fragmentation of habitat (Jahrsdoerfer and Leslie 1988; Leslie 2016).

While agriculture has historically been the primary driver of habitat loss and fragmentation in south Texas (Ellard and Patrick 1988; Jahrsdoerfer and Leslie 1988; Fulbright and Bryant 2002), urbanization is predicted to become the dominant cause of habitat destruction, degradation, and fragmentation in the Lower Rio Grande Valley (Marzluff and Ewing 2001). Despite the potential for improved suitability surrounding the McAllen–Edinburg–Mission and Brownsville–Harlingen–San Benito metropolitan areas predicted by SSP3 and the inland expansion of suitable habitat under both SSP2 and SSP3, if predicted urban growth and development come to fruition and surrounding agricultural land is converted for urban use, we can expect a decline in habitat

suitability as urban areas estimated to be poor-quality habitat expand and human-driven landscapes become increasingly dissimilar from native habitat (e.g., Marzluff and Ewing 2001).

The current and future predicted habitat suitability models consistently place the core of suitable habitat within Willacy, Cameron, and Hidalgo counties. Even under different scenarios of climate change, the centroid of the habitat distribution is predicted to undergo a maximum southwestern shift of ca. 15.2 km and remain positioned along the Willacy–Cameron County line, northwest of Laguna Atascosa NWR. Future predictions of habitat suitability place areas of improved suitability within one of the fastest-growing areas of the United States, where our models already display a strong incompatibility between urban landscapes and suitable newt habitat. Predicted expansions of suitable habitat occurring along the inland margins of the distribution may aid in the expansion of newt range only if individuals are geographically and physiologically capable of dispersal to these areas. Our recent detections of Texas Black-spotted Newts and the estimation of high suitability habitat in these areas suggests that tracts of relatively undisturbed native habitat are critical for the presence and persistence of this populations, particularly in Cameron and Hidalgo counties, where land conversion for urban use is most prominent.

Table 7.1. Occurrence records used as training points for modeling the distribution of suitable habitat for the Texas Black-spotted Newt (*Notophthalmus meridionalis meridionalis*) with locality (state: county [USA] or municipality [Mexico]: locality), source, and observation type for each record. Specific GPS coordinates have been redacted in this table. Some training point localities are represented by additional, non-listed occurrence records. Training points attributed to Rappole and Klicka (1991) and Bare (2018) are visual observations collected as part of their respective survey work. TX = Texas, USA; TA = Tamaulipas, Mexico; CM = Carnegie Museum of Natural History; iNat = iNaturalist; KU = Biodiversity Institute, University of Kansas; KUDA = Kansas University Digital Archives; LSUMZ = Louisiana Museum of Natural History, Louisiana State University; SMBU = Mayborn Museum Complex, Strecker Museum, Baylor University; TNHC = Biodiversity Collections, University of Texas at Austin; TCWC = Biodiversity Research and Teaching Collections, Texas A&M University; UF = Florida Museum of Natural History, University of Florida; UMMZ = Museum of Zoology, University of Michigan; USNM = Smithsonian Institution, National Museum of Natural History.

Locality	Record	Observation Type
TX: Calhoun: Powderhorn Wildlife Management Area, midline fence pond	Collins 2022	eDNA
TX: Live Oak: Live Oak County Park, pond SE of parking area	Robinson et al. 2022	eDNA
TX: McMullen: TX Hwy 16, S of Tilden, 15 m N Nueces River bridge	KUDA 11223	Specimen
TX: Refugio: Bayside	TNHC 84147	Specimen
TX: San Patricio: 1.3 mi NW 300 degrees W; Aransas Pass	TCWC 97539	Specimen
TX: Kleberg: Caesar Kleberg Wildlife Research Institute; South Pasture	Rappole and Klicka 1991	Visual
TX: Kleberg: FM 772, 1 mi N Vattmannville	Rappole and Klicka 1991	Visual
TX: Kleberg: 3–5 mi E Riviera	TCWC 64831	Specimen
TX: Kleberg: US Hwy 77, 0.1 mi S jct FM 771	Rappole and Klicka 1991	Visual
TX: Kenedy: US Hwy 77, 17.0 mi S Armstrong	Rappole and Klicka 1991	Visual
TX: Kenedy: US Hwy 77, 21.7 mi S Armstrong	Rappole and Klicka 1991	Visual
TX: Hidalgo: 3–4 mi N Sal del Ray	KU 145283	Specimen
TX: Willacy: TX Hwy 186, San Perlita	iNat 564951	Photograph
TX: Willacy: San Perlita, 2 mi NNW	TNHC 101944	Specimen
TX: Willacy: East Foundation El Sauz Ranch, Newt Pond	TNHC 116644	Specimen
TX: Hidalgo: Brushline Rd S	Bare 2018	Visual
TX: Willacy: US Hwy 77, 1 mi S Raymondville	LSUMZ 113854	Specimen
TX: Willacy: Grace Heritage Ranch, main pond	Bare 2018	Visual
TX: Cameron: Laguna Atascosa National Wildlife Refuge, Newt Pond	Collins 2022	eDNA
TX: Starr: Old Military Hwy, ca. 2.6 rd km ESE jct Co Rd 2360	Collins 2022	eDNA

TX: Cameron: Laguna Atascosa National Wildlife Refuge, Grebe Tank	Bare 2018	Visual
TX: Cameron: Laguna Atascosa National Wildlife Refuge, Prairie Trail pond #2	Robinson et al. 2022	eDNA
TX: Hidalgo: 1 mi E of Bentsen State Park	CM 62295	Specimen
TX: Cameron: pond S of Port Isabel High School Tarpon Stadium	Robinson et al. 2022	eDNA
TX: Cameron: 4 mi W of Los Fresnos	SMBU 15144	Specimen
TX: Hidalgo: Santa Ana National Wildlife Refuge, 11 mi S of Pharr	LSUMZ 113847	Specimen
TX: Cameron: Esp Santo Rd, ca. 1.2 rd km E jct Co Rd 1847 (Paredes Line Rd)	TNHC 116782	Specimen
TX: Cameron: Palo Alto Battlefield National Historical Park, First Tank	TNHC 116786	Specimen
TX: Cameron: Southmost Preserve, Overlook Resaca	Bare 2018	Visual
TA: Matamoros: Matamoros, 28 mi S on 101	TNHC 84196	Specimen
TA: Reynosa: State Road 97, 38.0 mi S Mexico 2	UF 176945	Specimen
TA: Matamoros: Hwy 101, 35.1 mi N Jct. Hwy 97	Rappole and Klicka 1991	Visual
TA: San Fernando: El Tejon, 9.5 mi NE on 101	TNHC 84448	Specimen
TA: San Fernando: K-202 on Rt 101 S of Matamoros	UMMZ 170191	Specimen
TA: Soto la Marina: San Jose de Las Rusias, 0.25 mi N of, 17.8 mi S from jct of MX Routes 70 and 180, on MX Route 180	USNM 258643	Specimen

Table 7.2. Environmental variables considered for inclusion in the final habitat distribution model. Variables shown in bold with an asterisk were retained for use in the final model.

Environmental Variable	Code	Source
Elevation*	**dem**	USGS (2000)
Bioclimatic		Fick and Hijmans (2017)
Annual mean temperature	bio01	
Mean diurnal range*	**bio02**	
Isothermality	bio03	
Temperature seasonality	bio04	
Maximum temperature of warmest month	bio05	
Minimum temperature of coldest month	bio06	
Temperature annual range	bio07	
Mean temperature of wettest quarter	bio08	
Mean temperature of driest quarter	bio09	
Mean temperature of warmest quarter	bio10	
Mean temperature of coldest quarter	bio11	
Annual precipitation	bio12	
Precipitation of wettest month	bio13	
Precipitation of driest month*	**bio14**	
Precipitation seasonality	bio15	
Precipitation of wettest quarter	bio16	
Precipitation of driest quarter	bio17	
Precipitation of warmest quarter*	**bio18**	
Precipitation of coldest quarter	bio19	
Land cover		USFWS (2020)
Wetland water regime*	**ephemerality**	
Soil		Poggio et al. (2021)
Sand content (g/kg)	sand	
Clay content (g/kg)*	**clay**	
Soil organic carbon (dg/kg)	carbon	

Table 7.3. Area (km^2) of suitable habitat for *Notophthalmus meridionalis meridionalis* and dynamics of change under four combinations of climate change scenario and year.

Climate Scenario, Year	Gain	Loss	Unchanged	Total Suitable	Net change
SSP2-4.5, 2070	1186.80	1323.05	40604.79	41791.59	-136.25
SSP2-4.5, 2090	1614.95	446.53	41481.31	43096.26	1168.42
SSP3-7.0, 2070	6073.23	7.57	41920.27	47993.51	6065.67
SSP3-7.0, 2090	5071.09	70.38	41857.46	46928.55	5000.71

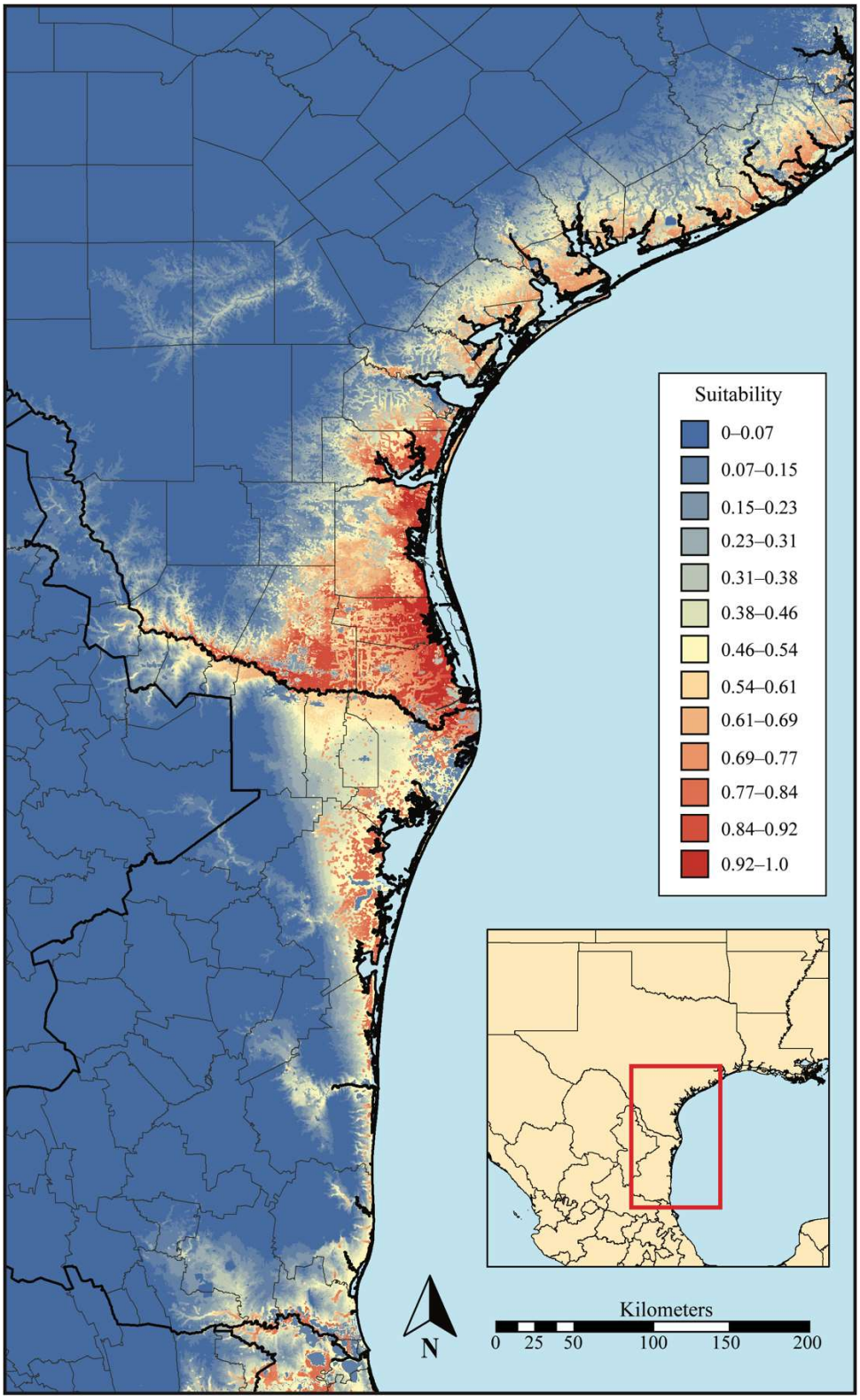

Figure 7.1. Current habitat suitability model for *Notophthalmus meridionalis meridionalis* across southern Texas, USA, and northeastern Mexico. Warmer colors indicate higher habitat suitability.

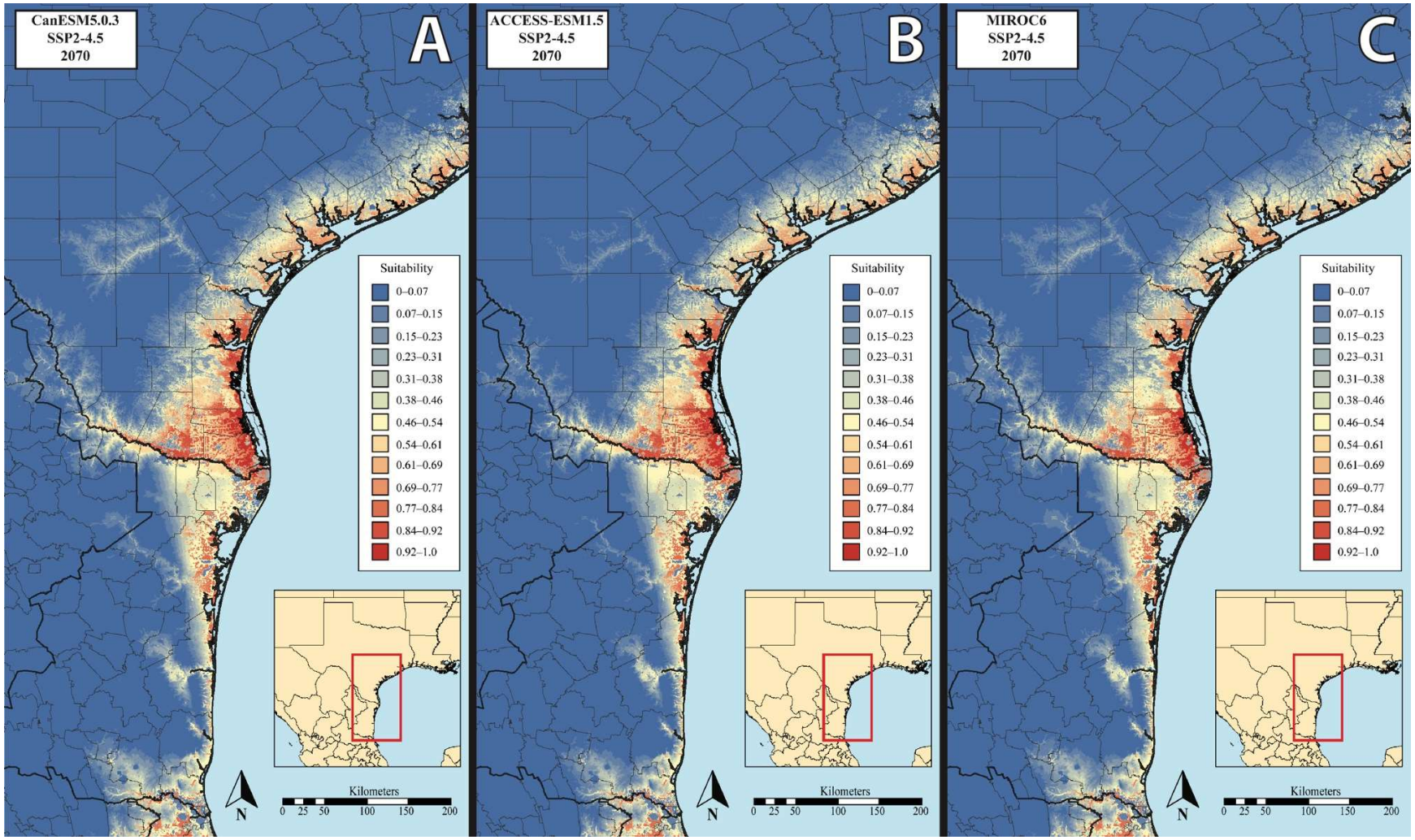

Figure 7.2. Future habitat suitability models for *Notophthalmus meridionalis meridionalis* across southern Texas, USA, and northeastern Mexico under SSP2-4.5 in 2070 using CanESM5.0.3 (A), ACCESS-ESM1.5 (B), and MIROC6 (C) general circulation models.

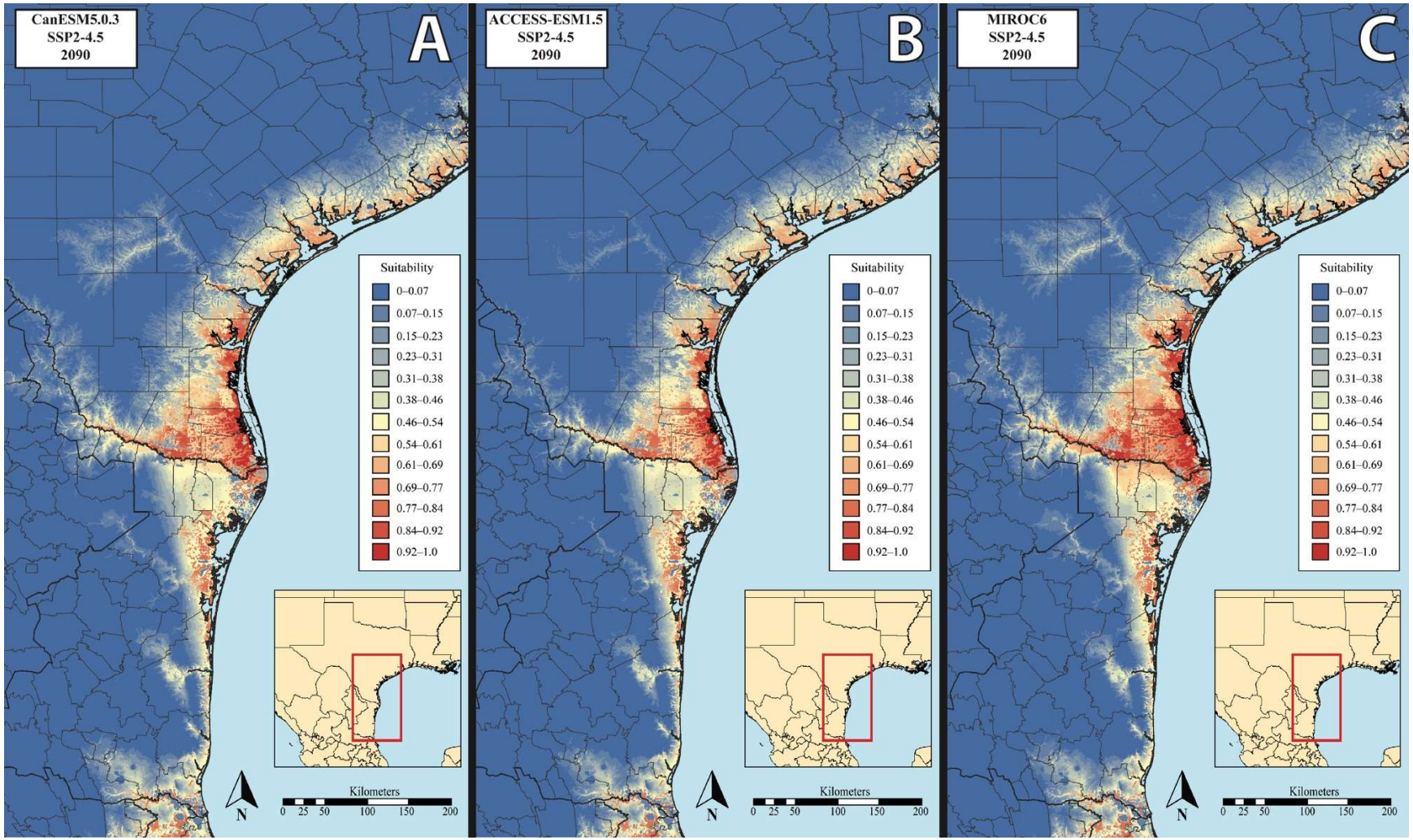

Figure 7.3. Future habitat suitability models for *Notophthalmus meridionalis meridionalis* across southern Texas, USA, and northeastern Mexico under SSP2-4.5 in 2090 using CanESM5.0.3 (A), ACCESS-ESM1.5 (B), and MIROC6 (C) general circulation models.

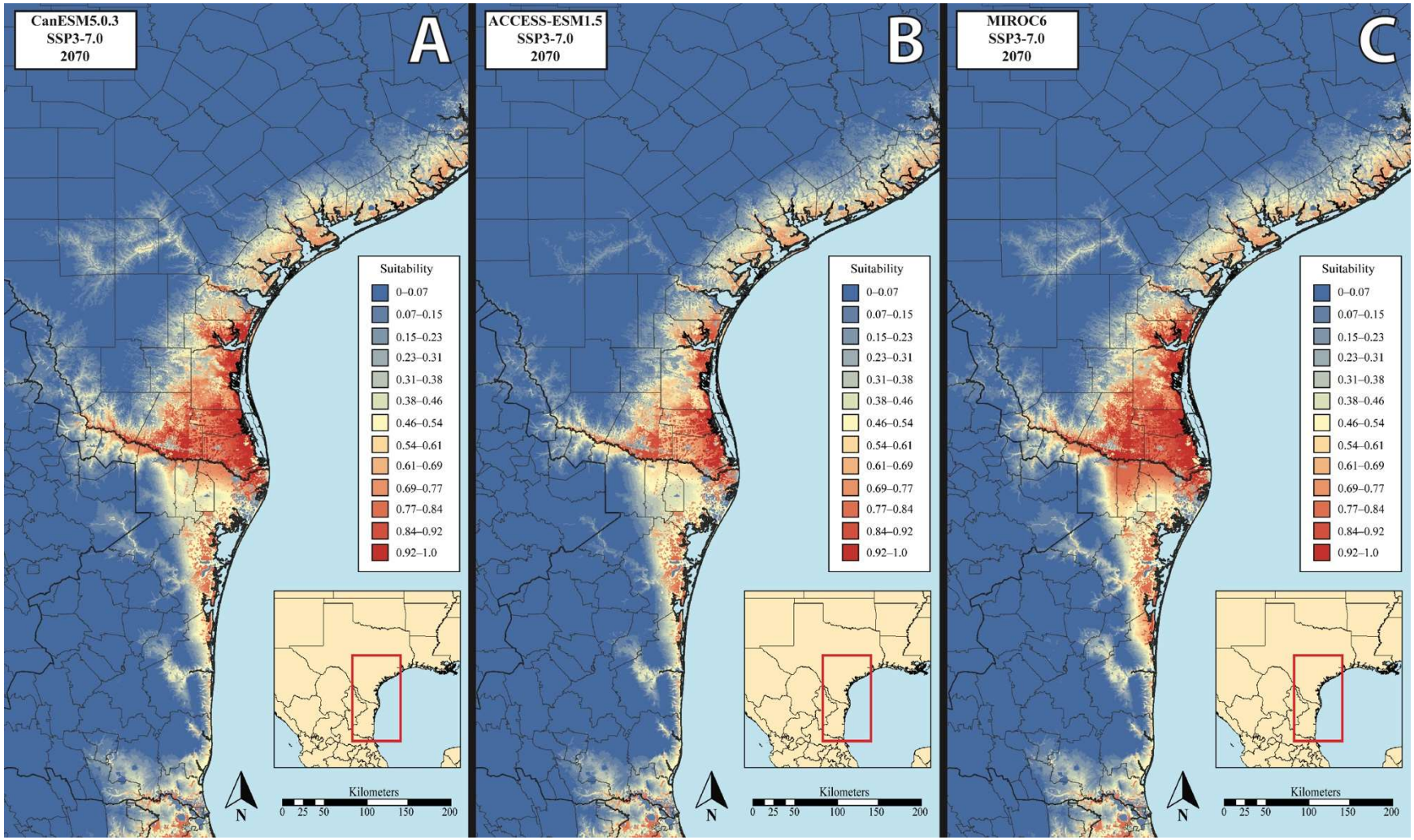

Figure 7.4. Future habitat suitability models for *Notophthalmus meridionalis meridionalis* across southern Texas, USA, and northeastern Mexico under SSP3-7.0 in 2070 using CanESM5.0.3 (A), ACCESS-ESM1.5 (B), and MIROC6 (C) general circulation models.

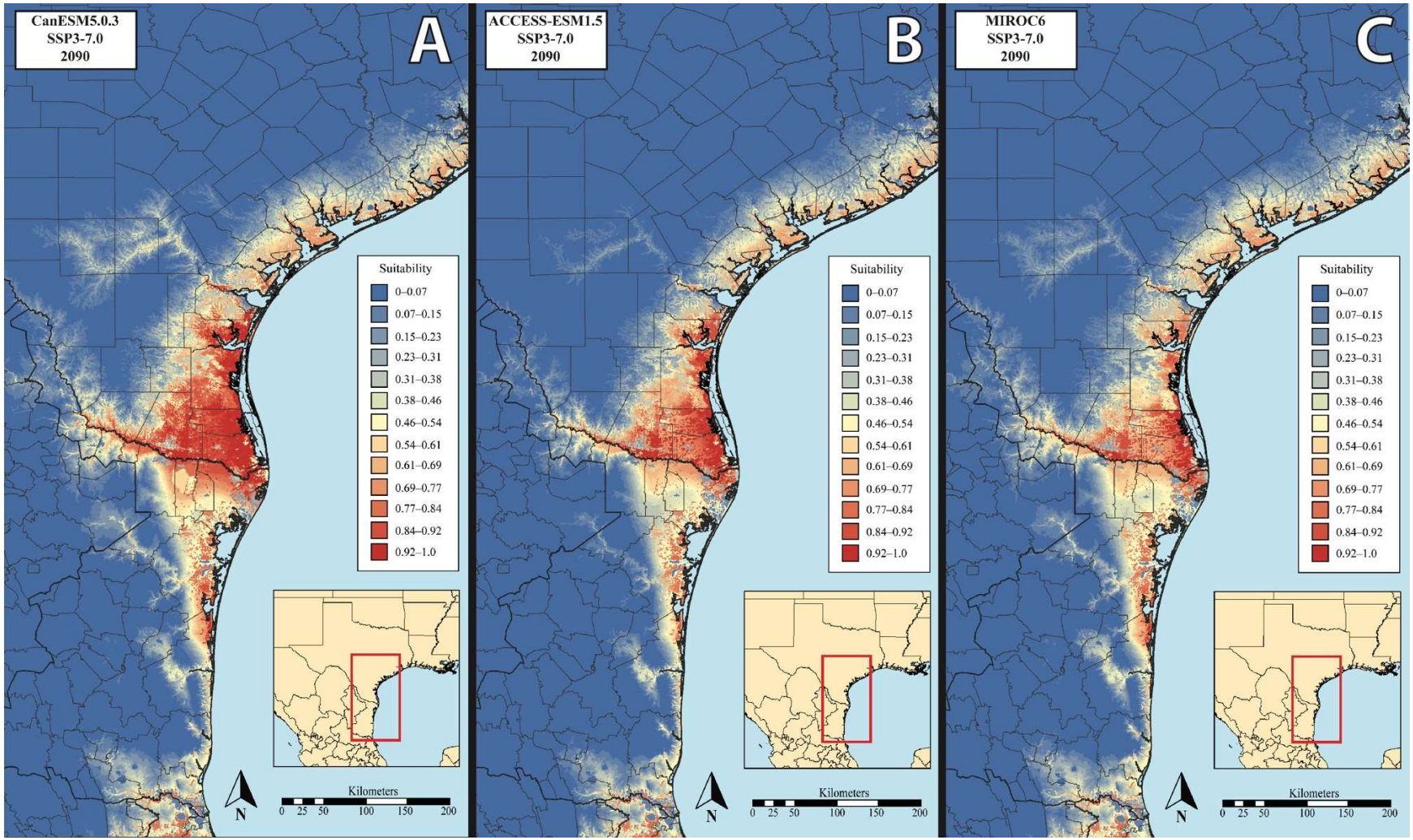

Figure 7.5. Future habitat suitability models for *Notophthalmus meridionalis meridionalis* across southern Texas, USA, and northeastern Mexico under SSP3-7.0 in 2090 using CanESM5.0.3 (A), ACCESS-ESM1.5 (B), and MIROC6 (C) general circulation models.

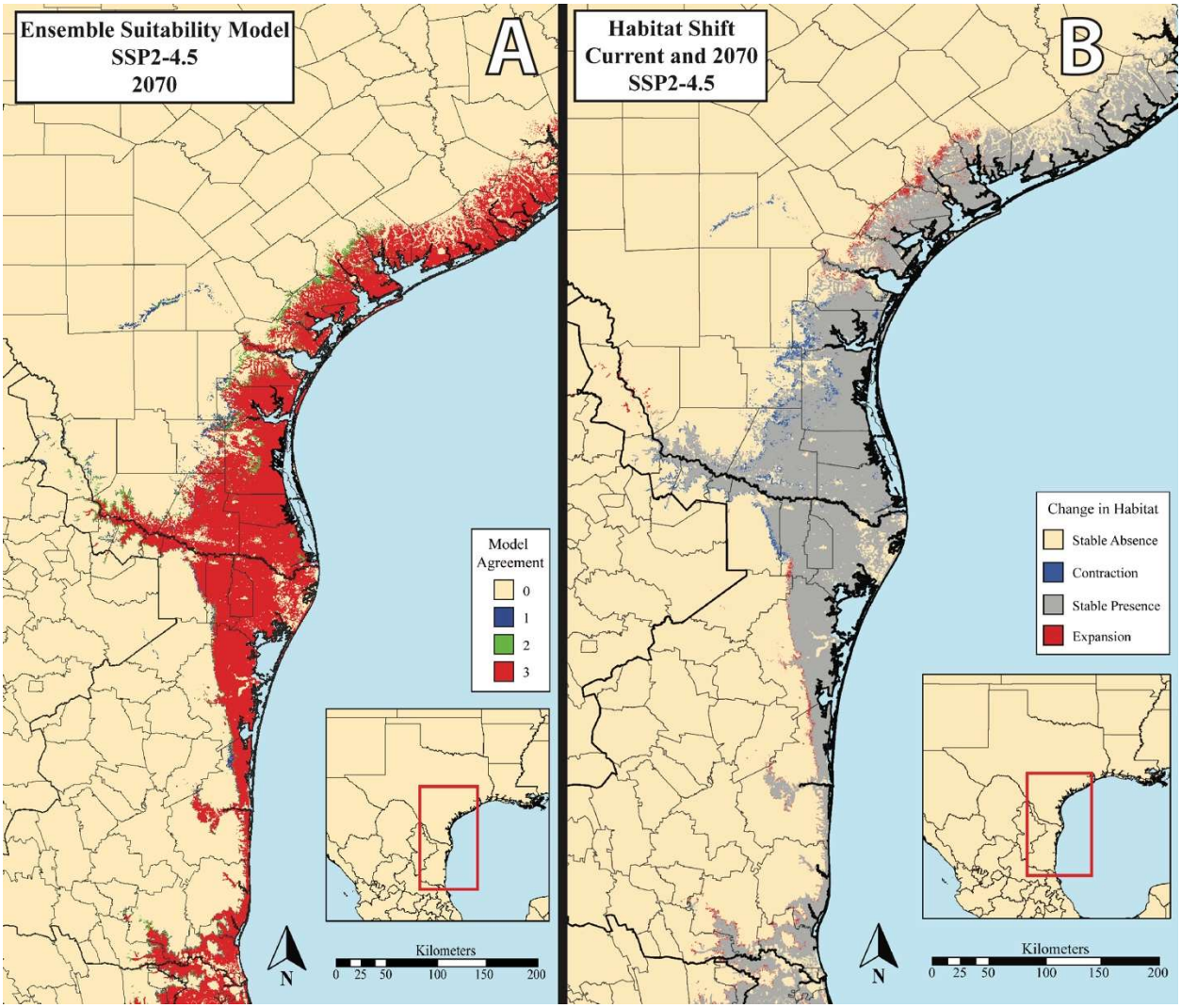

Figure 7.6. Predictive models of *Notophthalmus meridionalis meridionalis* habitat in southern Texas, USA, and northeastern Mexico under SSP2-4.5 in 2070: A) ensemble model showing agreement of three general circulation models; B) distribution of suitable habitat and the dynamics of change compared to the current distribution.

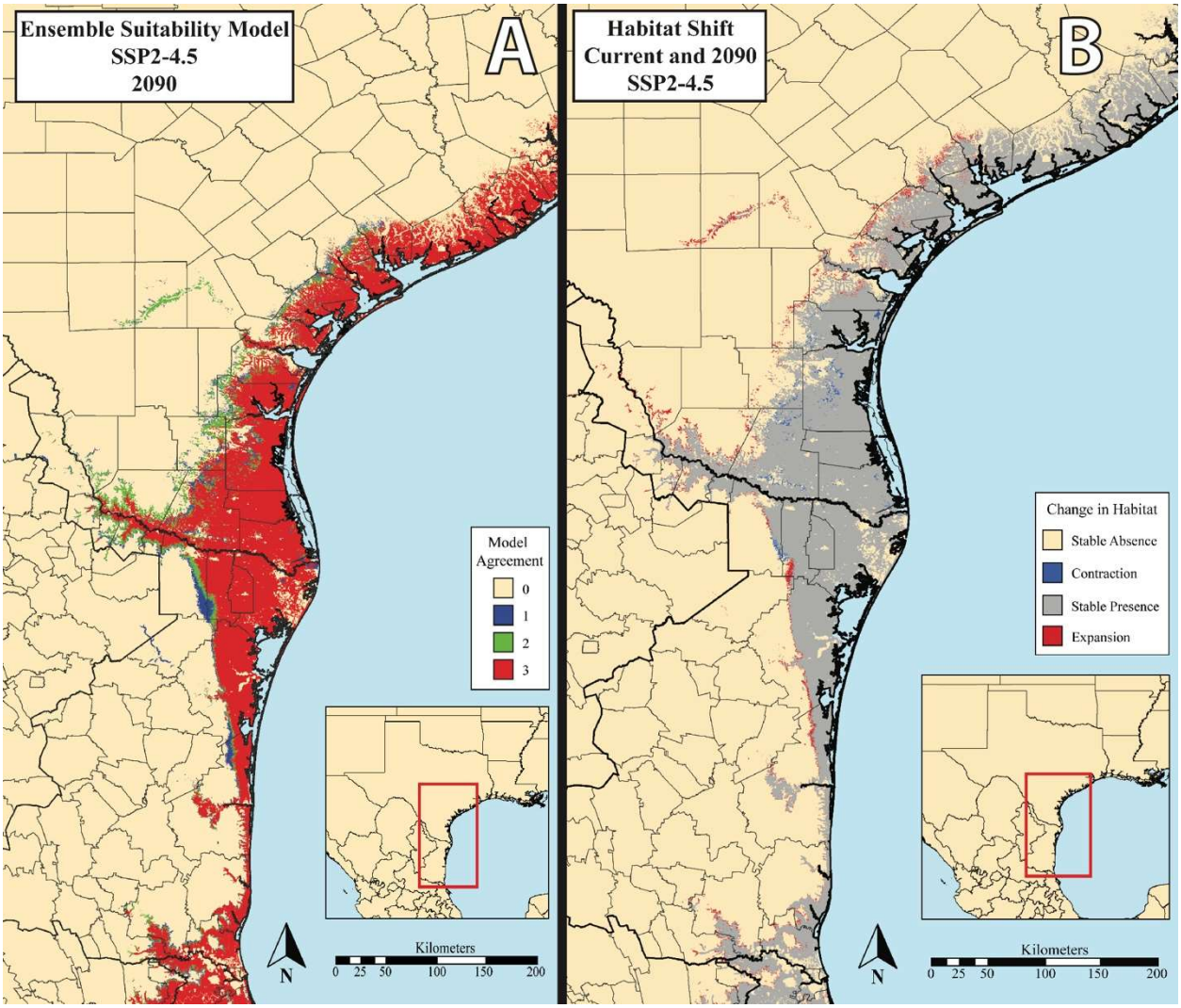

Figure 7.7. Predictive models of *Notophthalmus meridionalis meridionalis* habitat in southern Texas, USA, and northeastern Mexico under SSP2-4.5 in 2090: A) ensemble model showing agreement of three general circulation models; B) distribution of suitable habitat and the dynamics of change compared to the current distribution.

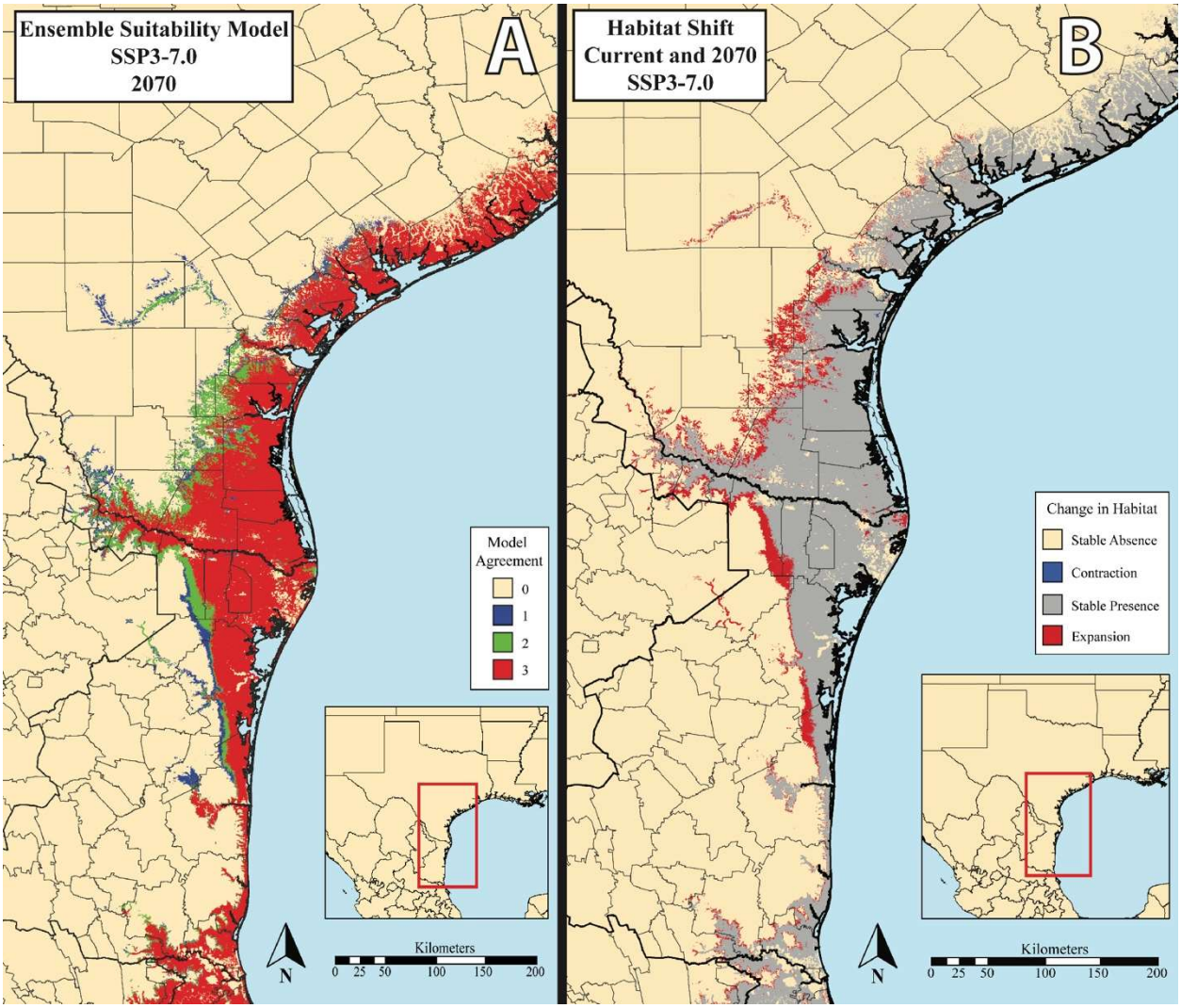

Figure 7.8. Predictive models of *Notophthalmus meridionalis meridionalis* habitat in southern Texas, USA, and northeastern Mexico under SSP3-7.0 in 2070: A) ensemble model showing agreement of three general circulation models; B) distribution of suitable habitat and the dynamics of change compared to the current distribution.

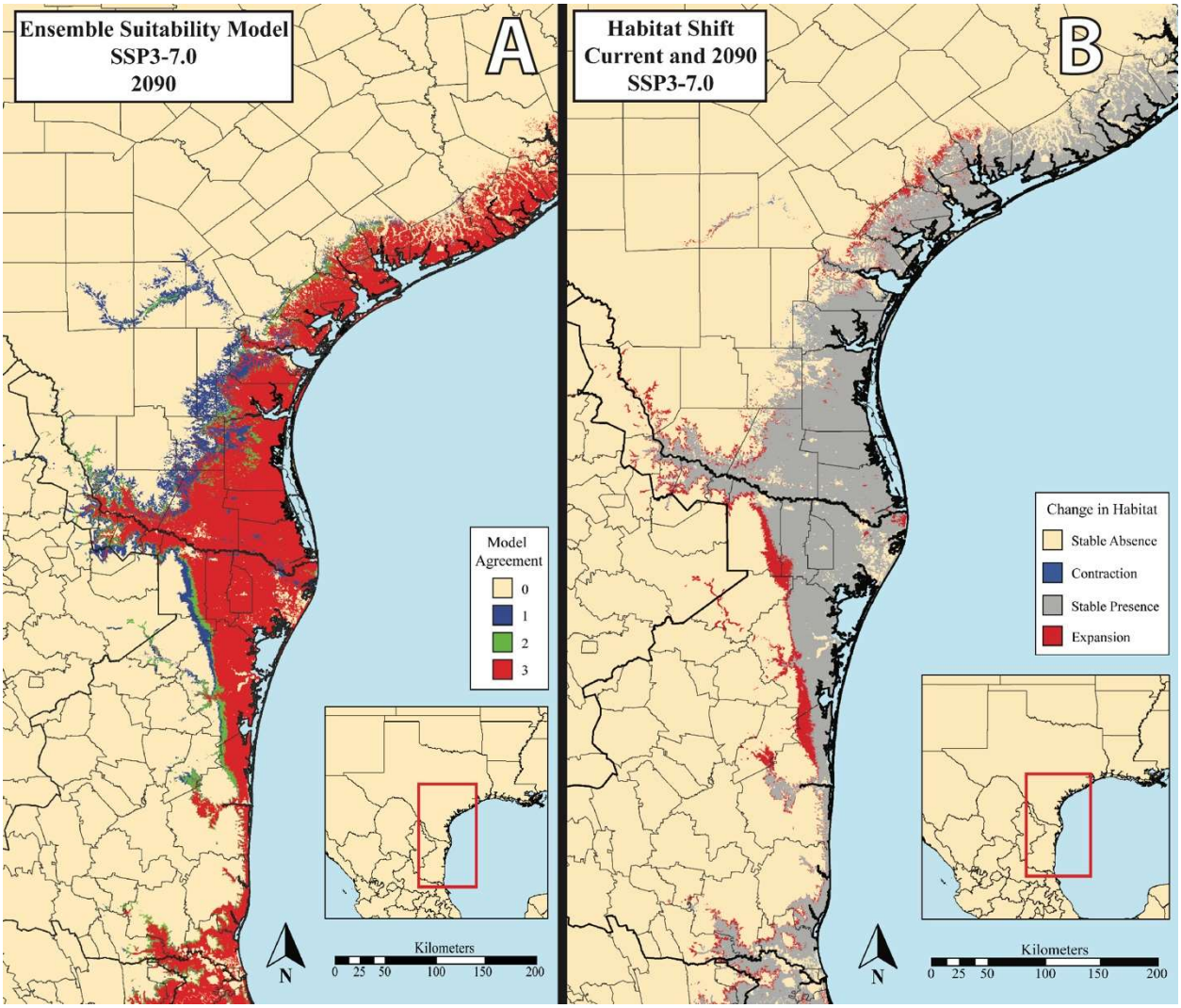

Figure 7.9. Predictive models of *Notophthalmus meridionalis meridionalis* habitat in southern Texas, USA, and northeastern Mexico under SSP3-7.0 in 2090: A) ensemble model showing agreement of three general circulation models; B) distribution of suitable habitat and the dynamics of change compared to the current distribution.

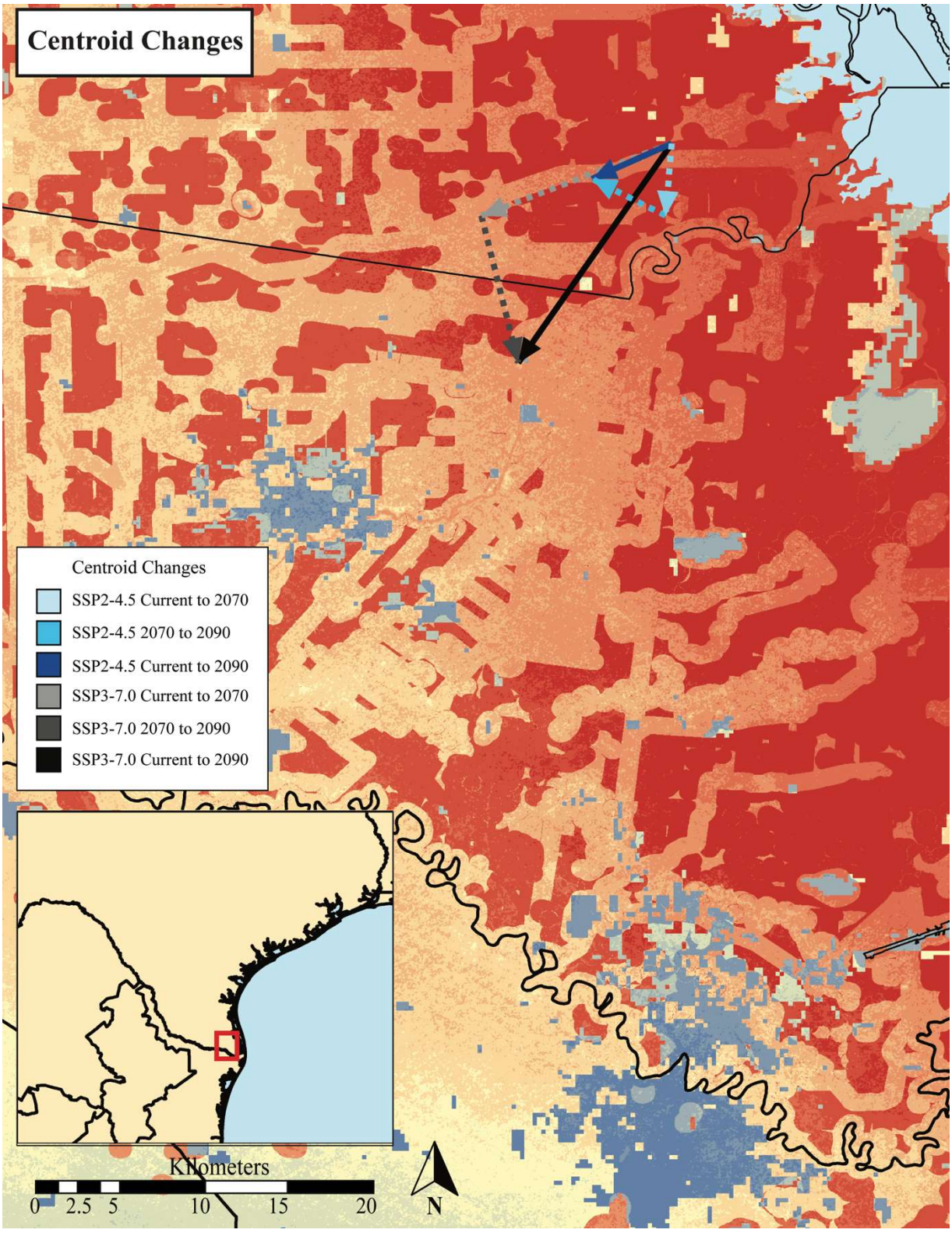

Figure 7.10. Changes to the centroid of *Notophthalmus meridionalis meridionalis* suitable habitat under SSP2-4.5 and SSP3.7.0 in 2070 and 2090 compared to the current centroid. Changes to the centroid are overlaid on the current habitat suitability map (Figure 7.1).

LITERATURE CITED

Abrahms B, DiPietro D, Graffis A, Hollander A. 2017. Managing biodiversity under climate change: challenges, frameworks, and tools for adaptation. *Biodiversity and Conservation* 26:2277–2293.

Altig R, McDiarmid RW. 2015. Handbook of Larval Amphibians of the United States and Canada. Cornell University Press, Ithaca, New York. xvii + 357 pp.

Andersen M, Beauvais G. 2013. Predictive distribution modeling of species of greatest conservation need in Texas. Final report for the Texas Natural Diversity Database, Texas Parks and Wildlife Department, Austin, Texas. 31 pp.

Anderson RP, Raza A. 2010. The effect of the extent of the study region on GIS models of species geographic distributions and estimates of niche evolution: preliminary tests with montane rodents (genus *Nephelomys*) in Venezuela. *Journal of Biogeography* 37:1378–1393.

Anderson RP, Lew DC, Peterson AT. 2003. Evaluating predictive models of species' distributions: criteria for selecting optimal models. *Ecological Modelling* 162:211–232.

Araújo MB, Anderson RP, Márcia Barbosa A, Beale CM, Dormann CF, Early R, Garcia RA, Guisan A, Maiorano L, Naimi B, O'Hara RB, Zimmermann NE, Rahbek C. 2019. Standards for distribution models in biodiversity assessments. *Science Advances* 5:eaat4858.

Arias PA, Bellouin N, Coppola E, Jones RG, Krinner G, Marotzke J, Naik V, Palmer MD, Plattner G-K, Rogelj J, Rojas M, Sillman J, Storelvmo T, Thorne PW, Trewin B, Achuta Rao K, Adhikary B, Allan RP, Armour K, Bala G, Barimalala R, Berger S, Canadell JG, Cassou C, Cherchi A, Collins W, Collins WD, Connors SL, Corti S, Cruz F, Dentener FJ, Dereczynski C, Di Luca A, Diongue Niang A, Doblas-Reyes FJ, Dosio A, Douville H, Engelbrecht F, Eyring V, Fischer E, Forster P, Fox-Kemper B, Fuglestvedt JC, Fyfe JC, Gillett NP, Goldfarb L, Gorodetskaya JM, Gutierrez JM, Hamdi R, Hawkins E, Hewitt HT, Hope P, Islam AS, Jones C, Kaufman DS, Kopp RE, Kosaka Y, Kossin J, Krakovska S, Lee J-Y, Li J, Mauritsen T, Maycock TK, Meinshausen M, Min S-K, Monteiro PMS, Ngo-Duc T, Otto F, Pinto I, Pirani A, Raghavan K, Ranasinghe R, Ruane AC, Ruiz L, Sallée JB, Samset BH, Sathyendranath S, Seneviratne SI, Sörensson AA, Szopa S, Takayabu I, Tréguier A-M, van den Hurk B, Vautard R, von Schuckmann K, Zaehle S, Zhang X, Zickfeld K. 2021. Technical Summary, Climate Change 2021: The Physical Science Basis. Contribution of Working Group I to the Sixth Assessment Report of the Intergovernmental Panel on Climate Change. Cambridge University Press, Cambridge, UK and New York, New York, USA.

Barbet-Massin M, Jiguet F, Albert CH, Thuiller W. 2012. Selecting pseudo-absences for species distribution models: how, where and how many? *Methods in Ecology and Evolution* 3:327–338.

Bare EA. 2018. Regional distribution, non-invasive detection, and genetic diversity of the black-spotted newt (*Notophthalmus meridionalis*). M.S. Thesis, The University of Texas Rio Grande Valley. x + 95 pp.

Bare EA, Kline RJ. 2017. *Notophthalmus meridionalis* (black-spotted newt). Habitat use. *Herpetological Review* 48:827–828.

Beng KC, Corlett RT. 2020. Applications of environmental DNA (eDNA) in ecology and conservation: opportunities, challenges and prospects. *Biodiversity and Conservation* 29:2089–2121.

Biggs J, Ewald N, Valentini A, Gaboriaud C, Dejean T, Griffiths R, Foster J, Wilkinson J, Arnell A, Brotherton P, Williams P, Dunn F. 2014. Using eDNA to develop a national citizen science-based monitoring programme for the great crested newt (*Triturus cristatus*). *Biological Conservation* 183:19–28.

Bishop SC. 1947. Handbook of Salamanders: The Salamanders of the United States, of Canada, and of Lower California. Cornell University Press, Ithaca, New York. xiv + 555 pp.

Bogolin AP. 2020. Comparing novel and traditional sampling methodologies to analyze the population status of the Rio Grande cooter (*Pseudemys gorzugi*). M.S. Thesis, The University of Texas Rio Grande Valley. xiv + 178 pp.

Bohmann K, Evans A, Gilbert MTP, Carvalho GR, Creer S, Knapp M, Yu DW, de Bruyn M. 2014. Environmental DNA for wildlife biology and biodiversity monitoring. *Trends in Ecology and Evolution* 29:358–367.

Boria RA, Olson LE, Goodman SM, Anderson RP. 2014. Spatial filtering to reduce sampling bias can improve the performance of ecological niche models. *Ecological Modelling* 275:73–77.

Boundy J. 1994. County records for Texas amphibians and reptiles. *Herpetological Review* 25:129.

Boyer F, Mercier C, Bonin A, Bras YL, Taberlet P, Coissac E. 2016. Obitools: a unix-inspired software package for DNA metabarcoding. *Molecular Ecology Resources* 16:176–182.

Boyer R, Grue CE. 1995. The need for water quality criteria for frogs. *Environmental Health Perspectives*, 103:352–357.

Brooks T, Mittermeier R, Mittermeier C, Fonseca G, Rylands A, Konstant W, Flick P, Pilgrim J, Oldfield S, Magin G, Hilton-Taylor C. 2002. Habitat loss and extinction in the hotspots of biodiversity. *Conservation Biology* 16:909–923.

Brown JL. 2014. SDMtoolbox: a python-based GIS toolkit for landscape genetic, biogeographic and species distribution model analyses. *Methods in Ecology and Evolution* 5:694–700.

Brown JL, Yoder AD. 2015. Shifting ranges and conservation challenges for lemurs in the face of climate change. *Ecology and Evolution* 5:1131–1142.

Brozio S, Manson C, Gourevitch E, Burns TJ, Greener MS, Downie JR, Hoskisson PA. 2017. Development and application of an eDNA method to detect the critically endangered Trinidad golden tree frog (*Phytotriades auratus*) in bromeliad phytotelmata. *PLoS ONE* 12:e0170619.

Brühl C, Schmidt T, Pieper S, Alscher A. 2013. Terrestrial pesticide exposure of amphibians: an underestimated cause of global decline? *Scientific Reports* 3:1135.

Buxton A, Groombridge J, Zakaria N, Griffiths RA. 2017. Seasonal variation in environmental DNA in relation to population size and environmental factors. *Scientific Reports* 7:46294.

Bylemans J, Gleeson DM, Duncan RP, Hardy CM, Furlan EM. 2019. A performance evaluation of targeted eDNA and eDNA metabarcoding analyses for freshwater fishes. *Environmental DNA* 1:402–414.

Carbajal-Márquez R, Díaz G, Martínez de la Vega G. 2014. Geographic distribution: *Notophthalmus meridionalis* (black-spotted newt). *Herpetological Review* 45:650.

Clarke KR, Gorley RN. 2006. Primer v6: User Manual/Tutorial (Plymouth Routines in Multivariate Ecological Research). PRIMER-E, Plymouth.

Coghlan SA, Currier CA, Freeland J, Morris TJ, Wilson CC. 2021. Community eDNA metabarcoding as a detection tool for documenting freshwater mussel (Unionidae) species assemblages. *Environmental DNA* 3:1172–1191.

Colburn EA. 2004. Vernal Pools: Natural History and Conservation. The MacDonald and Woodward Publishing Company, Blacksburg, Virginia. 426 pp.

Collins SM. 2022. Examination of amphibian community and environmental relationships using environmental DNA. M.S. Thesis, The University of Texas Rio Grande Valley. vii + 102 pp.
Cowardin LM, Carter V, Golet FC, LaRoe ET. 1979. Classification of Wetlands and Deepwater Habitats of the United States. U.S. Department of the Interior, Fish and Wildlife Service, Washington, D.C. vi + 131 pp.
Curtis AN, Tiemann JS, Douglass SA, Davis MA, Larson ER. 2021. High stream flows dilute environmental DNA (eDNA) concentrations and reduce detectability. *Diversity and Distributions* 27:1918–1931
Cushman SA. 2006. Effects of habitat loss and fragmentation on amphibians: a review and prospectus. *Biological Conservation* 128:231–240.
Darling JA, Mahon AR. 2011. From molecules to management: adopting DNA-based methods for monitoring biological invasions in aquatic environments. *Environmental Research* 111:978–988.
Davis DR, Bogolin AP, Rahman MS, Kline RJ, Rahman AF. 2020. Development and application of a novel suite of field survey methods to inform conservation of the Rio Grande cooter, *Pseudemys gorzugi*. Final report to Texas Comptroller of Public Accounts. 89 pp.
Dean TL, Richardson J. 1999. Responses of seven species of native freshwater fish and a shrimp to low levels of dissolved oxygen. *New Zealand Journal of Marine and Freshwater Research* 33:99–106.
Dejean T, Valentini A, Miquel C, Taberlet P, Bellemain E, Miaud C. 2012. Improved detection of an alien invasive species through environmental DNA barcoding: the example of the American bullfrog *Lithobates catesbeianus*. *Journal of Applied Ecology* 49:953–959.
Dixon JR. 2000. Amphibians and Reptiles of Texas: with Keys, Taxonomic Synopses, Bibliography, and Distribution Maps. Second Edition. Texas A&M University Press, College Station, Texas. 421 pp.
Dixon JR. 2013. Amphibians and Reptiles of Texas with Keys, Taxonomic Synopses, Bibliography, and Distribution Maps. Third Edition. Texas A&M University Press, College Station, Texas. viii + 447 pp.
Dodd Jr. CK. 1993. Cost of living in an unpredictable environment: the ecology of striped newts *Notophthalmus perstriatus* during a prolonged drought. *Copeia* 1993:605–614.
Dormann CF, Elith J, Bacher S, Buchmann C, Carl G, Carré G, Marquéz JRG, Gruber B, Lafourcade B, Leitão PJ, Münkemüller T, McClean C, Osborne PE, Reineking B, Schröder B, Skidmore AK, Zurell D, Lautenbach S. 2013. Collinearity: a review of methods to deal with it and a simulation study evaluating their performance. *Ecography* 36:27–46.
Dorsey A, Ingerman L, Swarts S. 2004. Toxicological profile for copper. U.S. Department of Health and Human Services, Public Health Service, Agency for Toxic Substances and Disease Registry, Atlanta, Georgia. xx + 272 + [22] pp.
Duran M. 2021. An annotated checklist of the amphibians and reptiles of North Padre Island, Texas, USA, with comparisons to adjacent barrier island and mainland herpetofauna. *ZooKeys* 1073:119.
Dvořák J. 1987. Production-ecological relationships between aquatic vascular plants and invertebrates in shallow waters and wetlands—a review. *Archiv fur Hydrobiologie Beiheft Ergebnisse der Limnologie* 27:181–184
Eichmiller JJ, Miller LM, Sorensen PW. 2016. Optimizing techniques to capture and extract environmental DNA for detection and quantification of fish. *Molecular Ecology Resources* 16:56–68.

Egea-Serrano A, Relyea RA, Tejedo M, Torralva M. 2012. Understanding of the impact of chemicals on amphibians: a meta-analytic review. *Ecology and Evolution* 2:1382–1397.

Elith J, Graham CH, Anderson RP, Dudík M, Ferrier S, Guisan A, Hijmans RJ, Huettmann F, Leathwick JR, Lehmann A, Li J, Lohmann LG, Loiselle BA, Manion G, Moritz C, Nakamura M, Nakazawa Y, Overton JM, Peterson AT, Phillips SJ, Richardson K, Scachetti-Pereira R, Schapire RE, Soberón J, Williams S, Wisz MS, Zimmermann NE. 2006. Novel methods improve prediction of species' distributions from occurrence data. *Ecography* 29:129–151.

Elith J, Phillips SJ, Hastie T, Dudík M, Chee YE, Yates CJ. 2011. A statistical explanation of MaxEnt for ecologists. *Diversity and Distributions* 17:43–57.

Ellard CJ, Patrick JM. 1988. Changing land use patterns in the Lower Rio Grande Valley: a case study of Cameron and Hidalgo counties. *Journal of Borderland Studies* 3:97–105.

Evans NT, Li Y, Renshaw MA, Olds BP, Deiner K, Turner CR, Jerde CL, Lodge DM, Lamberti GA, Pfrender ME. 2017. Fish community assessment with eDNA metabarcoding: effects of sampling design and bioinformatic filtering. *Canadian Journal of Fisheries and Aquatic Sciences* 74:1362–1374.

Eyre AC, Briscoe NJ, Harley DKP, Lumsden LF, McComb LB, Lentini PE. 2022. Using species distribution models and decision tools to direct surveys and identify potential translocation sites for a critically endangered species. *Diversity and Distributions* 28:700–711.

Ficetola GF, Miaud C, Pompanon F, Taberlet P. 2008. Species detection using environmental DNA from water samples. *Biology Letters* 4:423–425.

Fick SE, Hijmans RJ. 2017. WorldClim 2: new 1-km spatial resolution climate surfaces for global land areas. *International Journal of Climatology* 37:4302–4315.

Flores S, Herrera D. 2010. NORMA Oficial Mexicana NOM-059-SEMARNAT-2010, Proteccion Ambiental-Especies Nativas de Mexico de Flora Y Fauna Silvestres-Categor.as de Riesgo Y Especificaciones Para Su Inclusion, Exclusion O Cambio-Lista de Especies En Riesgo. Available at: https://www.dof.gob.mx/normasOficiales/4254/semarnat/semarnat.htm. Accessed 31 Jan 2023.

Flores-Villela O, Parra-Olea G, Hammerson GA, Wake D, Irwin K. 2008. *Notophthalmus meridionalis*. The IUCN Red List of Threatened Species 2008.e.T59452A11944420. Available at: https://dx.doi.org/10.2305/IUCN.UK.2022-2.RLTS.T59452A53987990.en. Accessed 31 Jan 2023.

Fonseca VG. 2018. Pitfalls in relative abundance estimation using eDNA metabarcoding. *Molecular Ecology Resources* 18:923–926.

Fulbright TE, Bryant FC. 2002. The Last Great Habitat. Caesar Kleberg Wildlife Research Institute, Texas A&M University-Kingsville, Special Publication No. 1, Kingsville, Texas. 32 pp.

Fulbright TE, Diamond DD, Rappole J, Norwine J. 1990. The coastal sand plain of southern Texas. *Rangelands Archives* 12:337–340.

Gatiboni L. 2022. Soils and plant nutrients. In: Moore KA, Bradley LK (eds.), North Carolina Extension Gardener Handbook. Second Edition. NC State Extension, Raleigh, North Carolina. Available at: https://content.ces.ncsu.edu/extension-gardener-handbook/1-soils-and-plant-nutrients. Accessed 31 Jan 2023.

Gill DE. 1978. Effective population size and interdemic migration rates in a metapopulation of the red-spotted Newt, *Notophthalmus viridescens* (Rafinesque). *Evolution* 32:839–849.

Gold Z, Curd EE, Goodwin KD, Choi ES, Frable BW, Thompson AR, Walker Jr HJ, Burton RS, Kacev D, Martz LD, Barber PH. 2021. Improving metabarcoding taxonomic assignment: a case study of fishes in a large marine ecosystem. *Molecular Ecology Resources* 21:2546–2564.

Goldberg CS, Pilliod DS, Arkle RS, Waits LP. 2011. Molecular detection of vertebrates in stream water; a demonstration using Rocky Mountain tailed frogs and Idaho giant salamanders. *PLoS ONE* 6:e22746.

Goldberg C, Ray A, Baumgardt J, Waits L. 2013. Environmental DNA as a new method for early detection of New Zealand mudsnails (*Potamopyrgus antipodarum*). *Freshwater Science* 32:792–800.

Goldberg C, Strickler K, Pilliod D. 2015. Moving environmental DNA methods from concept to practice for monitoring aquatic organisms. *Biological Conservation* 183:1–3.

Goldberg CS, Turner CR, Deiner K, Klymus KE, Thomsen PF, Murphy MA, Spear SF, McKee A, Oyler-McCance SJ, Cornman RS, Laramie MB, Mahon AR, Lance RF, Pilliod DS, Strickler KM, Waits LP, Fremier AK, Takahara T, Herder JE, Taberlet P. 2016. Critical considerations for the application of environmental DNA methods to detect aquatic species. *Methods in Ecology and Evolution* 7:1299–130.

Groff LA, Marks SB, Hayes MP. 2014. Using ecological niche models to direct rare amphibian surveys: a case study using the Oregon spotted frog (*Rana pretiosa*). *Herpetological Conservation and Biology* 9:354–368.

Grosjean S, Ohler A, Chuaynkern Y, Cruaud C, Hassanin A. 2015. Improving biodiversity assessment of anuran amphibians using DNA barcoding of tadpoles. Case studies from Southeast Asia. *Comptes Rendus Biologies* 338:351–361.

Gutzler DS. 2013. Regional climatic considerations for borderlands sustainability. *Ecosphere* 4:7.

Hallam J, Clare EL, Jones JI, Day JJ. 2021. Biodiversity assessment across a dynamic riverine system: a comparison of eDNA metabarcoding versus traditional fish surveying methods. *Environmental DNA* 3:1247–1266.

Harper LR, Handley LL, Hahn C, Boonham N, Rees HC, Gough KC, Lewis E, Adams IP, Brotherton P, Phillips S, Hänfling B. 2018. Needle in a haystack? A comparison of eDNA metabarcoding and targeted qPCR for detection of the great crested newt (*Triturus cristatus*). *Ecology and Evolution* 8:6330–6341.

Harper LR, Handley LL, Hahn C, Boonham N, Rees HC, Lewis E, Adams IP, Brotherton P, Phillips S, Hänfling B. 2020. Generating and testing ecological hypotheses at the pondscape with environmental DNA metabarcoding: a case study on a threatened amphibian. *Environmental DNA* 2:184–199.

Harris RMB, Grose MR, Lee G, Bindoff NL, Porfirio LL, Fox-Hughes P. 2014. Climate projections for ecologists. *WIREs Climate Change* 5:621–637.

Hauck LL, Weitemier KA, Penaluna BE, Garcia TS, Cronn R. 2019. Casting a broader net: using microfluidic metagenomics to capture aquatic biodiversity data from diverse taxonomic targets. *Environmental DNA* 1:251–267.

Hausfather Z. 2019. CMIP6: the next generation of climate models explained. Available at: www.carbonbrief.org/cmip6-the-next-generation-of-climate-models-explained/. Accessed 11 Nov 2022.

Healy WR. 1975a. Terrestrial activity and home range in efts of *Notophthalmus viridescens*. *American Midland Naturalist* 93:131–138.

Healy WR. 1975b. Breeding and postlarval migrations of the redspotted newt, *Notophthalmus viridescens*, in Massachusetts. *Ecology* 56:673–680.

Hecnar SJ, M'Closkey RT. 1996. Amphibian species richness and distribution in relation to pond water chemistry in south-western Ontario, Canada. *Freshwater Biology* 36:7–15.
Hecnar SJ, M'Closkey RT. 1997. The effects of predatory fish on amphibian species richness and distribution. *Biological Conservation* 79:123–31.
Herbert PD, Ratnasingham S, deWaard JR. 2003. Barcoding animal life: cytochrome c oxidase subunit 1 divergences among closely related species. *Proceedings of the Royal Society of London B, Biological Sciences* 270:S96–S99.
Heyer WR, Donnelly MA, McDiarmid RW, Hayek LC, Foster MS (eds.). 1994. Measuring and Monitoring Biological Diversity: Standard Methods for Amphibians. Smithsonian Institution Press, Washington, D.C. xix + 364 pp.
Hijmans RJ. 2012. Cross-validation of species distribution models: removing spatial sorting bias and calibration with a null model. *Ecology* 93:679–688.
Hirzel AH, Le Lay G. 2008. Habitat suitability modelling and niche theory. *Journal of Applied Ecology* 45:1372–1381.
Hirzel AH, Le Lay G, Helfer V, Randin C, Guisan A. 2006. Evaluating the ability of habitat suitability models to predict species presences. *Ecological Modeling* 199:142–152.
Hof AR, Jansson R, Nilsson C. 2012. The usefulness of elevation as a predictor variable in species distribution modelling. *Ecological Modelling* 246:86–90.
Huang Y, Fipps G. 2011. Landsat satellite multi-spectral image classification of land cover change for GIS-based urbanization analysis in irrigation districts: evaluation in the Lower Rio Grande Valley. Texas Water Resources Institute Technical Report No. 378, Texas A&M University System, College Station, Texas. 17 pp.
Hunter ME, Ferrante JA, Meigs-Friend G, Ulmer A. 2019. Improving eDNA yield and inhibitor reduction through increased water volumes and multi-filter isolation techniques. *Scientific Reports* 9:5259.
(IPCC) Intergovernmental Panel on Climate Change. 2021. Climate Change 2021: The Physical Science Basis. Contribution of Working Group I to the Sixth Assessment Report of the Intergovernmental Panel on Climate Change. Cambridge University Press, Cambridge, UK. xiii + 2391 pp.
(IPCC) Intergovernmental Panel on Climate Change. 2022. Climate Change 2022: Mitigation of Climate Change. Working Group III Contribution to the Sixth Assessment Report of the Intergovernmental Panel on Climate Change. Cambridge University Press, Cambridge, UK. ix + 1977 pp.
Irwin KJ. 1993. A preliminary survey and management recommendations of the herpetofauna of the Lower Rio Grande Valley National Wildlife Refuge. Final report to U.S. Fish and Wildlife Service. 25 pp.
Jackson M, Myrholm C, Shaw C, Ramsfield T. 2017. Using nested PCR to improve detection of earthworm eDNA in Canada. *Soil Biology and Biochemistry* 113:215–218.
Jahrsdoerfer SE, Leslie DM. 1988. Tamaulipan brushland of the Lower Rio Grande Valley of south Texas: description, human impact, and management options. USFWS Biological Report 88:63. viii + 63 pp.
Jochimsen DM, Peterson CR, Andrews KM, Gibbons JW. 2004. A literature review of the effects of roads on amphibians and reptiles and the measures used to minimize those effects. Idaho Fish and Game Department, Boise, Idaho. 79 pp.

Judd FW. 1985. Status of *Siren intermedia texana*, *Notophthalmus meridionalis*, and *Crotaphytus reticulatus*. Final report to the Office of Endangered Species, U.S. Fish and Wildlife Service, Department of the Interior, Washington, D.C. iv + 60 pp.

Khwarahm NR, Ararat K, Qader S, Sabir DK. 2021. Modeling the distribution of the Near Eastern fire salamander (*Salamandra infraimmaculata*) and Kurdistan newt (*Neurergus derjugini*) under current and future climate conditions in Iraq. *Ecological Informatics* 63:101309.

Klymus KE, Marshall NT, Stepien CA. 2017. Environmental DNA (eDNA) metabarcoding assays to detect invasive invertebrate species in the Great Lakes. *PLoS ONE* 12:e0177643.

Kolmogorov AN. 1933. Sulla determinazione empirica di una legge di distribuzione. *Giornale dell' Instituto Italiano degli Attuari* 4:83–91.

Kramer-Schadt S, Niedballa J, Pilgrim JD, Schröder B, Lindenborn J, Reinfelder V, Stillfried M, Heckmann I, Scharf AK, Augeri DM, Cheyne SM, Hearn AJ, Ross J, Macdonald DW, Mathai J, Eaton J, Marshall AJ, Semiadi G, Rustam R, Bernard H, Alfred R, Samejima H, Duckworth JW, Breitenmoser-Wuersten C, Belant JL, Hofer H, Wilting A. 2013. The importance of correcting for sampling bias in MaxEnt species distribution models. *Diversity and Distributions* 19:1366–1379.

Lacoursière-Roussel A, Dubois Y, Normandeau E, Bernatchez L. 2016. Improving herpetological surveys in eastern North America using the environmental DNA method. *Genome* 59:991–1007.

Lane S, Hamer A, Mahony M. 2007. Habitat correlates of five amphibian species and of species-richness in a wetland system in New South Wales, Australia. *Applied Herpetology* 4:65–82.

Laramie MB, Pilliod DS, Goldberg CS, Strickler KM. 2015. Environmental DNA sampling protocol—filtering water to capture DNA from aquatic organisms. USGS Numbered Series, U.S. Geological Survey, Reston, Virginia. iv + 15 pp.

Lee JL, Kent BW. 2020. *Notophthalmus viridescens viridescens* (red-spotted newt). Habitat use. *Herpetological Review* 50:292–293.

Leslie Jr. DM. 2016. An international borderland of concern: conservation of biodiversity in the Lower Rio Grande Valley. U.S. Geological Survey Scientific Investigations Report No. 2016–5078, Reston, Virginia. xi + 119 pp.

Levene H. 1960. Robust tests for equality of variances. In Olkin I, Ghurye SG, Hoeffding W, Madow WG, Mann HB (eds.), Contributions to Probability and Statistics: Essays in Honor of Harold Hotelling, pp. 278–292. Stanford University Press, Stanford, California.

Levesque R. 2007. SPSS Programming and Data Management. A Guide for SPSS and SAS Users. Fourth Edition. SPSS Inc., Chicago, Illinois.

Li C, Zwiers F, Zhang X, Li G, Sun Y, Wehner MF. 2021. Changes in annual extremes of daily temperature and precipitation in CMIP6 models. *Journal of Climate* 34:3441–3460.

Lombardi JV, Perotto-Baldivieso HL, Tewes ME. 2020. Land cover trends in south Texas (1987–2050): potential implications for wild felids. *Remote Sensing* 12:659.

Loredo I, Van Vuren D, Morrison ML. 1996. Habitat use and migration behavior of the California tiger salamander. *Journal of Herpetology* 30:282–285.

Low BW, Zeng Y, Tan HH, Yeo DCJ. 2021. Predictor complexity and feature selection affect Maxent model transferability: evidence from global freshwater invasive species. *Diversity and Distributions* 27:497–511.

Mann HB, Whitney DR. 1947. On a test of whether one of two random variables is stochastically larger than the other. *The Annals of Mathematical Statistics* 18:50–60.

Marzluff JM, Ewing K. 2001. Restoration of fragmented landscapes for the conservation of birds: a general framework and specific recommendations for urbanizing landscapes. *Restoration Ecology* 9:280–292.

Mazerolle MJ, Bailey LL, Kendall WL, Royle JA, Converse SJ, Nichols JD. 2007. Making great leaps forward: accounting for detectability in herpetological field studies. *Journal of Herpetology* 41:672–689.

McKee AM, Calhoun DL, Barichivich WJ, Spear SF, Goldberg CS, Glenn TC. 2015. Assessment of environmental DNA for detecting presence of imperiled aquatic amphibian species in isolated wetlands. *Journal of Fish and Wildlife Management 6:*498–510.

Mecham JS. 1967. *Notophthalmus viridescens*. *Catalogue of American Amphibians and Reptiles* 53:53.1–53.4.

Mecham JS. 1968a. *Notophthalmus meridionalis*. *Catalogue of American Amphibians and Reptiles* 74:74.1–74.2.

Mecham JS. 1968b. On the relationships between *Notophthalmus meridionalis* and *Notophthalmus kallerti*. *Journal of Herpetology* 2:121–127.

Merow C, Smith MJ, Silander Jr JA. 2013. A practical guide to MaxEnt for modeling species' distributions: what it does, and why inputs and settings matter. *Ecography* 36:1058–1069.

Minamoto T, Naka T, Moji K, Maruyama A. 2016. Techniques for the practical collection of environmental DNA: filter selection, preservation, and extraction. *Limnology* 17:23–32.

Nadkarni N, Longino J. 1990. Invertebrates in canopy and ground organic matter in a neotropical montane forest, Costa Rica. *Biotropica* 22:286–289.

National Toxicology Program. 2022. Ethidium bromide (1239-45-8). Chemical Effects in Biological Systems (CEBS). Research Triangle Park, NC (USA): National Toxicology Program (NTP). Available at: www.manticore.niehs.nih.gov/cebssearch/test_article/1239-45-8. Accessed 11 Nov 2022.

NatureServe. 2019. *Notophthalmus meridionalis* Black-spotted Newt. NatureServe Explorer. Available at: https://explorer.natureserve.org/Taxon/ELEMENT_GLOBAL.2.101904/Notophthalmus_meridionalis. Accessed 31 Jan 2023.

Nester GM, Brauwer MD, Koziol A, West KM, DiBattista JD, White NE, Power M, Heydenrych MJ, Harvey E, Bunce M. 2020. Development and evaluation of fish eDNA metabarcoding assays facilitate the detection of cryptic seahorse taxa (family: Syngnathidae). *Environmental DNA* 2:614–626.

Nichols RV, Vollmers C, Newsom LA, Wang Y, Heintzman PD, Leighton M, Green RE, Shapiro B. 2018. Minimizing polymerase biases in metabarcoding. *Molecular Ecology Resources* 18:927–939.

Nix WA, Maher K, Pallansch MA, Oberste MS. 2010. Parechovirus typing in clinical specimens by nested or semi-nested PCR coupled with sequencing. *Journal of Clinical Virology* 48:202–207.

Olson Z, Briggler J, Williams R. 2013. An eDNA approach to detect eastern hellbenders (*Cryptobranchus a. alleganiensis*) using samples of water. *Wildlife Research* 39:629–636.

Pearson RG, Raxworthy CJ, Nakamura M, Peterson AT. 2007. Predicting species distributions from small numbers of occurrence records: a test case using cryptic geckos in Madagascar. *Journal of Biogeography* 34:102–117.

Peña EN. 2012. Using census data, urban land-cover classification, and dasymetric mapping to measure urban growth of the Lower Rio Grande Valley, Texas. M.S. Thesis, University of Southern California. viii + 46 pp.

Peterman W, Crawford J, Kuhns A. 2013. Using species distribution and occupancy modeling to direct survey efforts and assess species status. *Journal of Nature Conservation* 21:114–121.

Peterson AT. 2003. Predicting the geography of species' invasions via ecological niche modeling. *The Quarterly Review of Biology* 78:419–433.

Peterson AT. 2006. Uses and requirements of ecological niche models and related distributional models. *Biodiversity Informatics* 3:59–72.

Peterson AT, Soberón J. 2012. Species distribution modeling and ecological niche modeling: getting the concepts right. Natureza & Conservação 10:1–6.

Peterson AT, Soberón J, Pearson RG, Anderson RP, Martínez-Meyer E, Nakamura M, Araújo MB. 2011. Ecological Niches and Geographic Distributions. Princeton University Press, Princeton, New Jersey. 328 pp.

Phillips SJ, Anderson RP, Schapire RE. 2006. Maximum entropy modeling of species geographic distributions. *Ecological Modeling* 190:231–259.

Phillips SJ, Dudík M, Elith J, Graham CH, Lehmann A, Leathwick J, Ferrier S. 2009. Sample selection bias and presence-only distribution models: implications for background and pseudo absence data. *Ecological Applications* 19:181–197.

Pilliod DS, Goldberg CS, Arkle RS, Waits LP. 2013. Estimating occupancy and abundance of stream amphibians using environmental DNA from filtered water samples. *Canadian Journal of Fisheries and Aquatic Sciences* 70:1123–1130.

Poggio L, de Sousa LM, Batjes NH, Heuvelink GBM, Kempen B, Ribeiro E, Rossiter D. 2021. SoilGrids 2.0: producing soil information for the globe with quantified spatial uncertainty. *SOIL* 7:217–240.

Radosavljevic A, Anderson RP. 2014. Making better Maxent models of species distributions: complexity, overfitting and evaluation. *Journal of Biogeography* 41:629–643.

Rappole JH, Klicka J. 1991. Status of the black-spotted newt (*Notophthalmus meridionalis*) in Texas and Mexico. Final report to the Lower Rio Grande Valley Wildlife Refuge, U.S. Fish and Wildlife Service, Alamo, Texas. 74 pp.

Rees H, Maddison B, Middleditch D, Patmore J, Gough K. 2014. REVIEW: The detection of aquatic animal species using environmental DNA – a review of eDNA as a survey tool in ecology. *Journal of Applied Ecology* 51:1450–1459.

Renan S, Gafny S, Perl R, Roll U, Malka Y, Vences M, Geffen E. 2017. Living quarters of a living fossil—uncovering the current distribution pattern of the rediscovered Hula painted frog (*Latonia nigriventer*) using environmental DNA. *Molecular Ecology* 26:6801–6812.

Renshaw MA, Olds BP, Jerde CL, McVeigh MM, Lodge DM. 2015. The room temperature preservation of filtered environmental DNA samples and assimilation into a phenol-chloroform-isoamyl alcohol DNA extraction. *Molecular Ecology Resources* 15:168–176.

Rhoden CM, Peterman WE, Taylor CA. 2017. Maxent-directed field surveys identify new populations of narrowly endemic habitat specialists. *PeerJ* 5:e3632.

Riahi K, van Vuuren DP, Kriegler E, Edmonds J, O'Neill BC, Fujimori S, Bauer N, Calvin K, Dellink R, Fricko O, Lutz W, Popp A, Cuaresma JC, KC S, Leimbach M, Jiang L, Kram T, Rao S, Emmerling J, Ebi K, Hasegawa T, Havlik P, Humpenöder F, Da Silva LA, Smith S, Stehfest E, Bosetti V, Eom J, Gernaat D, Masui T, Rogelj J, Strefler J, Drouet L, Krey V, Luderer G, Harmsen M, Takahashi K, Baumstark L, Doelman JC, Kainuma M, Klimont Z, Marangoni G, Lotze-Campen H, Obersteiner M, Tabeau A, Tavoni M. 2017. The Shared Socioeconomic Pathways and their energy, land use, and greenhouse gas emissions implications: an overview. *Global Environmental Change* 42:153–168.

Rinehart KA, Donovan TM, Mitchell BR, Long RA. 2009. Factors influencing occupancy patterns of eastern newts across Vermont. *Journal of Herpetology* 43:521–531.

Robinson PS. 2021. Status, distribution, and conservation of the black-spotted newt (*Notophthalmus meridionalis*) in south Texas. M.S. Thesis, The University of Texas Rio Grande Valley. x + 96 pp.

Robinson PS, Davis DR, Kline RJ. 2020. Geographic distribution: *Notophthalmus meridionalis* (black-spotted newt). *Herpetological Review* 51:531.

Robinson PS, Davis DR, Collins SM, Kline RJ. 2022. Defining the current distribution of the imperiled black-spotted newt across south Texas, USA. *Global Ecology and Conservation* 36:e02131.

Roffler GH, Allen JM, Massey A, Levi T. 2021. Metabarcoding of fecal DNA shows dietary diversification in wolves substitutes for ungulates in an island archipelago. *Ecosphere* 12:03297.

Rondinini C, Di Marco M, Chiozza F, Santulli G, Baisero D, Visconti P, Hoffmann M, Schipper J, Stuart SN, Tognelli MF, Amori G, Falcucci A, Maiorano L, Boitani L. 2011. Global habitat suitability models of terrestrial mammals. *Philosophical Transactions of the Royal Society B, Biological Sciences* 366:2633–2641.

Rourke ML, Fowler AM, Hughes JM, Broadhurst MK, DiBattista JD, Fielder S, Furlan EM. 2021. Environmental DNA (eDNA) as a tool for assessing fish biomass: a review of approaches and future considerations for resource surveys. *Environmental DNA* 4:9–33.

Rouse JD, Bishop CA, Struger J. 1999. Nitrogen pollution: an assessment of its threat to amphibian survival. *Environmental Health Perspectives* 107:799–803.

Roussel JM, Paillisson JM, Tréguier A, Petit E. 2015. The downside of eDNA as a survey tool in water bodies. *Journal of Applied Ecology* 52:823–826.

Ruppert KM. 2020. Development and assessment of an environmental DNA (eDNA) assay for the Rio Grande siren and review of eDNA metabarcoding applications. M.S. Thesis, The University of Texas Rio Grande Valley. ix + 177 pp.

Ruppert KM, Kline RJ, Rahman MS. 2019. Past, present, and future perspectives of environmental DNA (eDNA) metabarcoding: a systematic review in methods, monitoring, and applications of global eDNA. *Global Ecology and Conservation* 17:e00547.

Ruppert KM, Davis DR, Rahman MS, Kline RJ. 2022. Development and assessment of an environmental DNA (eDNA) assay for a cryptic Siren (Amphibia: Sirenidae). *Environmental Advances* 7:100163.

Sakata MK, Watanabe T, Maki N, Ikeda K, Kosuge T, Okada H, Yamanaka H, Sado T, Miya M, Minamoto T. 2021. Determining an effective sampling method for eDNA metabarcoding: a case study for fish biodiversity monitoring in a small, natural river. *Limnology* 22:221–235.

Sakata MK, Kawata MU, Kurabayashi A, Kurita T, Nakamura M, Shirako T, Kakehashi R, Nishikawa, K, Hossman MY, Nishijima T, Kabamoto J, Miya M, Minamoto T. 2022. Development and evaluation of PCR primers for environmental DNA (eDNA) metabarcoding of Amphibia. *Metabarcoding and Metagenomics* 6:15–26.

Sakin E. 2012. Organic carbon organic matter and bulk density relationships in arid-semi arid soils in southeast Anatolia region. *African Journal of Biotechnology* 11:1373–1377.

Sasso T, Lopes CM, Valentini A, Dejean T, Zamudio KR, Haddad CF, Martins M. 2017. Environmental DNA characterization of amphibian communities in the Brazilian Atlantic Forest: potential application for conservation of a rich and threatened fauna. *Biological Conservation* 215:225–232.

Schenekar T, Schletterer M, Lecaudey LA, Weiss SJ. 2020. Reference databases, primer choice, and assay sensitivity for environmental metabarcoding: lessons learnt from a re-evaluation of an eDNA fish assessment in the Volga headwaters. *River Research and Applications* 36:1004–1013.

Schmidley DJ, Parker NC, Baker RJ. 2001. Texas Parks and Wildlife for the 21st Century. Texas Tech University, Lubbock, Texas. 46 pp.

Schulte EE, Hopkins BG. 1996. Estimation of soil organic matter by weight loss-on-ignition. In Magdoff FR, Tabatabai MA, Hanlon Jr. EA (eds.), Soil Organic Matter: Analysis and Interpretation, pp. 21–31. Soil Science Society of America Special Publications 46, Madison, Wisconsin.

Scott NJ. 1996. Evolution and management of the North American grassland herpetofauna. In Finch DM (ed.), Ecosystem Disturbances and Wildlife Conservation in Western Grasslands – A Symposium Proceedings. September 22–26, 1994, pp. 40–53. U.S. Department of Agriculture-Forest Service, General Technical Report RM-GTR-285, Fort Collins, Colorado.

Singer VL, Lawlor TE, Yue S. 1999. Comparison of SYBR® Green I nucleic acid gel stain mutagenicity and ethidium bromide mutagenicity in the *Salmonella*/mammalian microsome reverse mutation assay (Ames test). *Mutation Research/Genetic Toxicology and Environmental Mutagenesis* 439:37–47.

Small M, Bonner T, Baccus J. 2009. Hydrologic alteration of the Lower Rio Grande terminus: a quantitative assessment. *River Research and Applications* 25:241–252.

Smart A, Weeks A, Rooyen A, Moore A, McCarthy M, Tingley R. 2016. Assessing the cost-efficiency of environmental DNA sampling. *Methods in Ecology and Evolution* 7:1291–1298.

Soberón J, Peterson AT. 2005. Interpretation of models of fundamental ecological niches and species' distributional areas. *Biodiversity Informatics* 2:1–10.

Solberg E, Evans I, Penny D. 1999. Copper deficiency: diagnosis and correction. Agri-Facts, Agdex 532-3, Alberta Agriculture, Food and Rural Development, Edmonton. 9 pp.

Strickler K, Fremier A, Goldberg C. 2015. Quantifying effects of UV-B, temperature, and pH on eDNA degradation in aquatic microcosms. *Biological Conservation* 183:85–93.

Stubbs MJ, Rister ME, Lacewell RD, Ellis JR, Sturdivant AW, Robinson JRC, Fernandez L. 2003. Evolution of irrigation districts and operating institutions: Texas, Lower Rio Grande Valley. Texas Water Resources Institute Technical Report No. 228, Texas A&M University, College Station, Texas. viii + 60 pp.

Swart NC, Cole JNS, Kharin VV, Lazare M, Scinocca JF, Gillett NP, Anstey J, Arora V, Christian JR, Hanna S, Jiao Y, Lee WG, Majaess F, Saenko OA, Seiler C, Seinen C, Shao A, Sigmond M, Solheim L, von Salzen K, Yang D, Winter B. 2019. The Canadian Earth System Model version 5 (CanESM5.0.3). *Geoscientific Model Development* 12:4823–4873.

Syfert MM, Smith MJ, Coomes DA. 2013. The effects of sampling bias and model complexity on the predictive performance of MaxEnt species distribution models. *PLoS ONE* 8:e55158.

Taggart TW. 1997. Geographic distribution: *Notophthalmus meridionalis* (black-spotted newt). *Herpetological Review* 28:47.

Tatebe H, Ogura T, Nitta T, Komuro Y, Ogochi K, Takemura T, Sudo K, Sekiguchi M, Abe M, Saito F, Chikira M, Watanabe S, Mori M, Hirota N, Kawatani Y, Mochizuki T, Yoshimura K, Takata K, O'ishi R, Yamazaki D, Suzuki T, Kurogi M, Kataoka T, Watanabe M, Kimoto M. 2019. Description and basic evaluation of simulated mean state, internal variability, and climate sensitivity in MIROC6. *Geoscientific Model Development* 12:2727–2765.

Thomsen P, Kielgast J, Iversen L, Wiuf C, Rasmussen M, Gilbert M, Orlando L, Willerslev E. 2012. Monitoring endangered freshwater biodiversity using environmental DNA. *Molecular Ecology* 21:2565–2573.

Thornton OW. 1977. The impact of man upon herpetological communities in the Lower Rio Grande Valley, Texas. M.S. Thesis, Texas A&M University, College Station, Texas. ix + 96 pp.

Tipton BL, Hibbitts TL, Hibbitts TD, Hibbitts TJ, Laduc TJ. 2012. Texas Amphibians. A Field Guide. University of Texas Press, Austin, Texas. xiv + 309 pp.

Todd BD, Winne CT, Willson JD, Gibbons JW. 2007. Getting the drift: examining the effects of timing, trap type and taxon on herpetofaunal drift fence surveys. *The American Midland Naturalist* 158:292–305.

(TPWD) Texas Parks and Wildlife Department. 2020. Rare, Threatened, and Endangered Species of Texas. Available at: https://tpwd.texas.gov/gis/rtest/. Accessed 31 Jan 2023.

Tronstad LM, Brown KM, Andersen MD. 2018. Using species distribution models to guide field surveys for an apparently rare aquatic beetle. *Journal of Fish and Wildlife Management* 9:330–339.

Tsuji S, Takahara T, Doi H, Shibata N, Yamanaka H. 2019. The detection of aquatic macroorganisms using environmental DNA analysis—a review of methods for collection, extraction, and detection. *Environmental DNA* 1:99–108.

Turner CR, Barnes MA, Xu CC, Jones SE, Jerde CL, Lodge DM. 2014. Particle size distribution and optimal capture of aqueous macrobial eDNA. *Methods in Ecology and Evolution* 5:676–684.

(USDA) U.S. Department of Agriculture. 2013. Tiocano Series. National Cooperative Soil Survey. Available at: www.soilseries.sc.egov.usda.gov/OSD_Docs/T/TIOCANO.html. Accessed 21 January 2023.

(USDA) U.S. Department of Agriculture. 2019. Natural Resources Conservation Service Web Soil Survey. Available at: www.websoilsurvey.nrcs.usda.gov/app/. Accessed 21 January 2023.

(USFWS) U.S. Fish and Wildlife Service. 2020. National Wetlands Inventory. U.S. Department of the Interior, Washington, D.C. Available at: www.fws.gov/program/national-wetlands-inventory. Accessed 12 Nov 2022.

(USFWS) U.S. Fish and Wildlife Service. 2021. Endangered Species Program. National Domestic Listing Workplan: Fiscal Years 21-25. Available at: https://www.fws.gov/endangered/what-we-do/listing-workplan.html. Accessed 31 Jan 2023.

(USGS) U.S. Geological Survey. 2000. Shuttle Radar Topography Mission (SRTM) 1 Arc-Second Global. Earth Resources Observation and Science (EROS) Center, version 3.0. Available at: www.doi.org/10.5066/F7PR7TFT. Accessed 12 Nov 2022.

Valentini A, Taberlet P, Miaud C, Civade R, Herder J, Thomsen PF, Bellemain E, Besnard A, Coissac E, Boyer F, Gaboriaud C, Jean P, Poulet N, Roset N, Copp GH, Geniez P, Pont D, Argillier C, Baudoin J-M, Peroux T, Crivelli AJ, Olivier A, Acqueberge M, Le Brun M, Møller PR, Willerslev E, Dejean T. 2016. Next-generation monitoring of aquatic biodiversity using environmental DNA metabarcoding. *Molecular Ecology* 25:929–942.

Van Meter RJ, Glinski DA, Henderson WM, Purucker S. 2016. Soil organic matter content effects on dermal pesticide bioconcentration in American toads (*Bufo americanus*). *Environmental Toxicology and Chemistry* 35:2734–2741.

VanDerWal J, Shoo L, Graham C, Williams S. 2009. Selecting pseudo-absence data for presence only distribution modeling: How far should you stray from what you know? *Ecological Modelling* 220:589–594.
Veloz SD. 2009. Spatially autocorrelated sampling falsely inflates measures of accuracy for presence only niche models. *Journal of Biogeography* 36:2290–2299.
Vörös J, Márton O, Schmidt BR, Gál JT, Jelić D. 2017. Surveying Europe's only cave-dwelling chordate species (*Proteus anguinus*) using environmental DNA. *PLoS ONE* 12:e0170945.
Warren DL, Wright AN, Seifert SN, Shaffer HB. 2014. Incorporating model complexity and spatial sampling bias into ecological niche models of climate change risks faced by 90 California vertebrate species of concern. *Diversity and Distributions* 20:334–343.
Waudby HP, Petit S. 2017. Thermoregulatory value of cracking-clay soil shelters for small vertebrates during extreme desert conditions. *Integrative Zoology* 12:237–249.
Wehner MF. 2020. Characterization of long period return values of extreme daily temperature and precipitation in the CMIP6 models: Part 2, projections of future change. *Weather and Climate Extremes* 30:100284.
Wikston MJH. 2021. Comparative efficacy of eDNA and conventional methods for monitoring wetland anuran communities. M.S. Thesis, Trent University, Peterborough, Ontario. x + 85 pp.
Wilcoxon F. 1945. Some uses of statistics in plant pathology. *Biometrics Bulletin* 1:41–45.
Wilson IG. 1997. Inhibition and facilitation of nucleic acid amplification. *Applied and Environmental Microbiology* 63:3741–3751.
Wilson MC, Chen XY, Corlett RT, Didham RK, Ding P, Holt RD, Holyoak M, Hu G, Hughes AC, Jiang L, Laurance WF, Liu J, Pimm SL, Robinson SK, Russo SE, Si X, Wilcove DS, Wu J, Yu M. 2016. Habitat fragmentation and biodiversity conservation: key findings and future challenges. *Landscape Ecology* 31:219–227.
Wittig KP, Brown SC. 1977. Sodium balance in the newt, *Notophthalmus viridescens*. *Comparative Biochemistry and Physiology* 58:49–52.
Wyman R. 1988. Soil acidity and moisture and the distribution of amphibians in five forests of southcentral New York. *Copeia* 1988:394–399.
Yaegashi S, Tahir MSFB, Haga H. 2020. The effect of storm event on detection: the species diversity of insects using environmental DNA meta-barcoding. 22nd Congress of the International Association for Hydro-Environment Engineering and Research-Asia Pacific Division (IAHR-APD), Hokkaido University. 6 pp.
Yates M, Fraser D, Derry A. 2019. Meta-analysis supports further refinement of eDNA for monitoring aquatic species-specific abundance in nature. *Environmental DNA* 1:5–13.
Thomsen P, Kielgast J, Iversen L, Wiuf C, Rasmussen M, Gilbert M, Orlando L, Willerslev E. 2012. Monitoring endangered freshwater biodiversity using environmental DNA. *Molecular Ecology* 21:2565–2573.
Ziehn T, Chamberlain MA, Law RM, Lenton A, Bodman RW, Dix M, Stevens L, Wang Y-P, Srbinovsky J. 2020. The Australian Earth System Model: ACCESS-ESM1.5. *Journal of Southern Hemisphere Earth Systems Science* 70:193–214.

APPENDIX A

Environmental DNA Extraction Protocols

Modified Epoch GenCatch Blood and Tissue Genomic Mini-Prep Kit

- In a 1.7-mL microcentrifuge tube, add 10 µL of 10 mg/mL RNase A to pooled extract
    - Incubate at 37°C for 10 min
- Let sit at room temp for 1 min, add 10 µL of 10 mg/mL Proteinase-K, vortex every 15 min for 1 h
- Add 500 µL EX buffer and vortex
    - Incubate at 70°C for 20 min
    - In the interim, preheat 50 µL/sample elution buffer to 70°C
- Let sit at room temperature for 5 min, then add 500 µL 100% ethanol and vortex
- Pass 800 µL of the solution through a GenCatch column placed inside a 1.7-mL microcentrifuge tube and centrifuge at 8000 rpm for 2 min
    - This will have to be done two times to allow the entire volume to pass through
- Wash with 500 µL WS buffer twice, centrifuge at 8000 rpm for 2 min for the first wash and 15000 rpm for 2 min for the second wash
- In new 1.7-mL microcentrifuge tube, elute DNA with 50 µL heated elution buffer by centrifuging at 15000 rpm for 2 min. Add 50 µL nuclease free water to column and centrifuge at 15000 rpm for 2 min

Chloroform

- In a 1.7 mL-microcentrifuge tube, add 500 µL chloroform to pooled extract, let sit at room temperature for 1 min, then centrifuge at 12000 rpm for 2 min
- Extract supernatant into clean 1.7 mL-microcentrifuge tube, add 4 µL 15 mg/mL GlycoBlue Coprecipitant (Thermo Fisher Scientific, Waltham, MA, USA), then 500 µL 100% ethanol and invert until mixed, and centrifuge at 12000 rpm for 10 min
- Discard supernatant, do not disturb the DNA pellet, add 500 µL 95% ethanol, vortex for 30 s, and centrifuge at 12000 rpm for 2 min
- Discard supernatant, do not disturb the DNA pellet, add 500 µL 75% ethanol, vortex for 30 s, centrifuge at 12000 rpm for 2 min
    - Air dry pellet for 30+ min
- Add 50 µL 30% TE buffer
    - Place on heat block at 55°C for 5 min

PC-CTAB

- In a 1.7-mL microcentrifuge tube, add 4 µL 15 mg/mL GlycoBlue Coprecipitant (Thermo Fisher Scientific, Waltham, MA, USA) and 500 µL 100% ethanol to pooled extract, invert until mixed, then centrifuge at 12000 rpm for 10 min
- Discard supernatant, do not disturb the DNA pellet, add 500 µL 95% ethanol, vortex for 30 s, and centrifuge at 12000 rpm for 2 min
- Discard supernatant, do not disturb the DNA pellet, add 500 µL 75% ethanol, vortex for 30 s, centrifuge at 12000 rpm for 2 min
    - Air dry pellet for 30+ min

- Add 1 mL CTAB solution (40 µL 0.5M EDTA, 100 µL 1M TRIS, 280 µL 5M NaCl, 20 mg CTAB, 40 mg PVP, 5 µL β-mercaptoethanol, 515 µL water)
- Store at 4°C for 1 h, incubate at 65°C for 10 min, then cool at room temperature for 10 min
- Add 500 µL phenol-chloroform and vortex, then centrifuge at 12000 rpm for 5 min
- Transfer supernatant to clean 1.7-mL microcentrifuge tube, add 1 mL ice cold 100% ethanol, then add 20 µL 5M NaCl
    - Precipitate at -80°C for 1 h
- Centrifuge at 4°C at 12000 rpm for 15 min
    - Remove supernatant and air dry pellet for 30+ min
- Rehydrate with 50 µL 30% TE buffer
    - Place on heat block at 55°C for 5 min

PC-CTAB Double Extraction

- In a 1.7-mL microcentrifuge tube, add 500 µL chloroform to pooled extract, let sit at room temperature for 1 min, then centrifuge at 12000 rpm for 2 min
- Extract supernatant into clean 1.7-mL microcentrifuge tube, add 4 µL 15mg/mL GlycoBlue Coprecipitant (Thermo Fisher Scientific, Waltham, MA, USA), then 500 µL 100% ethanol and invert until mixed
- Centrifuge at 12000 rpm for 10 min
- Discard supernatant, do not disturb the DNA pellet, add 500 µL 95% ethanol, vortex for 30 s, and centrifuge at 12000 rpm for 2 min
- Discard supernatant, do not disturb the DNA pellet, add 500 µL 75% ethanol, vortex for 30 s, centrifuge at 12000 rpm for 2 min
    - Air dry pellet for 30+ min
- Add 50 µL 30% TE buffer
    - Place on heat block at 55°C for 5 min
- Add 1 mL CTAB solution (40 µL 0.5M EDTA, 100 µL 1M TRIS, 280 µL 5M NaCl, 20 mg CTAB, 40 mg PVP, 5 µL β-mercaptoethanol, 515 µL water)
    - Store at 4°C for 1 h, incubate at 65°C for 10 min, then cool at room temperature for 10 min
- Add 500 µL phenol-chloroform and vortex, then centrifuge at 12000 rpm for 5 min
- Transfer supernatant to clean 1.7-mL microcentrifuge tube, add 1 mL ice cold 100% ethanol, then add 20 µL 5M NaCl
    - Precipitate at -80°C for 1 h
- Centrifuge at 4°C at 12000 rpm for 15 min
    - Remove supernatant and airdry pellet for 30+ min
- Rehydrate with 50 µL 30% TE buffer
    - Place on heat block at 55°C for 5 min

APPENDIX B

Supplemental Metabarcoding Methods

OBITools3 Pipeline

OBITools3 was run using Ubuntu and the Windows subsystem for Linux. OBITools3 was activated using the source *obi3-env/bin/activate* command. The basic structure of the OBITools3 code is a command, followed by an input file, followed an output file. OBITools3 uses a data management system (DMS) to house files during analysis. A DMS is identified by the .obidms file extension. Each individual experiment, or NGS run, had its own DMS to make organization of data easier.

Forward and reverse reads were imported and parsed out into an experiment specific DMS using the *obi import* command. Forward and reverse reads were then aligned using *obi alignpairedend* command. The quality of alignment for each sequence was assessed using the *obi stats -a score_norm* command. Alignment quality is given on a scale from 0 to 1, where 0 is the worst alignment and 1 would be a perfect alignment. Sequences with an alignment score of 0.80 and above were used for further analysis. That selection was done using the *obi grep -p "sequence['score_norm'] > 0.8"* command. The *obi ngsfilter* command was then used to identify and separate specific primers and primer tag combinations. The *obi ngsfilter* command also trims the primers and tags from the sequence after it separates unique primer combinations. A NGS filter file was required for the *obi ngsfilter* command; the file needs to be in .txt format and needs to include sample number, primer tags, forward and reverse primer sequence, and any extra information related to the sample.

Following the *obi ngsfilter* step, unique sequences were identified and dereplicated, to reduce computing time and power required, using the *obi uniq* command. Extraneous metadata was then removed using the *obi annotate* command. Sequences that had a count greater than 1 and a length less than or equal to 80bp will then be pulled from the data set using the *obi grep -p "len(sequence)<=80 and sequence['COUNT']>=1"* command. Sequences were then cleaned and removed of any errors resulting from PCR/Sequencing using the *obi clean -s*. If analyzing a tagged sample or individual sample the command is modified to *obi clean -s MERGED_sample*. Sequences were compared to the locally generated reference database with the minimum required match of 97% using *obi ecotag -m 0.97* command. Assignments were tallied and viewed using the *obi stats -c SCIENTIFIC_NAME* command. Data analyzed using OBITools3 was also exported to Geneious Prime for visualization and the BLAST function was used to confirm the taxonomic assignments of OBITools3 and provide more resolution on sequences not identified by OBITools3.

Reference Database Creation

A new directory called Batrachia_RD was made to house the downloaded sequences using the *mkdir* command. All publicly available sequences except for human and environmental microbe sequences were downloaded from EMBL into the Batrachia_RD directory using the following command: *wget -nH –cut-dirs=5 -A rel_std_*.dat.gz -R rel_std_hum_*.dat.gz,rel_std_env_*.dat.gz -m ftp://ftp.ebi.ac.uk/pub/databases/embl/release/st*. All sequences were imported into a new directory, and parsed out into one file using the following command; *obi import –embl Batrachia_RD Val/embl_refs*. Following that step, the taxonomic information from NCBI was downloaded using the following command: *wget https://ftp.ncbi.nlm.nih.gov/pub/taxonomy/taxdump.tar.gz.* The taxonomy zip file was imported

into the directory using the command: *obi import –taxdump taxdump.tar.gz Val/taxonomy/my_tax.* After that an in-silico PCR reaction was simulated for all downloaded sequences to see how primers bind to available sequences. The in-silico PCR reaction command used was *obi ecopcr -e 3 -l 50 -L 160 -F ACACCGCCCGTCACCCT -R GTAYACTTACCATGTTACGACTT –taxonomy Val/taxonomy/my_tax Val/embl_refs Val/Bat_refs*. As entered, the command allows up to three errors along the sequence and the simulated fragment lengths range from 50–160 bp. After the in-silico PCR reaction, the simulated fragments were then checked to test if there is adequate taxonomic coverage for family, genus and species rankings using the command: *obi grep –require-rank=species –require-rank=genus –require-rank=family –taxonomy Val/taxonomy/my_tax Val/Bat_refs Val/Bat_refs_clean*. The reference database was then built with a minimum required match percentage of 97% using the command: *obi build_ref_db -t 0.97 –taxonomy Val/taxonomy/my_tax Val/Bat_refs_clean Val/Bat_db_97*.